Institut de radiophysique

13.12.2024

Master of Science EPFL-ETH
Degree in Nuclear Engineering
and Medical Radiation Physics

Physics of single-photon emission computed tomography (SPECT)

Siria Medici, PhD
SSRMP Medical Physicist
Institut de Radiophysique (IRA)
UNIL – CHUV

canton de vaud
LIBERTÉ ET PATRIE

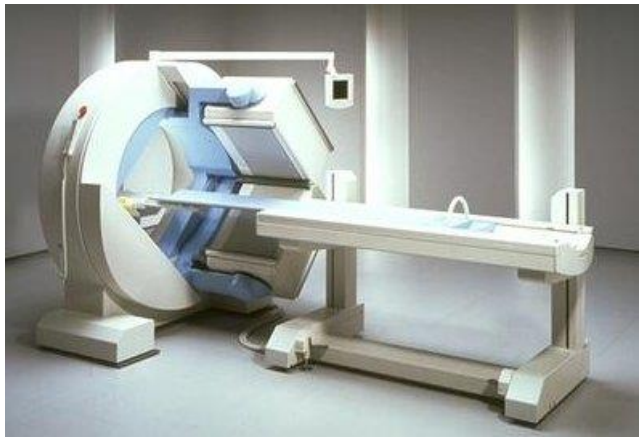

Contents:

- Principles of Gamma Camera
- Bases of Emission Computed Tomography in nuclear medicine
- Single Photon Emission Computed Tomography (SPECT)

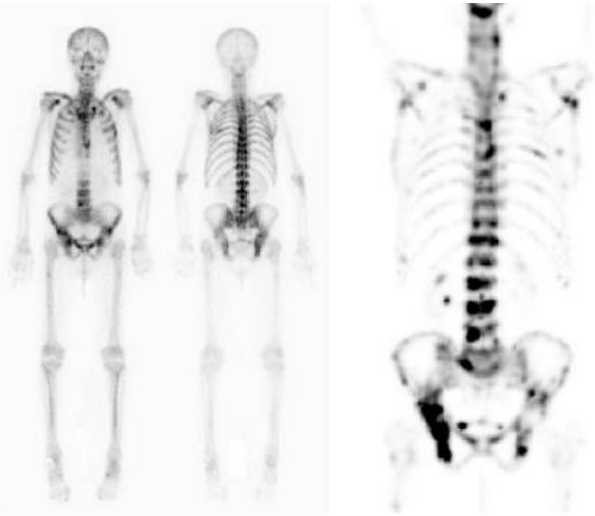

Preface

Don’t hesitate to tell if:

- it’s too complicated!
- It’s too easy !
- Something is not clear!

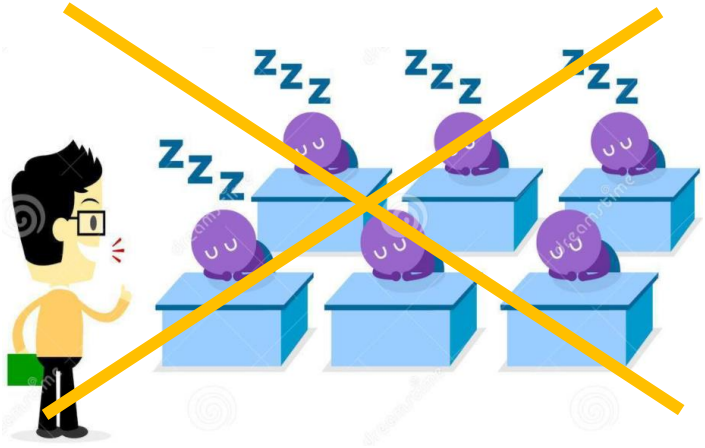

Preface

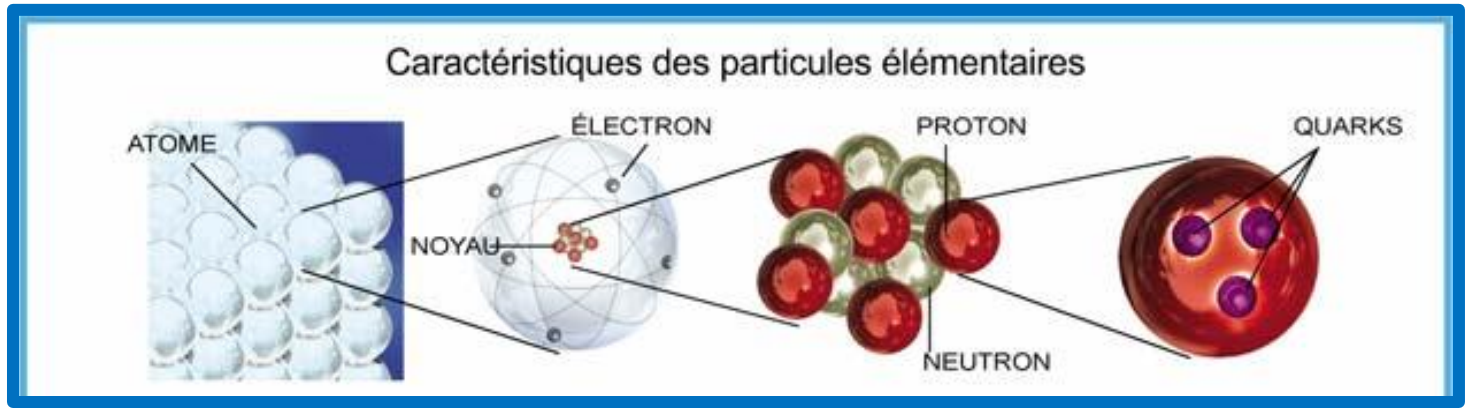

Photoelectric effect

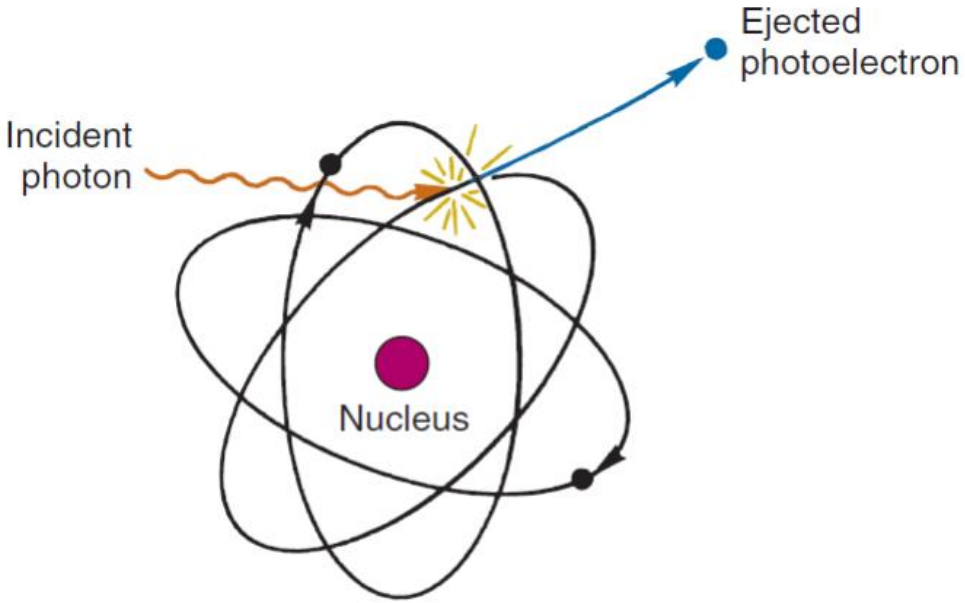

FIGURE 6-11 Schematic representation of the photoelectric effect. The incident photon transfers its energy to a photoelectron and disappears.

Compton effect

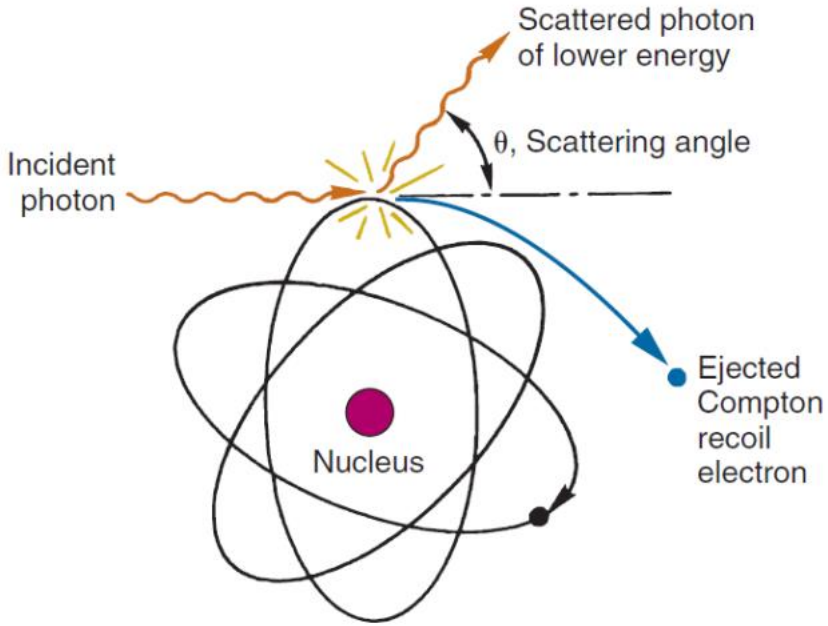

FIGURE 6-12 Schematic representation of Compton scattering. The incident photon transfers part of its energy to a Compton recoil electron and is scattered in another direction of travel (θ, scattering angle).

Gamma emission imaging … a long story!

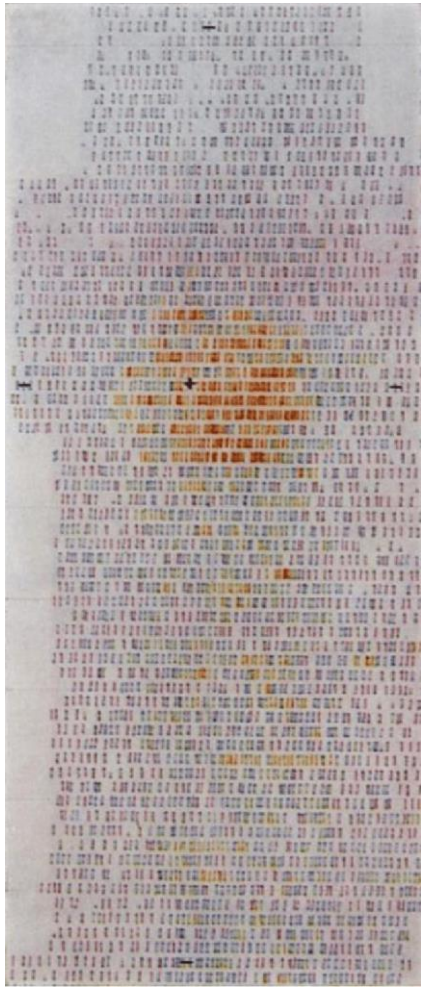

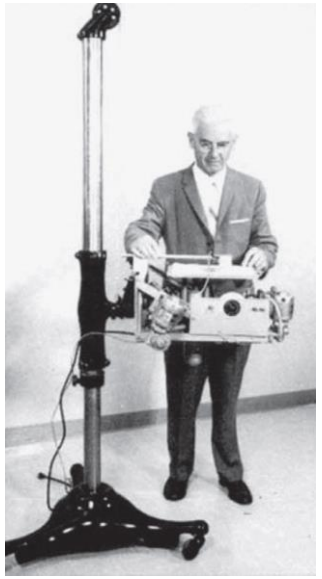

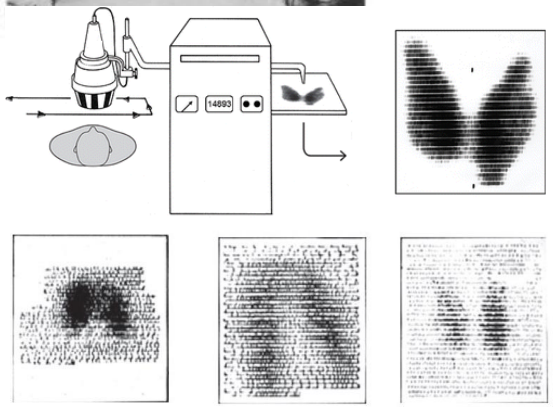

Rectilinear scanner by B. Cassen (1950)
Developed for planar images with I-131.
Scintillator counter scanning the area of interest.
Ink intensity ∝ measured photon count-rate.
Long imaging times due to limited field of view.

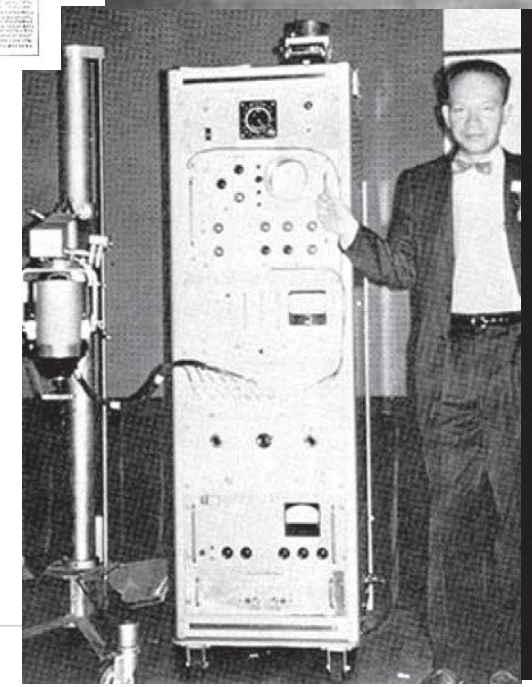

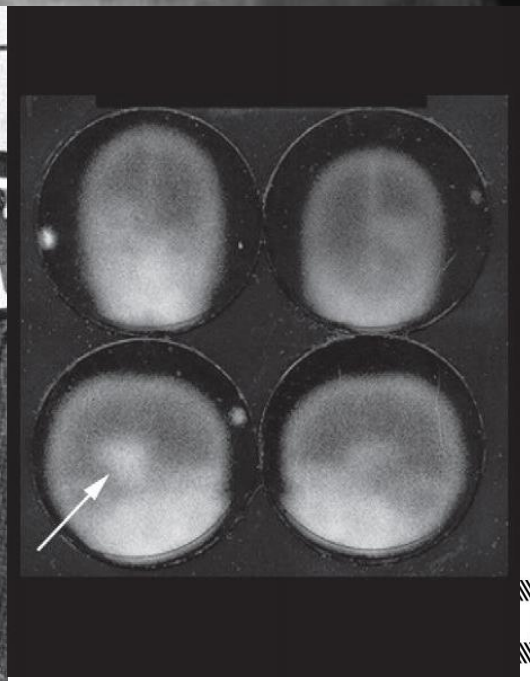

First Gamma Camera by
H. Anger (1958), using
Tc-99m Pertechnetate.
Brain scan of a patient with glioma.

Radiopharmaceuticals

Radioisotope

Specific binding site

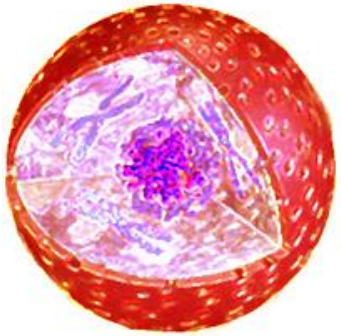

Radiotracer

Cell/Target tissue

Radio-**diagnostic** and/or radio-**therapeutic** (if both: "*theranostic*")

γ γ + β and/or α

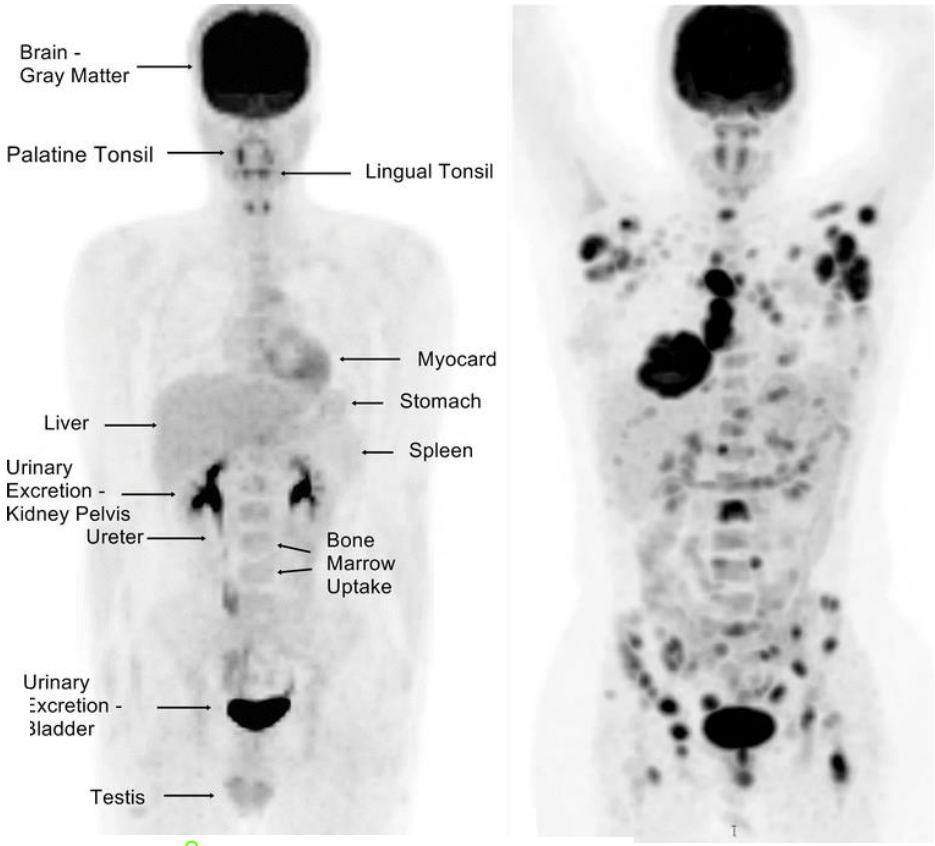

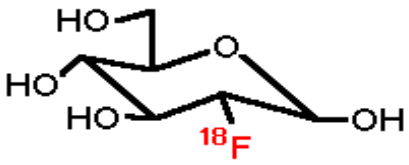

Vectors:

- Molecules, peptides, antobodies, microspheres, …

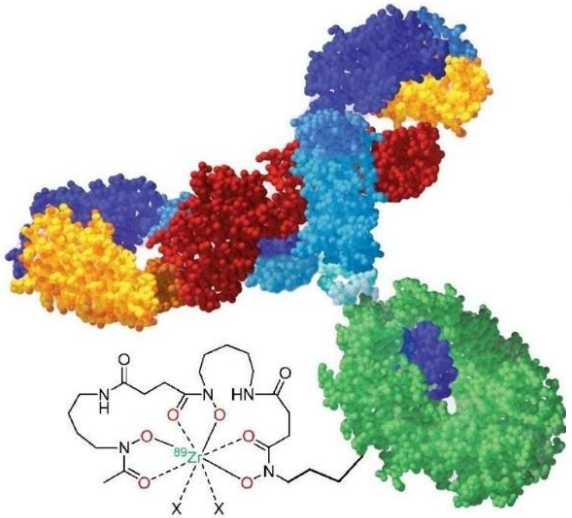

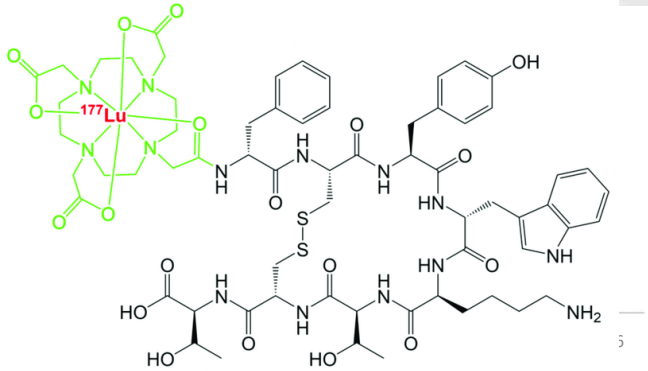

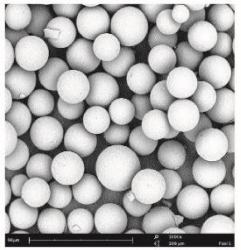

SELECTED CLINICAL NUCLEAR MEDICINE PROCEDURES

Radiopharmaceutical	Imaging	Measurement	Examples of Clinical Use
^{99m}Tc-MDP	Planar	Bone metabolism	Metastatic spread of cancer, osteomyelitis vs. cellulitis
^{99m}Tc-sestamibi (Cardiolite) ^{99m}Tc-tetrofosmin (Myoview) ^{201}Tl-thallous chloride	SPECT or planar	Myocardial perfusion	Coronary artery disease
^{99m}Tc-MAG3 ^{99m}Tc-DTPA	Planar	Renal function	Kidney disease
^{99m}Tc-HMPAO (Ceretec)	SPECT	Cerebral blood flow	Neurologic disorders
^{99m}Tc-ECD	SPECT	Cerebral blood flow	Neurologic disorders
^{123}I-sodium iodide ^{131}I-sodium iodide	Planar	Thyroid function	Thyroid disorders Thyroid cancer
^{67}Ga-gallium citrate	Planar	Sequestered in tumors	Tumor localization
^{99m}Tc-macroaggregated albumin and ^{133}Xe gas	Planar	Lung perfusion/ ventilation	Pulmonary embolism
^{111}In-labeled white blood cells	Planar	Sites of infection	Detection of inflammation
^{18}F-fluorodeoxyglucose	PET	Glucose metabolism	Cancer, neurological disorders, and myocardial diseases
^{82}Rb-rubidium chloride	PET	Myocardial perfusion	Coronary artery disease

MDP, methylene diphosphonate; MAG3, mercapto-acetyl-triglycine; DTPA, diethylenetriaminepenta-acetic acid; HMPAO, hexamethylpropyleneamine oxime; ECD, ethyl-cysteine-dimer; SPECT, single photon emission computed tomography; PET, positron emission tomography.

Production of radioisotopes for medical use

Three main routes of production:

1. **Reactor**-produced (fission fragments / neutron activation)

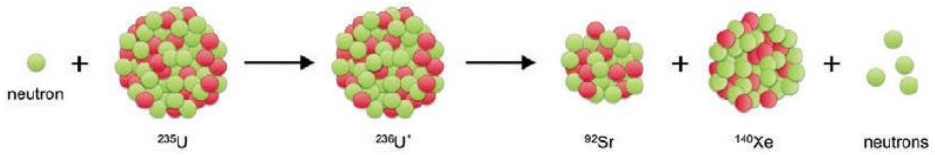

$$^{130}Te\ (n,\gamma)^{131}Te \xrightarrow{\beta-\ (25\ m)} \mathbf{^{131}I} \xrightarrow{\beta-,\gamma=364\ keV\ (8\ d)} {}^{131}Xe$$

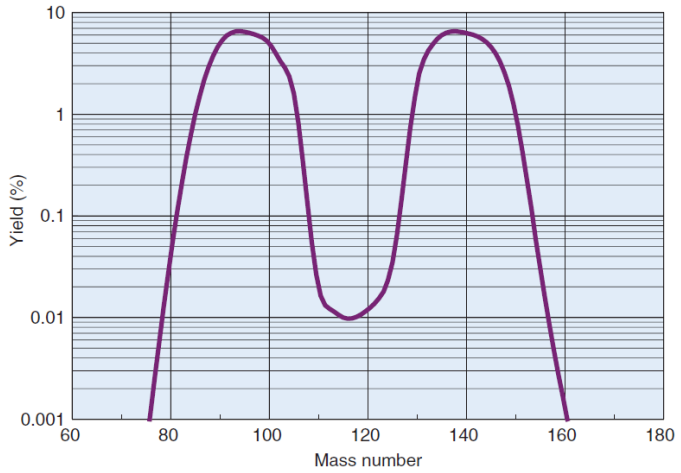

2. **Accelerator**-produced

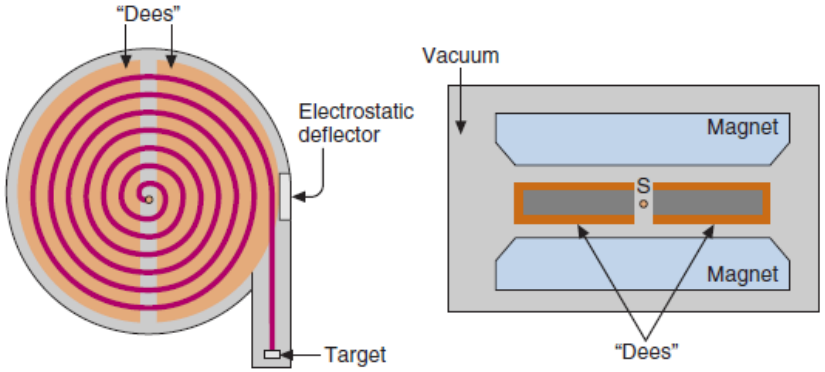

$$^{18}O(p,n)^{\mathbf{18}}\boldsymbol{F}$$

3. Radionuclide **generators** $^{99}Mo \xrightarrow{\beta-(66\ h)} \mathbf{^{99m}Tc}\ (6\ h)$

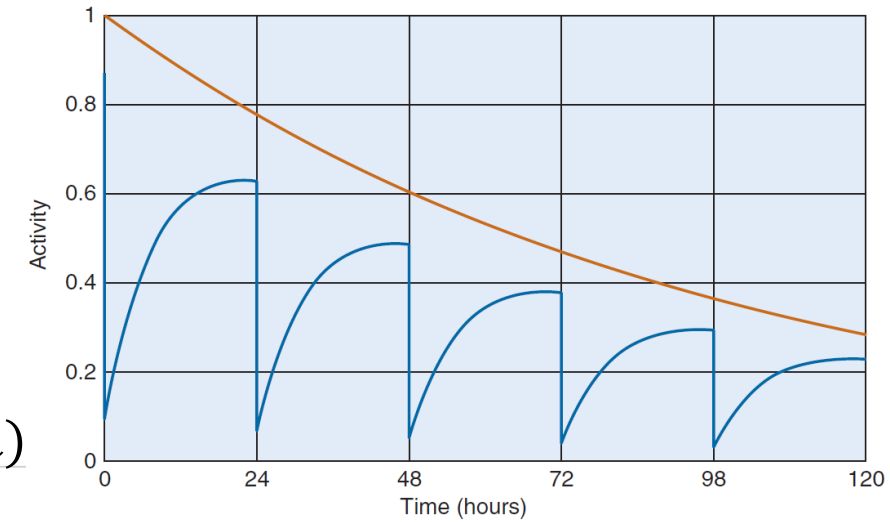

canton de vaud

1. Reactor-produced radionuclides: **fission fragments**

$$^{235}\mathrm{U} + \mathrm{n} \longrightarrow {}^{236}\mathrm{U}^{*} + \text{fission fragments}$$

$$^{99}_{39}Y \xrightarrow{\beta-(1.5\ s)} {}^{99}_{40}Zr \xrightarrow{\beta-(21\ s)} {}^{99}_{41}Nb \xrightarrow{\beta-(15\ s)} {}^{99}_{42}Mo \xrightarrow{\beta-(66\ h)} {}^{99m}_{43}\boldsymbol{Tc} \xrightarrow{\gamma=140\ keV\ (6\ h)} {}^{99}_{43}Tc \xrightarrow{\beta-(2.111\cdot 10^{5}\ \mathrm{y})} {}^{99}_{44}Ru$$

Fission products have excess of neutrons → β- decay.

Fission products may be carrier-free* (no stable isotope of the radionuclide of interest → high specific activity can be achieved after chemical separation).

Fission processes lack in specificity : low yield of the radionuclide of interest.

* carrier-free: no stable isotopes of the same elements are present.

1. Reactor-produced radionuclides: **neutron activation**

$$^{A}_{Z}X(n,\gamma)^{A+1}_{Z}X \qquad ^{A}_{Z}X(n,p)_{Z-1}^{A}Y$$

$$^{130}Te\ (n,\gamma)^{131}Te \xrightarrow{\beta-\ (25\ m)} \mathbf{^{131}I} \xrightarrow{\beta-,\gamma=364\ keV\ (8\ d)} {}^{131}Xe$$

Neutron activation products have excess of neutrons → β- decay

Most common production mode is (n,γ) → same element, not carrier-free.
Carrier-free by possible by using (n,p) reaction or by activating a short lived radionuclide using the (n,γ) reaction and waiting for its decay.

Small fraction of target nuclei are activated, even at high neutron fluxes
→ low specific activity due to presence of unactivated stable carrier (target).

NEUTRON-ACTIVATED RADIONUCLIDES OF IMPORTANCE IN BIOLOGY AND MEDICINE

Radionuclide	Decay Mode	Production Reaction
^{14}C	β^-	$^{14}N(n,p)^{14}C$
^{24}Na	(β^-,γ)	$^{23}Na(n,\gamma)^{24}Na$
^{32}P	β^-	$^{31}P(n,\gamma)^{32}P$ $^{32}S(n,p)^{32}P$
^{35}S	β^-	$^{35}Cl(n,p)^{35}S$
^{42}K	(β^-,γ)	$^{41}K(n,\gamma)^{42}K$
^{51}Cr	(EC,γ)	$^{50}Cr(n,\gamma)^{51}Cr$
^{59}Fe	(β^-,γ)	$^{58}Fe(n,\gamma)^{59}Fe$
^{75}Se	(EC,γ)	$^{74}Se(n,\gamma)^{75}Se$
^{125}I	(EC,γ)	$^{124}Xe(n,\gamma)^{125}Xe \xrightarrow{EC} {}^{125}I$
^{131}I	(β^-,γ)	$^{130}Te(n,\gamma)^{131}Te \xrightarrow{\beta^-} {}^{131}I$

2. **Accelerator**-produced radionuclides

$$\boxed{{}^{A}_{Z}X(p, n)_{Z+1}{}^{A}Y} \quad \boxed{{}^{A}_{Z}X(d, n)^{A+1}_{Z+1}Y}$$

$$^{18}O(p,n)^{18}F \qquad ^{109}Ag(\alpha,2n)^{111}In \qquad ^{122}Te(d,n)^{123}I$$

In most activation processes, positive charge is added to the nucleus
→ β+ / EC decay

Addition of positive charge changes to atomic number Z → generally different element, carrier-free.

Smaller quantities of radioactivity when compared to reactor-produced radionuclides (due to generally higher activation cross-section for neutrons than for charged particles + lower beam intensities).

SOME CYCLOTRON-PRODUCED RADIONUCLIDES USED IN NUCLEAR MEDICINE

Product	Decay Mode	Common Production Reaction
^{11}C	β^+, EC	$^{14}N(p,\alpha)^{11}C$
		$^{10}B(d,n)^{11}C$
^{13}N	β^+	$^{16}O(p,\alpha)^{13}N$
		$^{12}C(d,n)^{13}N$
^{15}O	β^+	$^{14}N(d,n)^{15}O$
		$^{15}N(p,n)^{15}O$
^{18}F	β^+, EC	$^{18}O(p,n)^{18}F$
		$^{20}Ne(d,\alpha)^{18}F$
^{67}Ga	(EC,γ)	$^{68}Zn(p,2n)^{67}Ga$
^{111}In	(EC,γ)	$^{109}Ag(\alpha,2n)^{111}In$
		$^{111}Cd(p,n)^{111}In$
^{123}I	(EC,γ)	$^{122}Te(d,n)^{123}I$
		$^{124}Te(p,3n)^{123}I$
^{201}Tl	(EC,γ)	$^{201}Hg(d,2n)^{201}Tl$

3. **Generator**-produced radionuclides

Mother (long-lived) → daughter

$$^{82}Sr \xrightarrow{EC\ (25\ d)} {}^{82}Rb\ (75\ s)$$

$$^{99}Mo \xrightarrow{\beta-(66\ h)} {}^{99m}Tc\ (6\ h)$$

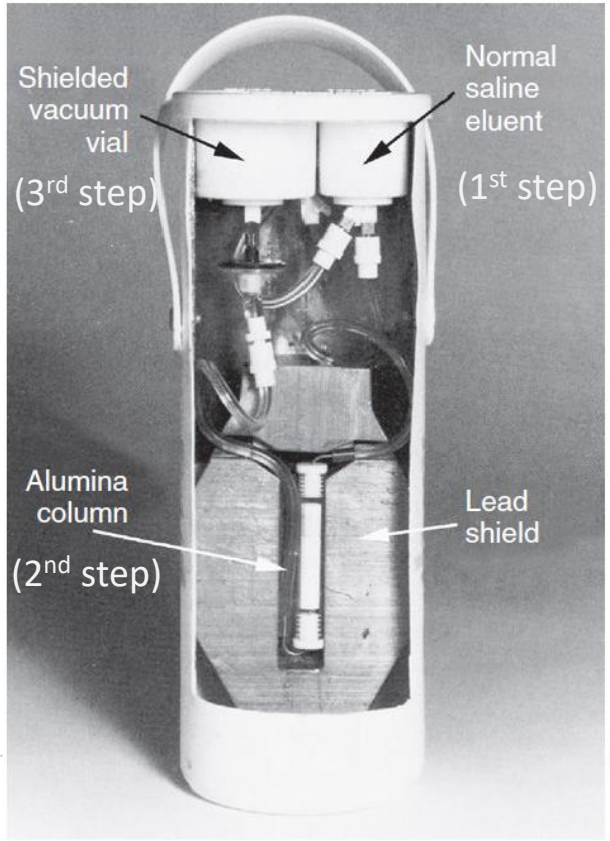

Elution efficiency may vary from one generator to the other.

Impurities (partial elution of the parent) may occur.

Dependent on reactor operations (shortages!)

FORBES > INNOVATION > HEALTHCARE

Technetium Is In Short Supply. Here's How That Affects Public Health

Omer Awan Senior Contributor
Dr. Omer Awan is a practicing physician who covers public health.

Follow

0

Oct 24, 2024, 06:45am EDT

"Technetium-99m, a critical nuclear imaging radioisotope, is in short supply and could cause delays or cancellations of over 40,000 medical imaging studies daily in the United States.

The global shortage of Tc-99m stems for issues related to its production. Normally, Tc-99m decays and is eluted from Molybdenum-99, which is generated from a high-flux reactor. The parent isotope Molybdenum-99 is only produced in a few nuclear reactors worldwide, such as in Petten, Netherlands. A structural issue within a pipe from this reactor in the Netherlands will require repair that may delay the production of Tc-99m well into November, according to reports from the Society of Nuclear Medicine and Molecular Imaging."

Sources: https://nap.nationalacademies.org/read/24909/chapter/5#14, https://www.forbes.com/sites/omerawan/2024/10/24/technetium-is-in-short-supply-heres-how-that-affects-public-health/

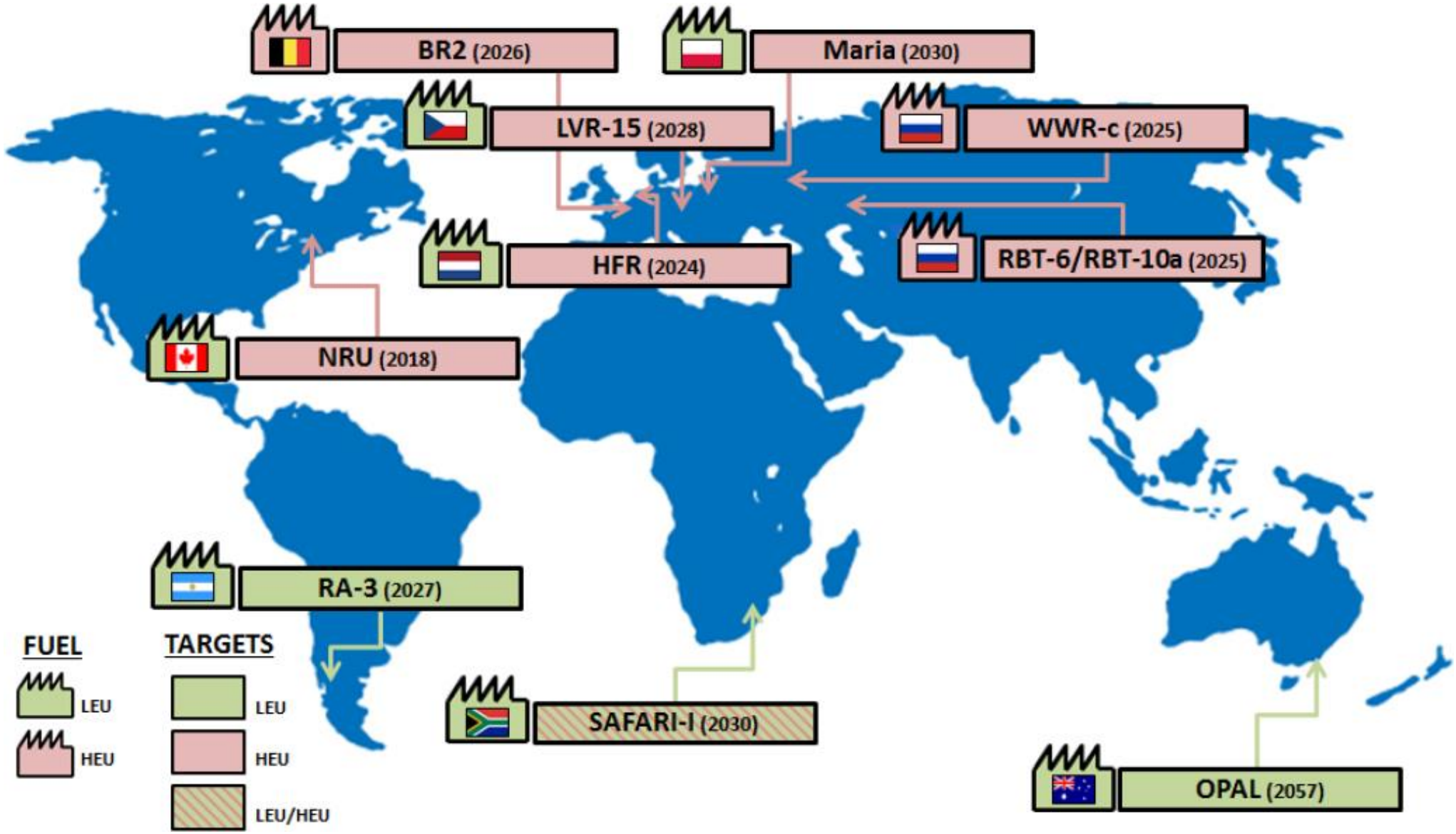

Current Mo-99 supply map as of July 2017. The estimated end of operation for the reactors is shown in parentheses. https://doi.org/10.17226/24909.

Sources: https://nap.nationalacademies.org/read/24909/chapter/5#14, https://www.forbes.com/sites/omerawan/2024/10/24/technetium-is-in-short-supply-heres-how-that-affects-public-health/

SOME RADIONUCLIDE GENERATORS USED IN NUCLEAR MEDICINE

Daughter*	Decay Mode	$T_{1/2}$	Parent	$T_{1/2}$
^{62}Cu	β^+,EC	9.7 min	^{62}Zn	9.3 hr
^{68}Ga	β^+,EC	68 min	^{68}Ge	271 d
^{82}Rb	β^+,EC	1.3 min	^{82}Sr	25 d
^{87m}Sr	IT	2.8 hr	^{87}Y	80 hr
^{99m}Tc	IT	6 hr	^{99}Mo	66 hr
^{113m}In	IT	100 min	^{113}Sn	120 d

The gamma camera
Introduction to basic principles

Gamma camera: main components

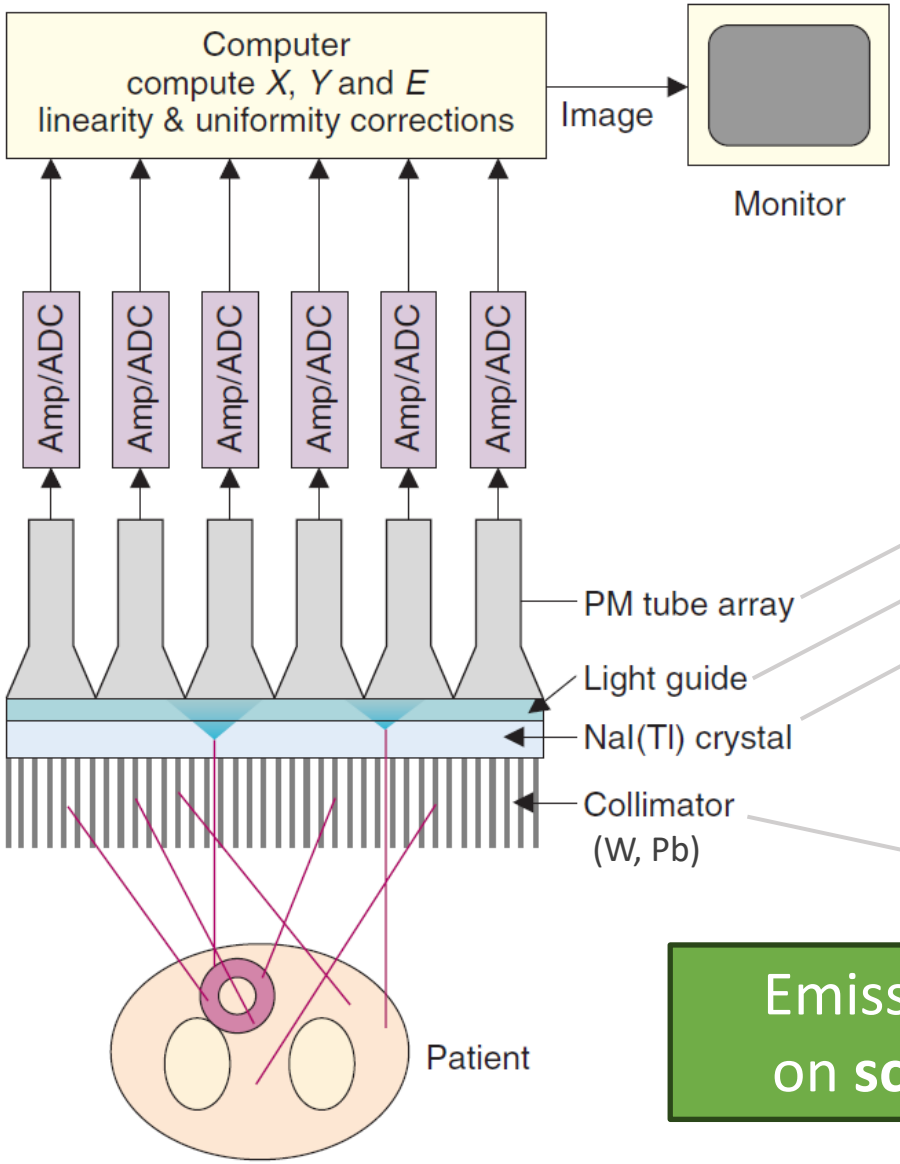

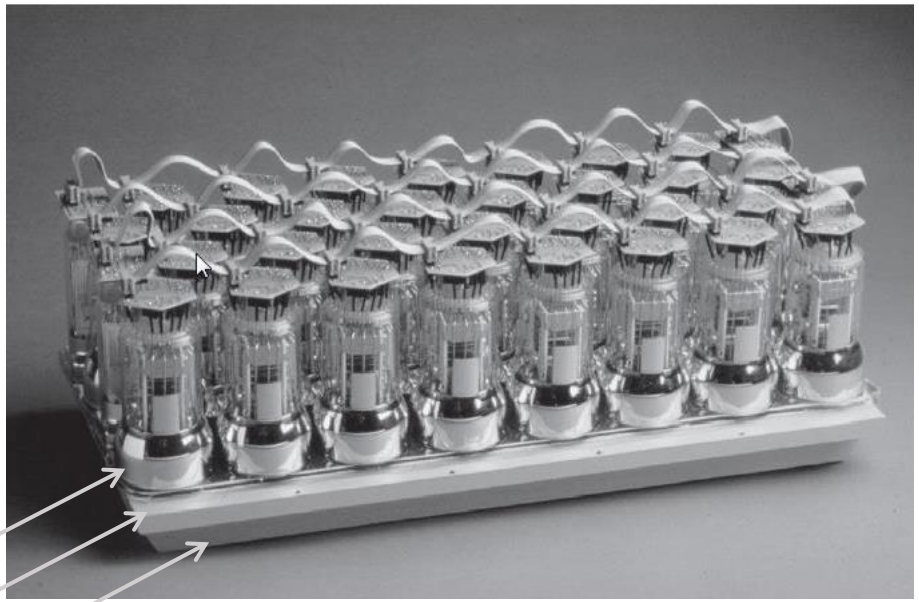

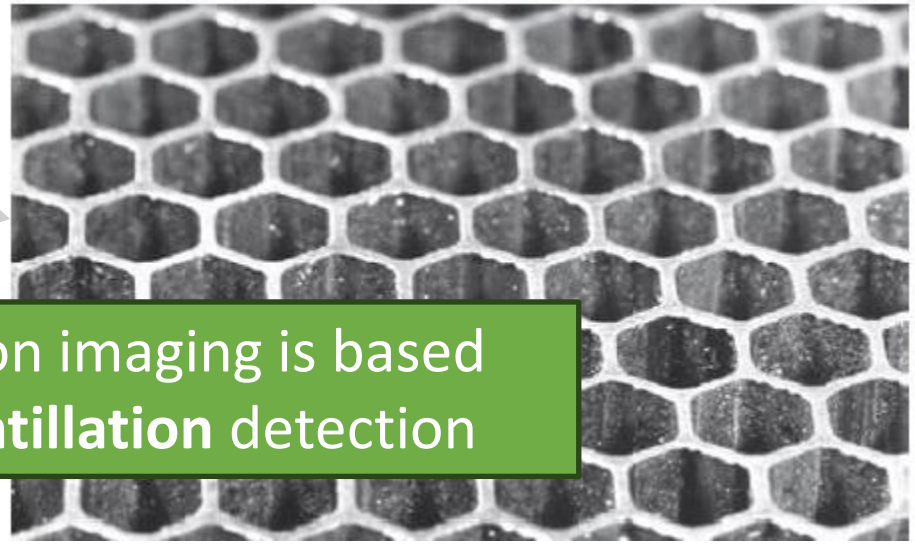

Parallel hole collimator

Emission imaging is based on **scintillation** detection

Radiation detectors - scintillation

1. *Gas-filled detectors*

   Ionization chambers

   Proportional counters

   Geiger-Müller counters

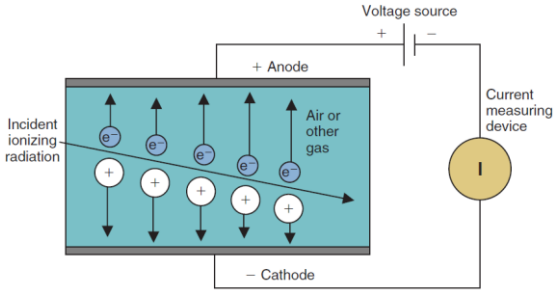

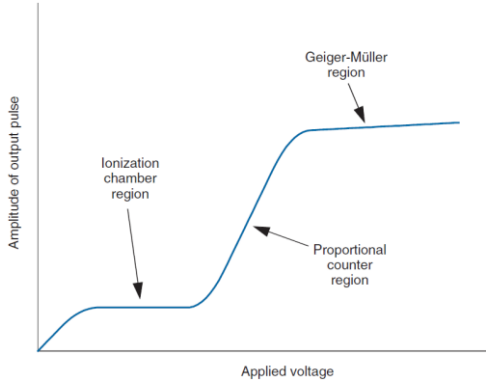

2. *Semiconductor detectors*

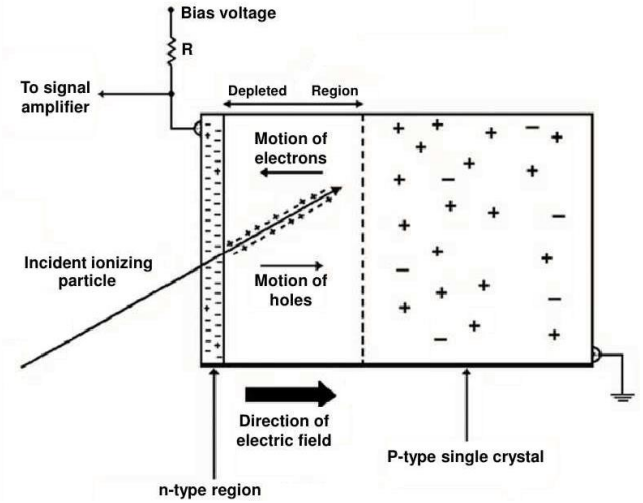

3. *Scintillation detectors*

   Inorganic

   Organic

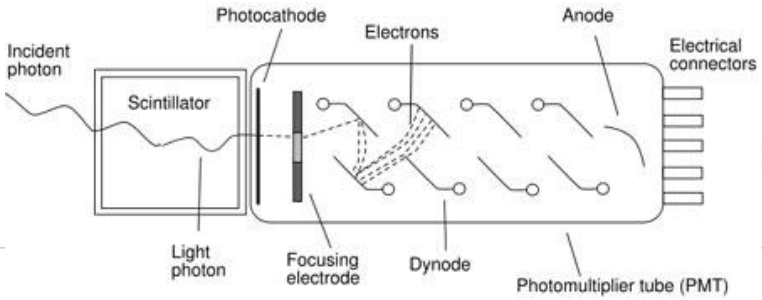

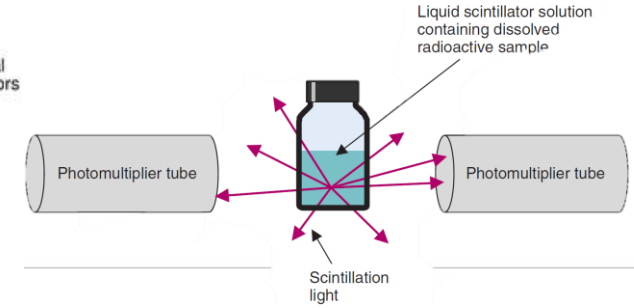

Scintillation detectors

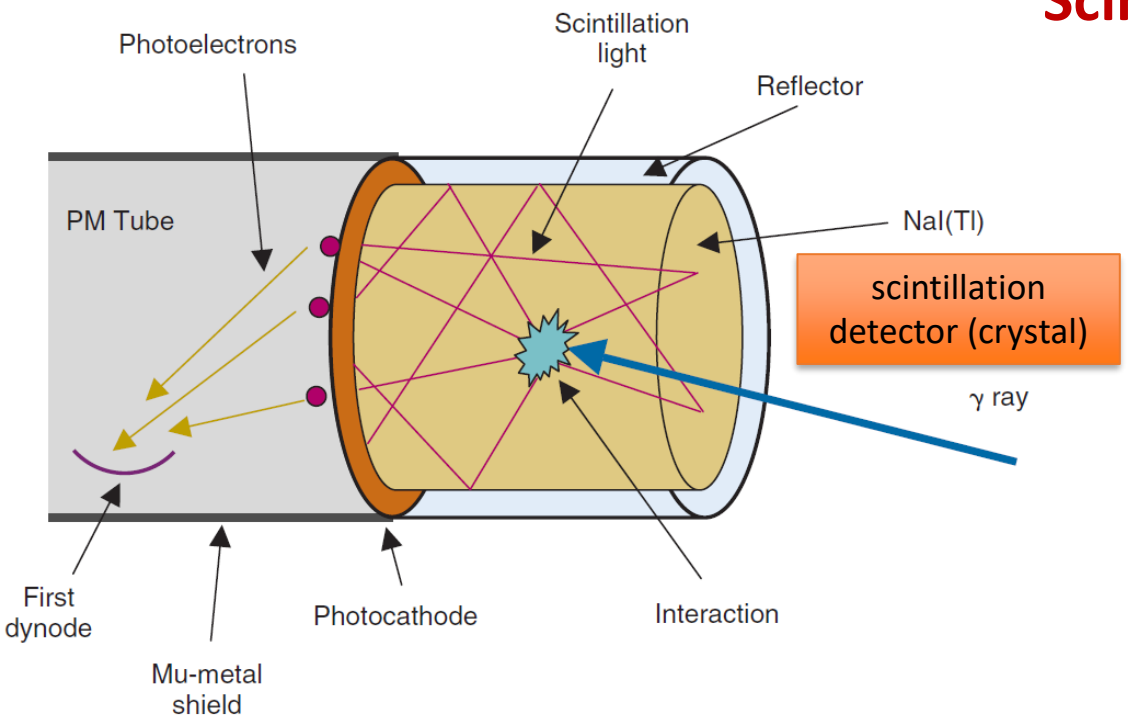

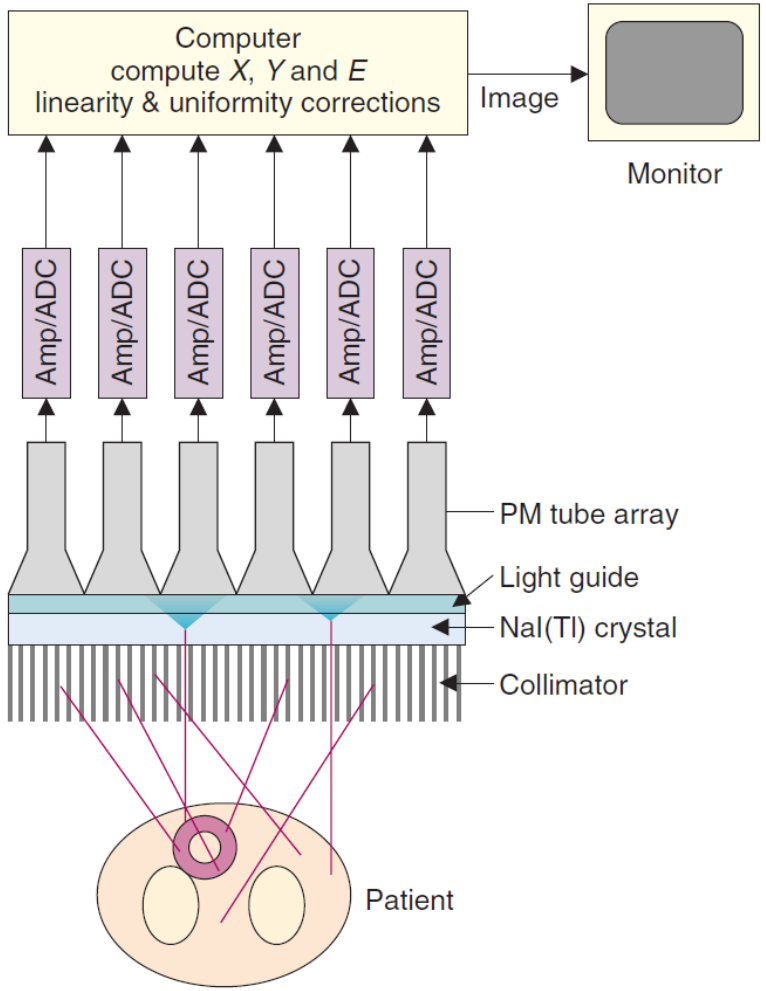

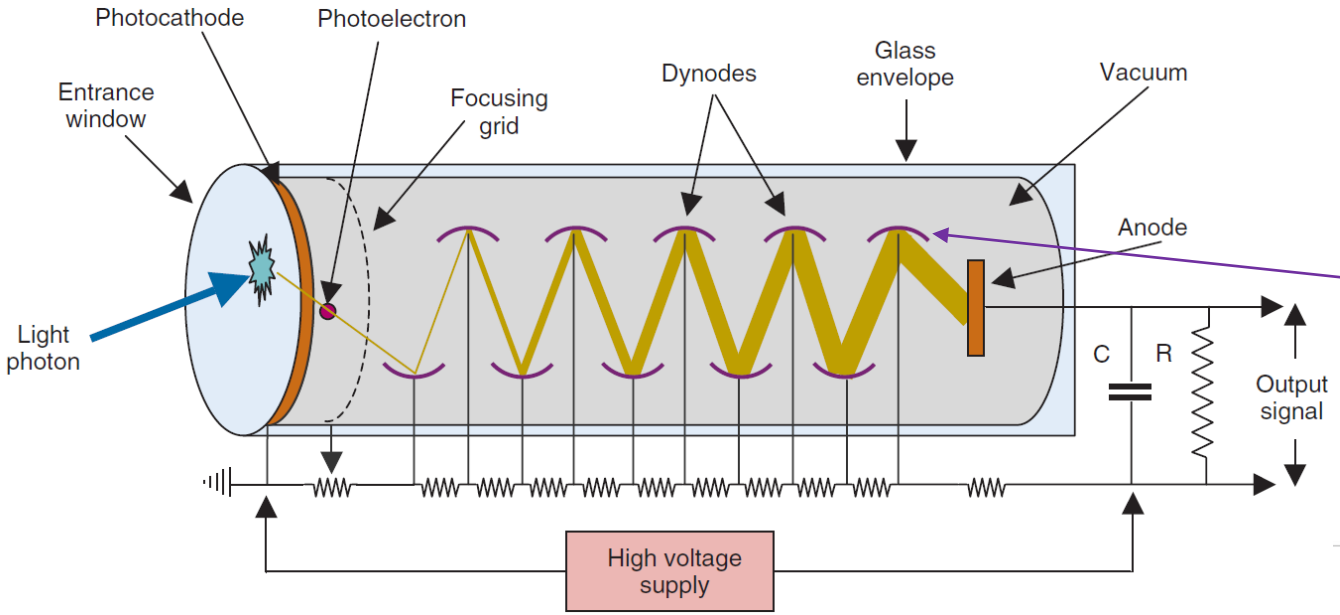

Electron multiplication factor at each dynode ~ x6

For a 10 dynode photomultiplier tube (PMT) ~ x 60’000’000

Scintillation detectors

Scintillation material
- Organic (liquids)
- Inorganic (crystals: NaI(Tl), BGO, LSO, GSO, CsI, $LaBr_3$, plastic,…)

PROPERTIES OF SOME SCINTILLATOR MATERIALS

Property	NaI(Tl)	BGO	LSO(Ce)	GSO(Ce)
Density (g/cm^3)	3.67	7.13	7.40	6.71
Effective atomic number	50	73	66	59
Decay time (nsec)	230	300	40	60
Photon yield (per keV)	38	8	20-30	12-15
Index of refraction	1.85	2.15	1.82	1.85
Hygroscopic	Yes	No	No	No
Peak emission (nm)	415	480	420	430

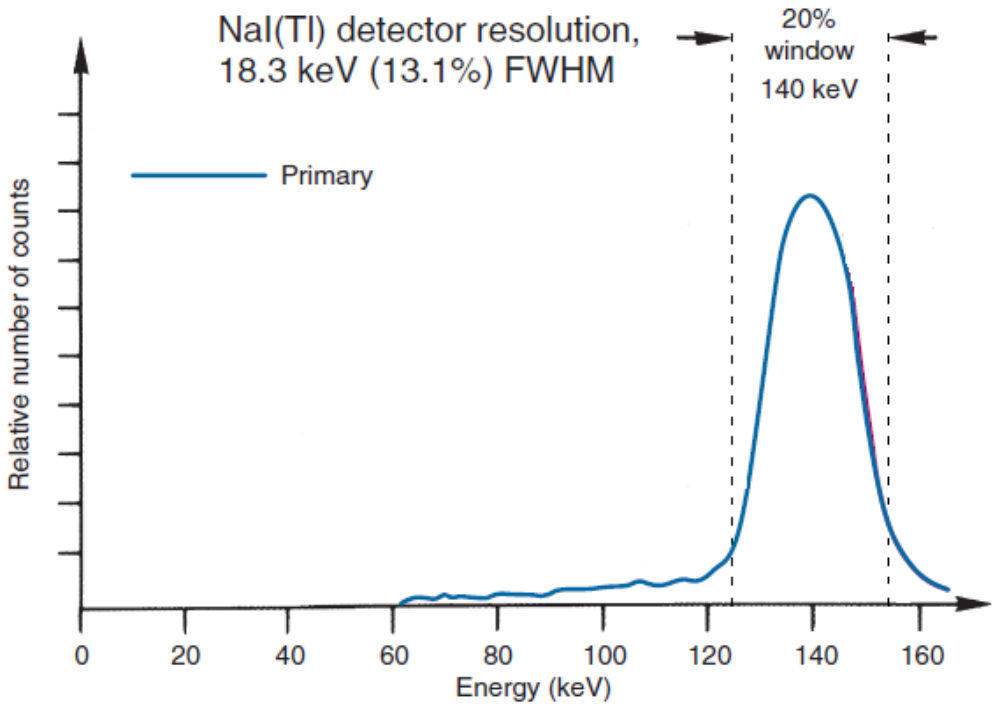

^{99m}Tc Eγ=140 keV → scintillation photon yield $= 38 \cdot 140 = 5320$

Amount of **scintillation light ∝ deposited energy**
→ energy discrimination possible

Scintillation detectors – sodium iodide (NaI)

Advantages of NaI detectors:

✓ Reasonably dense and contains I (relatively high atomic number):

- good absorber and efficient for penetrating radiations → ideal 50-250 keV photons.
- predominant interaction in this range → photoelectric effect.

✓ Efficient scintillator (high photon yield).

✓ Transparent to its own scintillation (limited light loss due to self-absorption).

✓ Relatively inexpensive to grow in large plates.

✓ Scintillation light emitted by NaI is optimal (good wavelength) for PMT operation.

Disadvantages of NaI detectors:

✗ Crystal is fragile and easily fractured by mechanical or thermal stress (fractures = reduced amount of light reaching the photocathode).

✗ NaI is hygroscopic (humidity creates yellowish stains → impair light transmission)

✗ At energies > 250 keV, Compton effect is predominant.

Gamma camera: problems in event localization

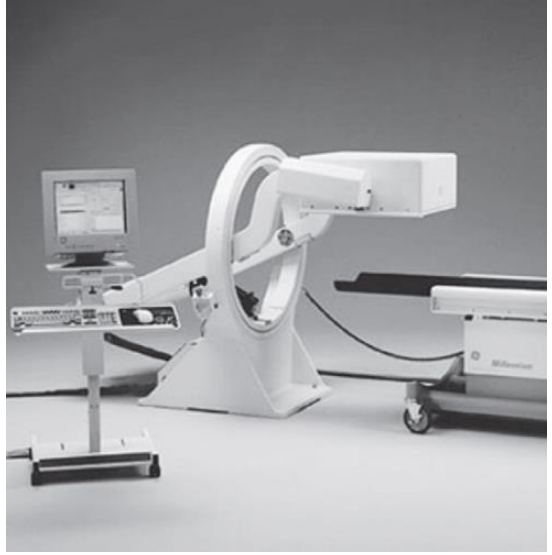

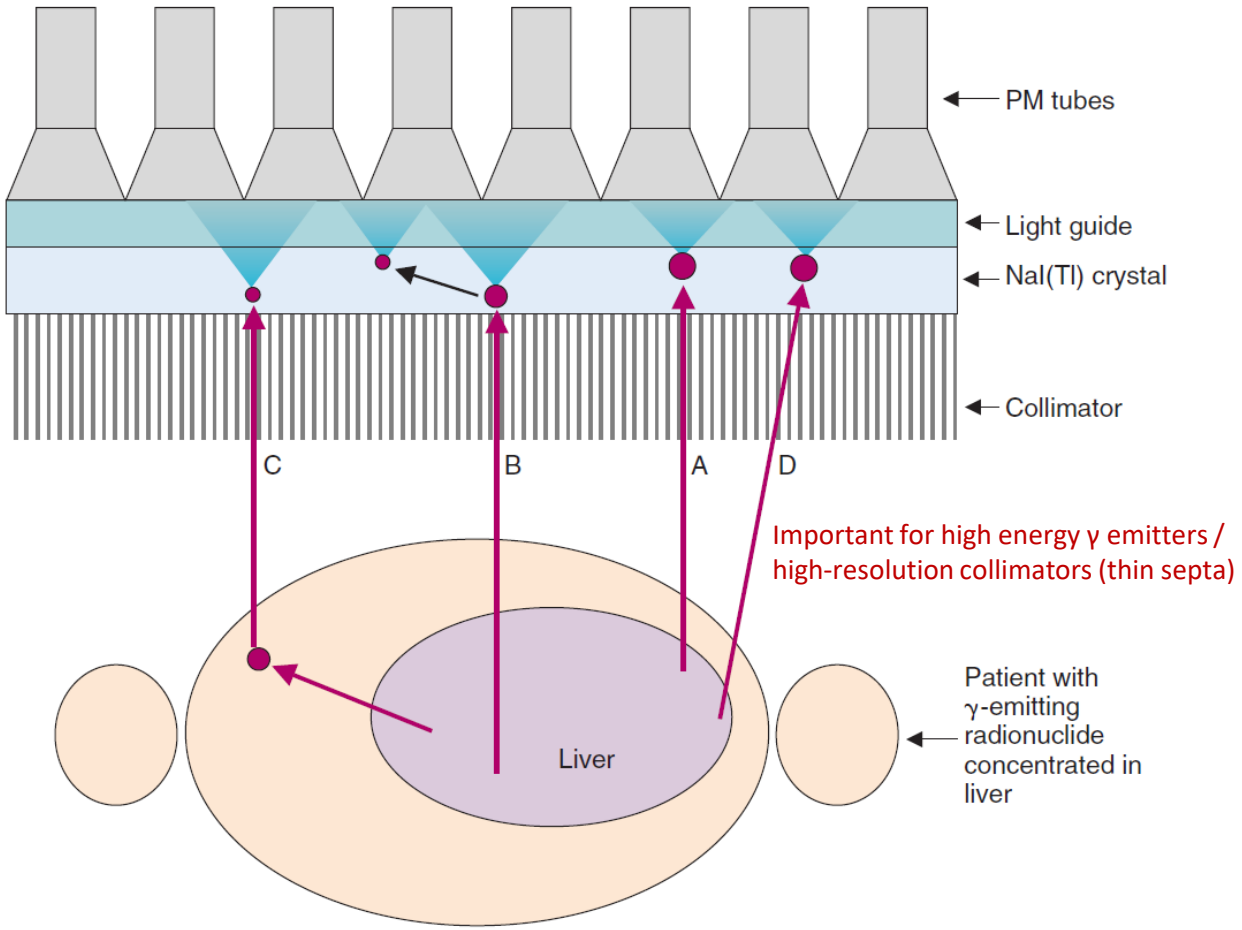

A) Valid event (useful for correct localization on the imaged region)

B) Scatter within the detector
C) Scatter within the patient
D) Septal penetration

Incorrect source localization !

(+ loss of contrast, blurring)

scatter = diffusion

Gamma camera: problems in event localization

1 dimension

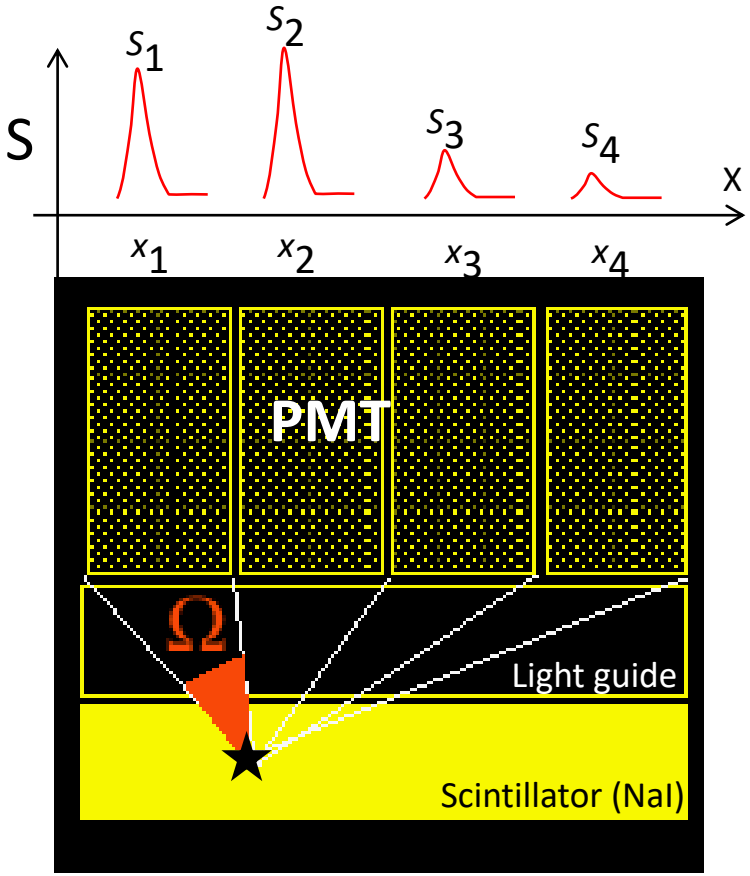

2D localisation on the crystal = weighted average (centroid) of the photomultiplier tube response

30-100 PMT

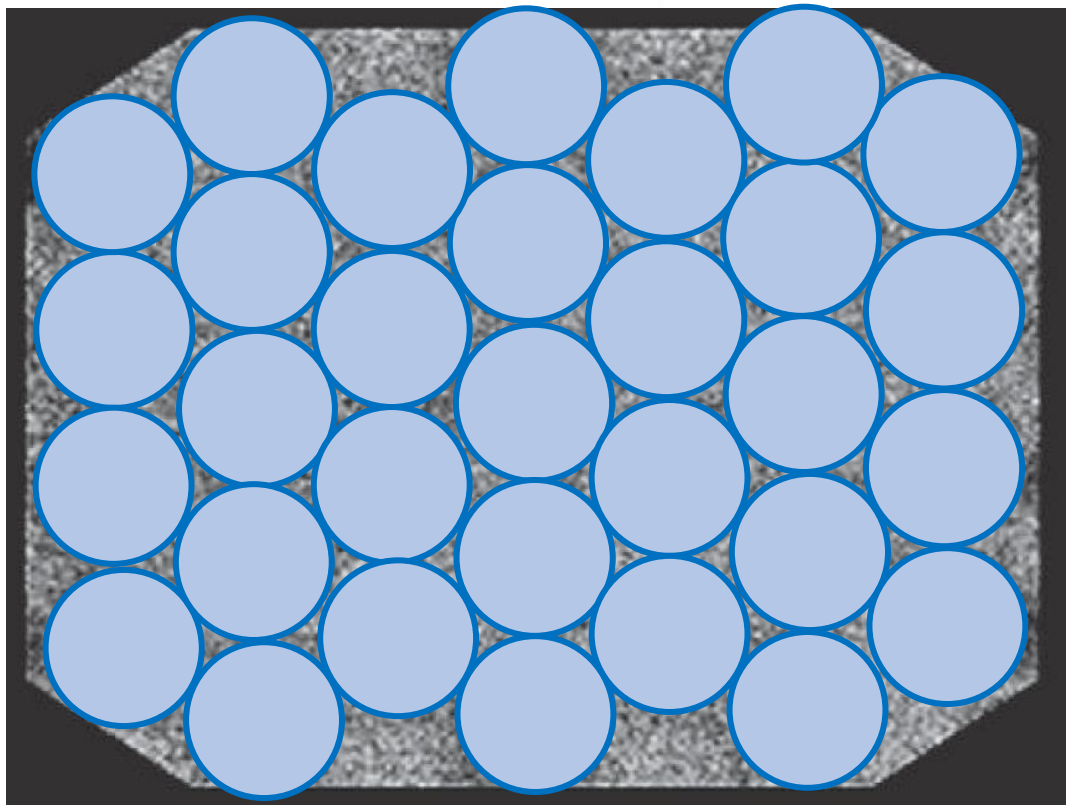

⚠ PMT response does not vary linearly with the interaction position + other non-uniformities (crystal inhomogeneities, light reflections, pulse-height spectrum ≠ among PMT …).

In digital cameras, output signal of each PMT is digitalized and event position is calculated by a software → take into account for non-linearity.

Gamma camera: problems in event localization

1 dimension

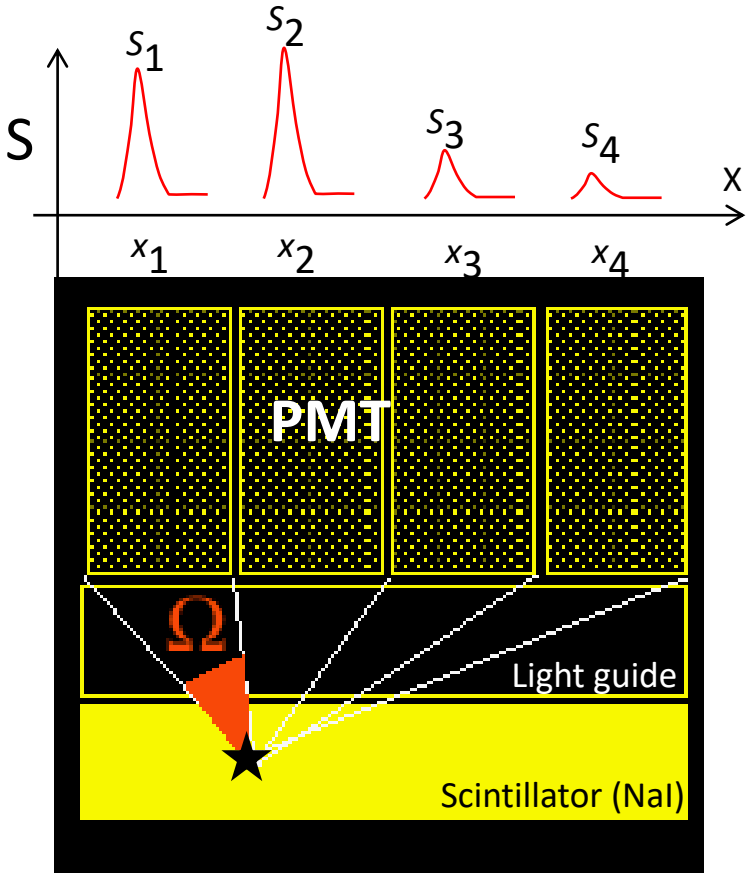

2D localisation on the crystal = weighted average (centroid) of the photomultiplier tube response

30-100 PMT

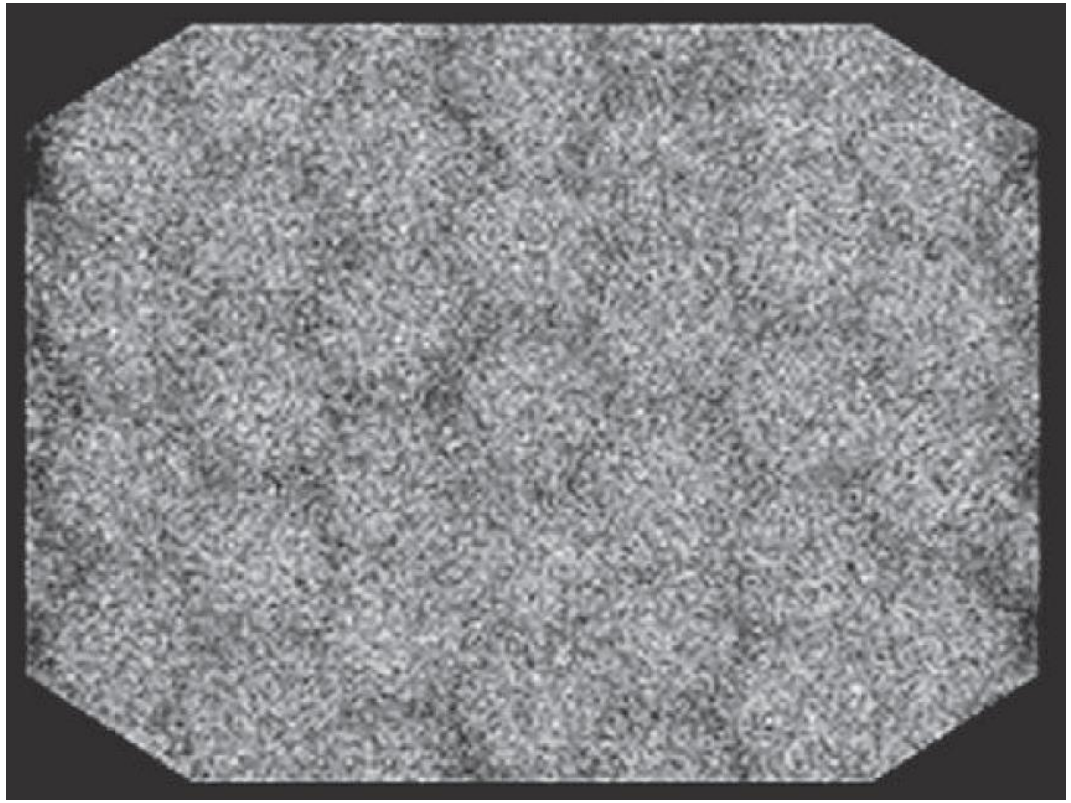

⚠ PMT response does not vary linearly with the interaction position + other non-uniformities (crystal inhomogeneities, light reflections, pulse-height spectrum ≠ among PMT …).

In digital cameras, output signal of each PMT is digitalized and event position is calculated by a software → take into account for non-linearity.

Gamma camera: problems in event localization

1 dimension

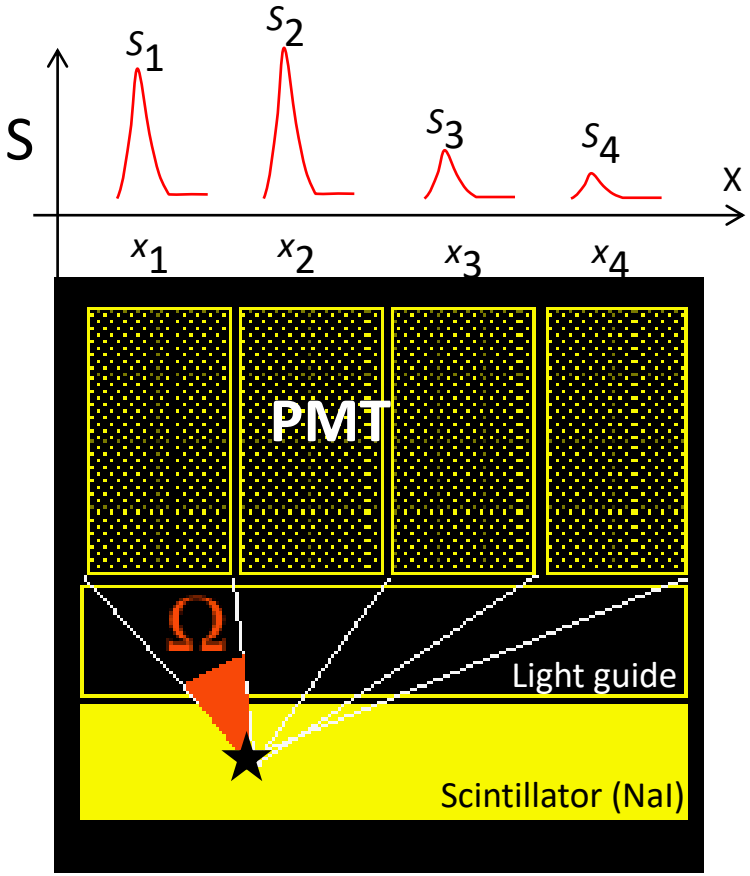

2D localisation on the crystal = weighted average (centroid) of the photomultiplier tube response

30-100 PMT

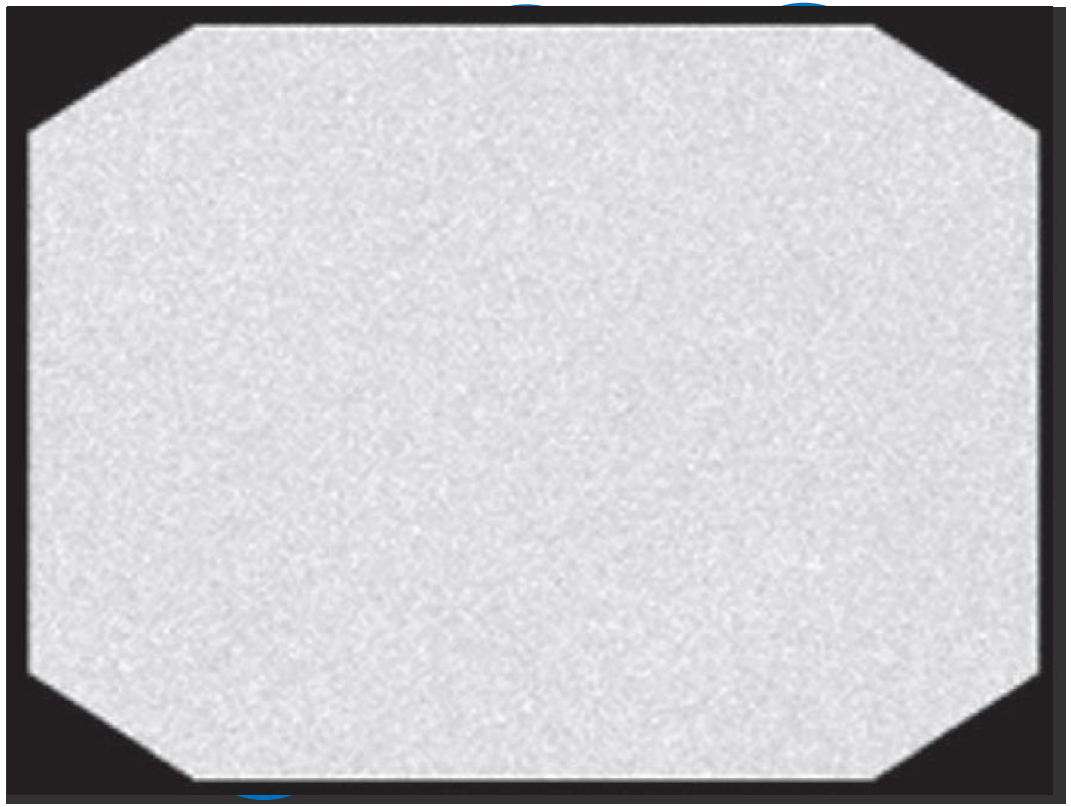

⚠ PMT response does not vary linearly with the interaction position + other non-uniformities (crystal inhomogeneities, light reflections, pulse-height spectrum ≠ among PMT …).

In digital cameras, output signal of each PMT is digitalized and event position is calculated by a software → take into account for non-linearity.

Gamma camera: energy determination

Why is energy discrimination so important ?

Scattered photons are undesirable : no useful information of the source distribution!

They also lose energy along their path → can be discriminated from using the pulse-height analyser (PHA) present on each PMT (signal amplitude ∝ scintillation light ∝ deposited energy in the crystal).

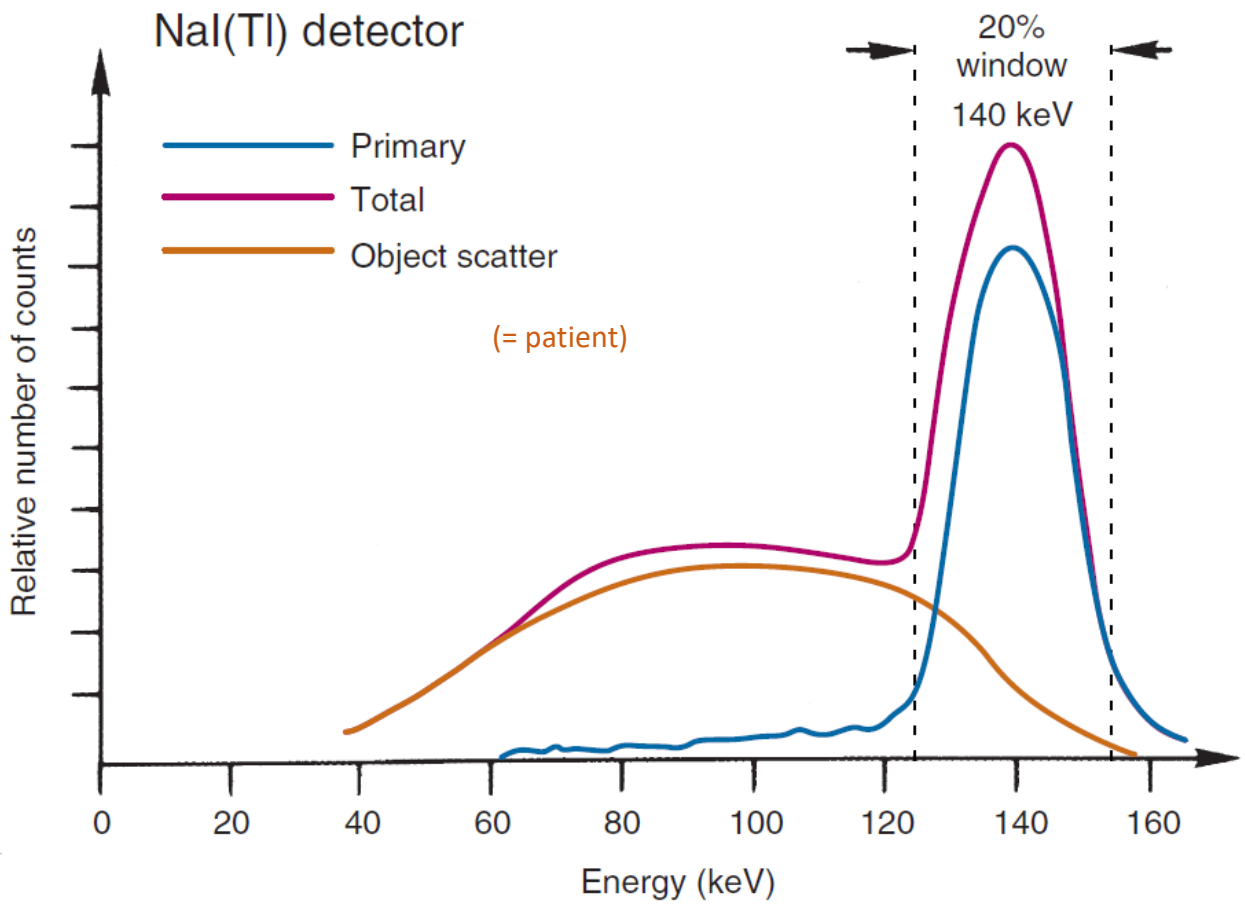

PE effect :

they mostly result in full deposition of the photons in the detector (photopeak).

Compton :

part of the energy is transferred to the detector via the recoil e-, the scattered photon may either be detected or escape the detector.

→ Only PE or Compton scattered at small angles should be accepted!

Gamma camera: energy determination

Why is energy discrimination so important ?

Scattered photons are undesirable : no useful information of the source distribution!

They also lose energy along their path → can be discriminated from using the pulse-height analyser (PHA) present on each PMT (signal amplitude ∝ scintillation light ∝ deposited energy in the crystal).

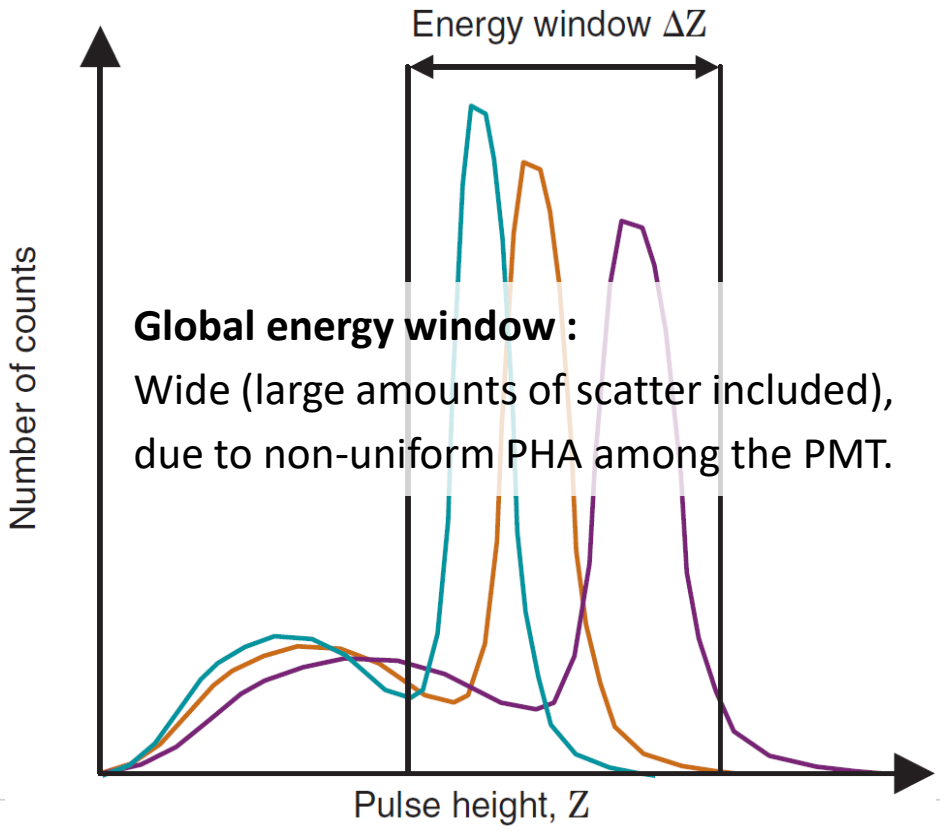

Global energy window :

Wide (large amounts of scatter included), due to non-uniform PHA among the PMT.

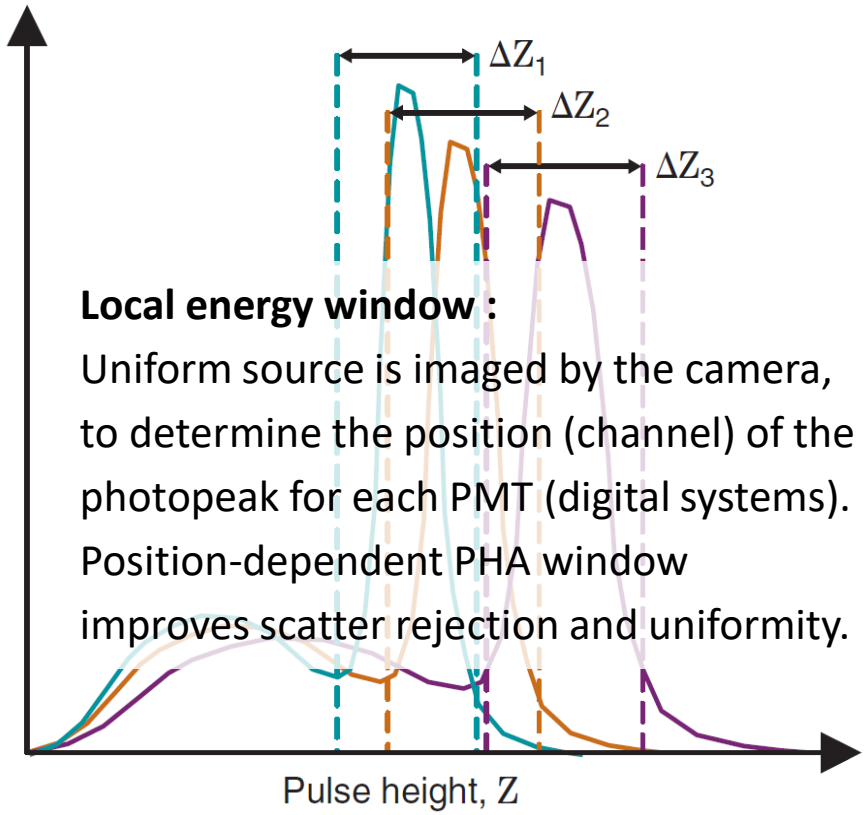

Local energy window :

Uniform source is imaged by the camera, to determine the position (channel) of the photopeak for each PMT (digital systems). Position-dependent PHA window improves scatter rejection and uniformity.

Gamma camera: energy determination → scatter correction

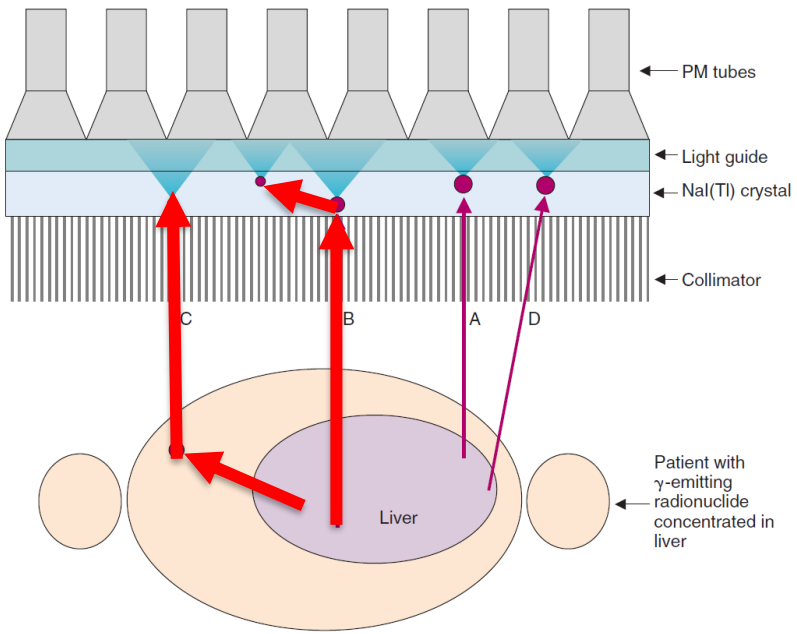

Diffusion, reduced contrast, overestimation of activity.

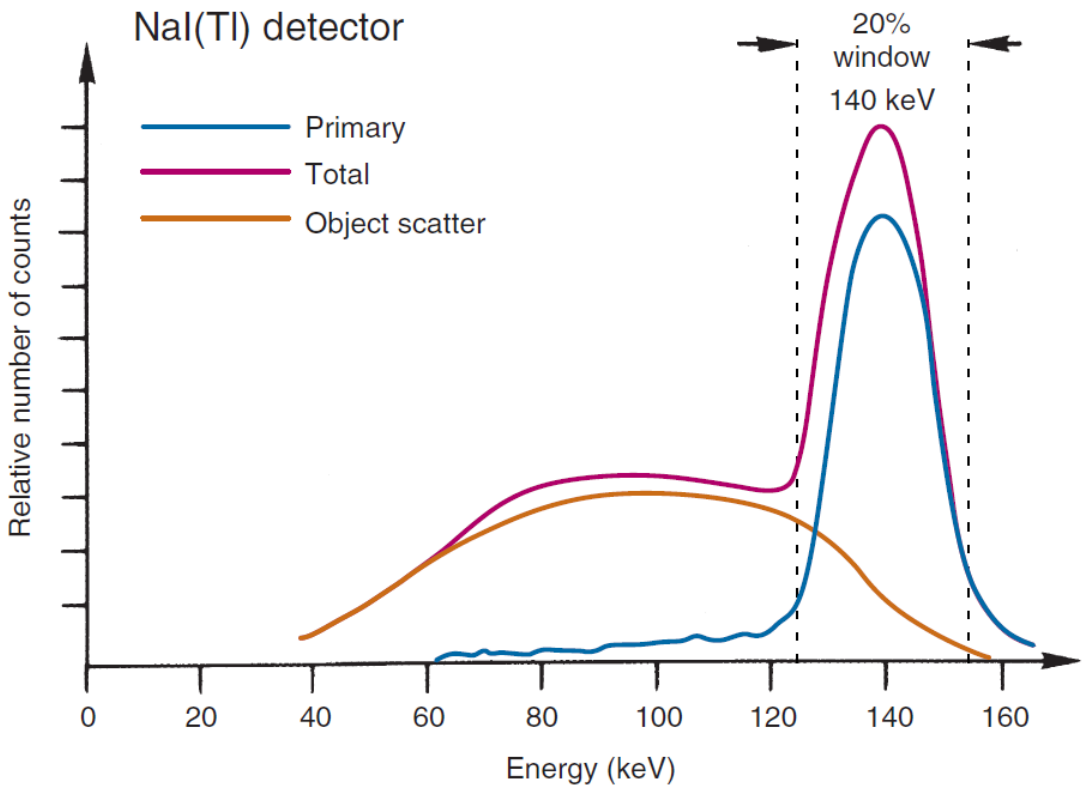

- Two (or more) energy windows: one for scattering and one for the photoelectric peak.
- The goal: to detect only those photons that have not scattered (= deviated from the path).
- For each projection, subtraction of the scattered events that fall into the window of the photopeak.

Gamma camera: energy determination → scatter correction

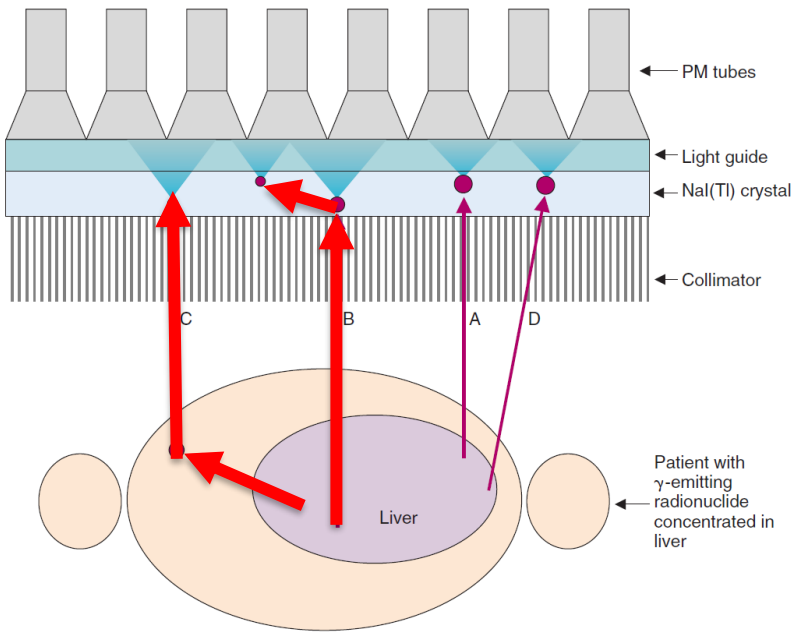

Diffusion, reduced contrast, overestimation of activity.

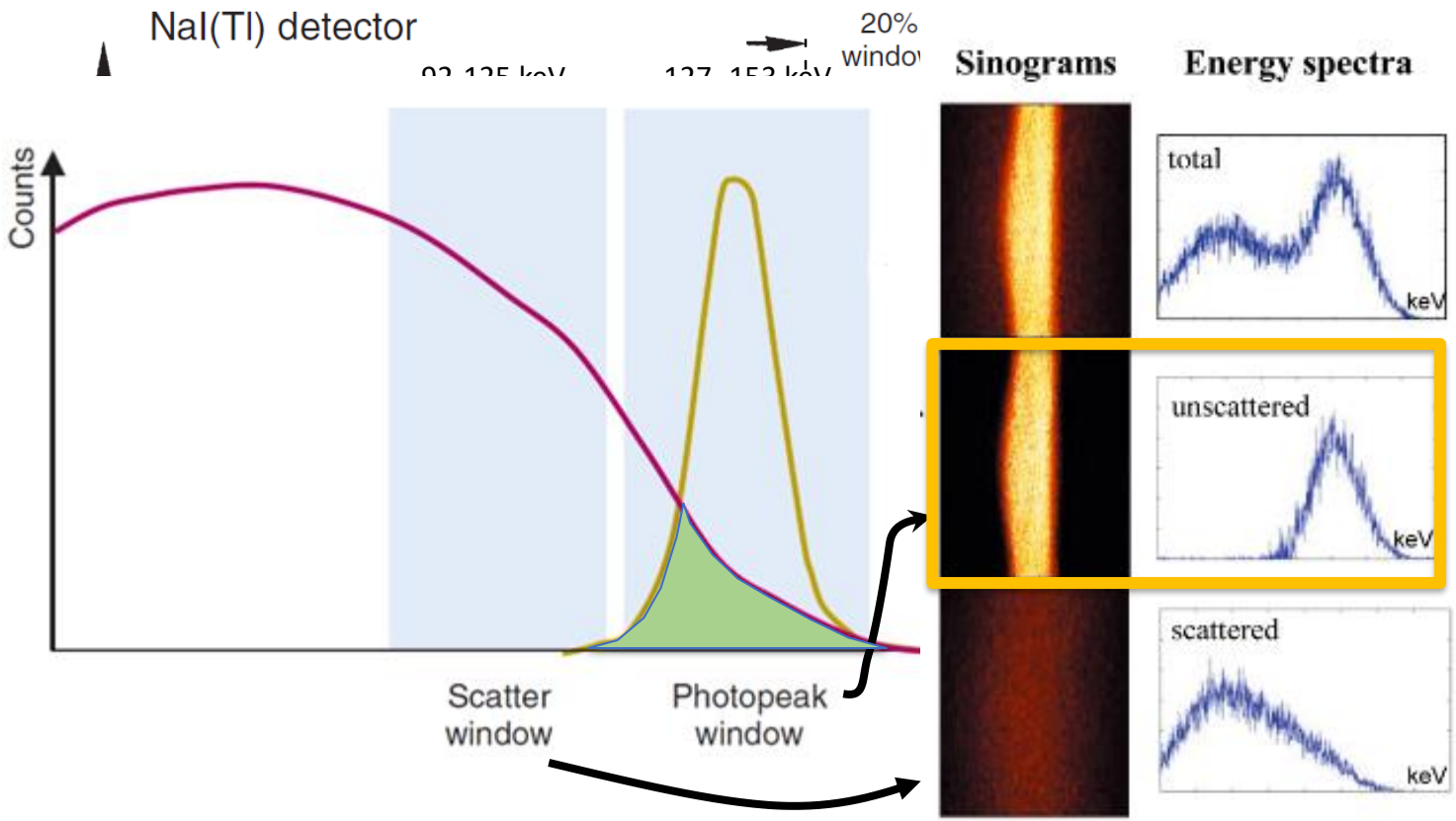

- Two (or more) energy windows: one for scattering and one for the photoelectric peak.
- The goal: to detect only those photons that have not scattered (= deviated from the path).
- For each projection, subtraction of the scattered events that fall into the window of the photopeak.

Spatial resolution

What defines the spatial resolution of an imaging device?

Ability to distinguish two adjacent structures as separate (sharpness/detail).

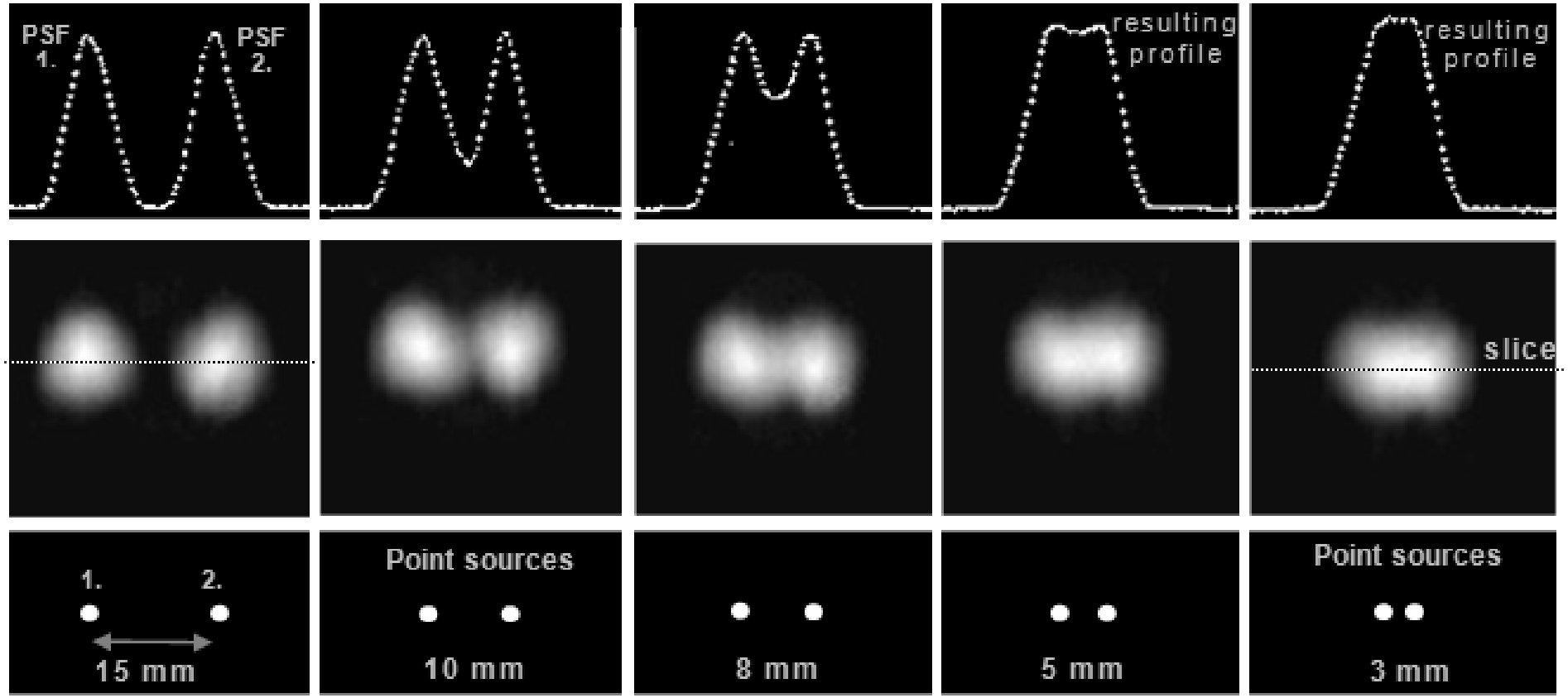

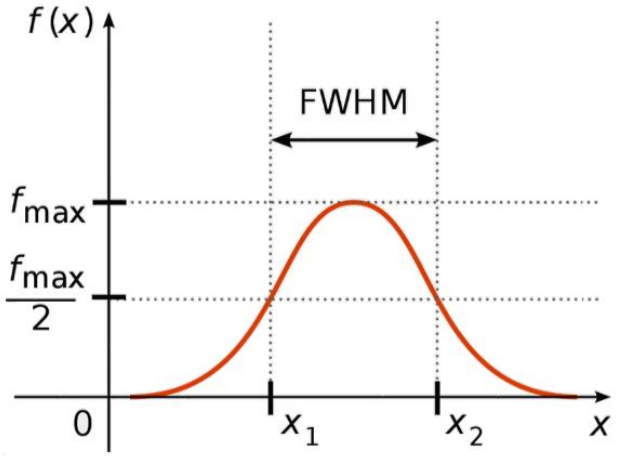

Small FWHM = Better resolution!

Spatial resolution

Intrinsic spatial resolution: achievable by the detector itself and electronics (no collimator). Depends on:

- **γ-ray energy** : low energy γ produce less scintillation photons per event → statistical fluctuations.
- **crystal thickness** : thicker detectors are more efficient in detecting radiation 👍(spoiler), but:
  - Increased light spreading before reaching PMT 👎
  - Greater probability of detecting multiple Compton-scattered events 👎

For modern cameras: ~ **3 – 4.5 mm** (of FWHM for Tc-99m)

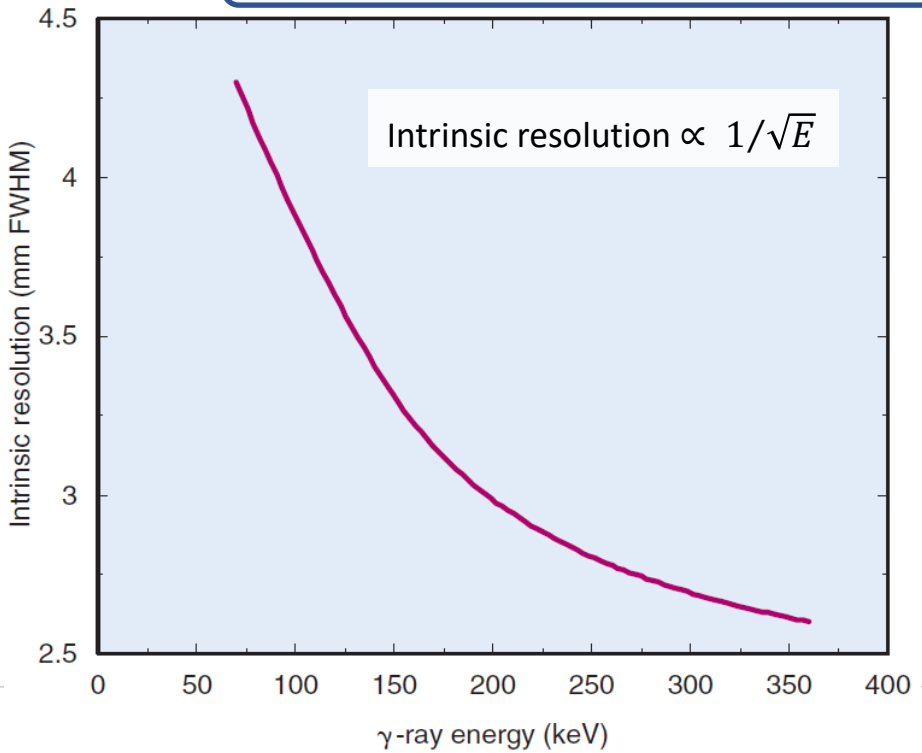

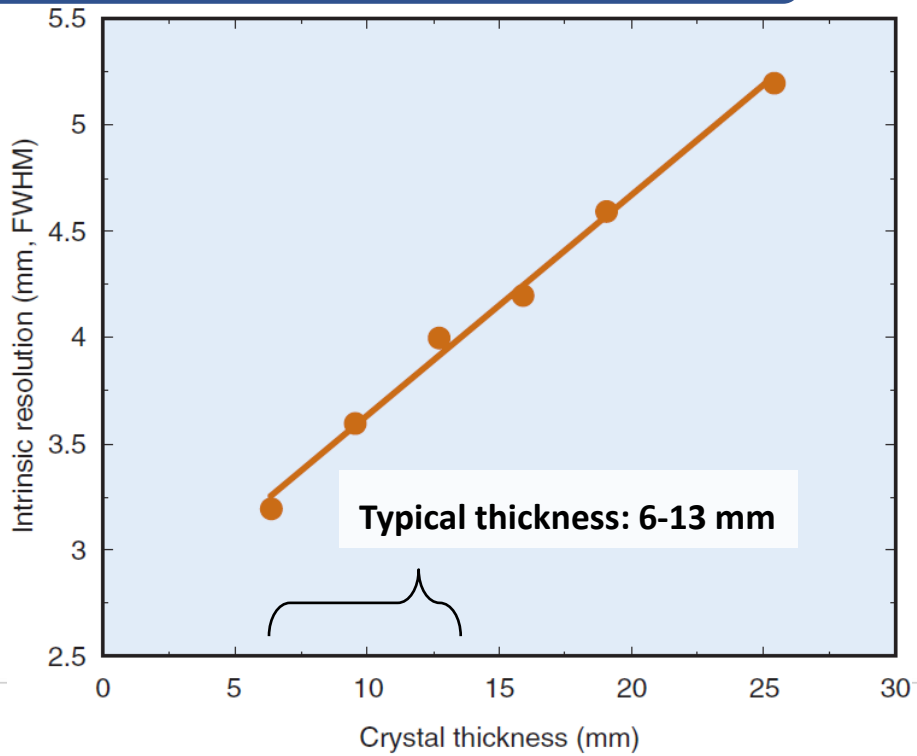

Spatial resolution

Intrinsic spatial resolution: achievable by the detector itself and electronics (no collimator). Depends on:

- **γ-ray energy** : low energy γ produce less scintillation photons per event → statistical fluctuations.
- **crystal thickness** : thicker detectors are more efficient in detecting radiation 👍(spoiler), but:
  - Increased light spreading before reaching PMT 👎
  - Greater probability of detecting multiple Compton-scattered events 👎

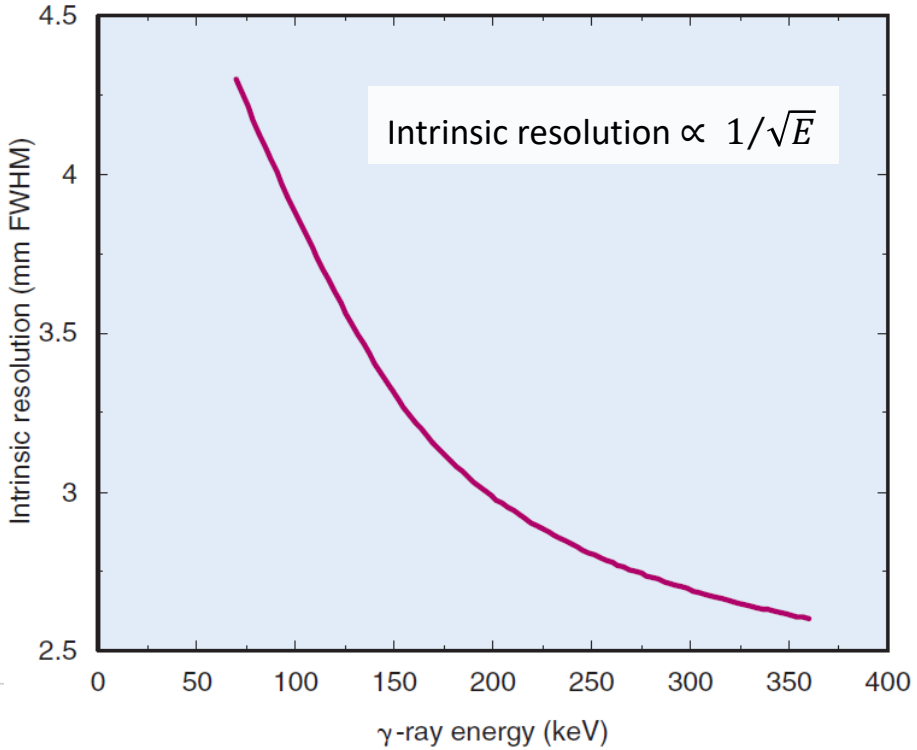

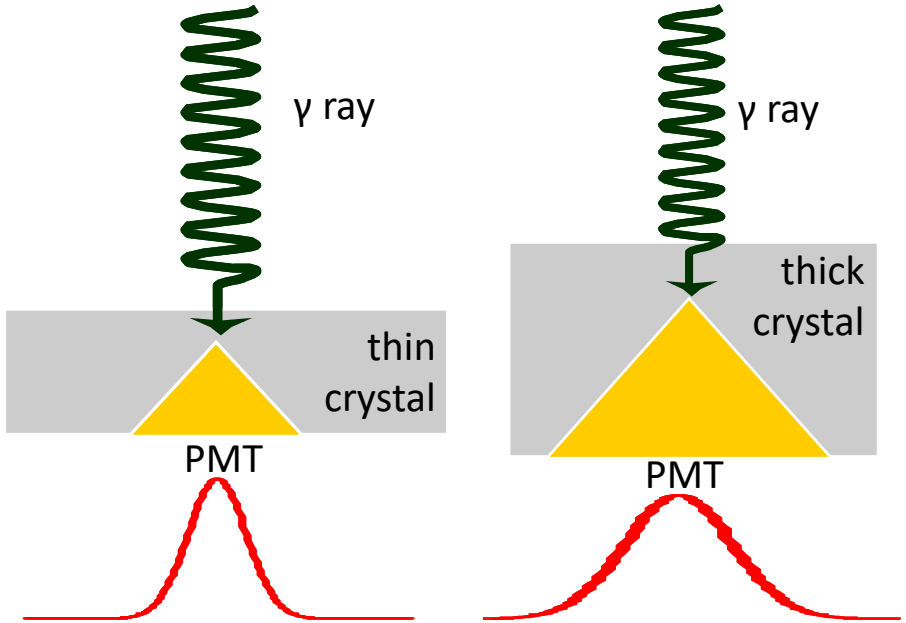

Spatial resolution

<u>Extrinsic</u> spatial resolution : also influenced by linear and angular sampling, reconstruction algorithm (incl. spatial smoothing) and mostly by the *presence of collimators*.

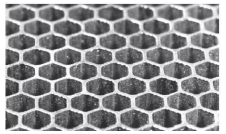

Collimators :

- 👍 improve source distribution localisation by selectively allowing only photons travelling in specific directions to hit the detector (absorptive collimation)
- 👎 degrade spatial resolution (weak link for the camera performance!).

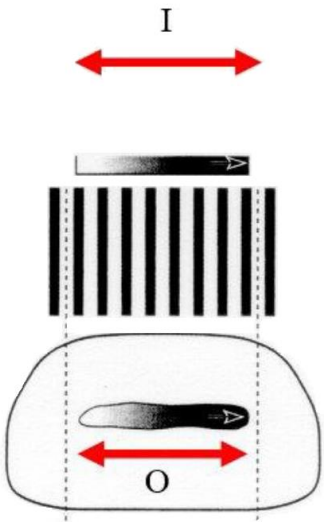

Parallel-hole
Image of the same size and orientation (most common)

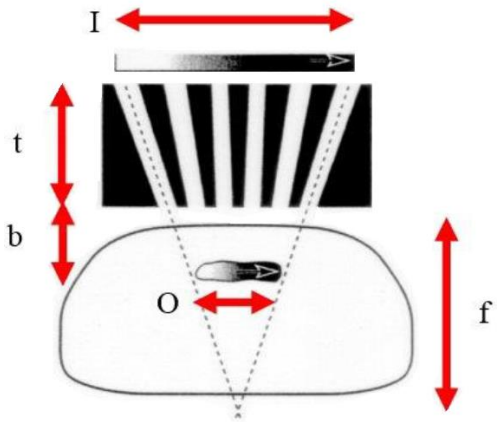

Converging
Noninverted image, generally magnified (for small objects, e.g. thyroid, mice)

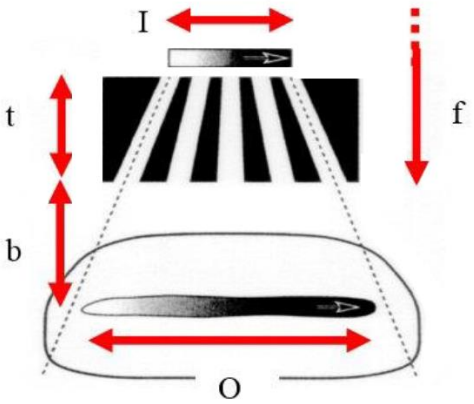

Diverging
Minified, noninverted image (for big objects on small cameras, e.g. liver)

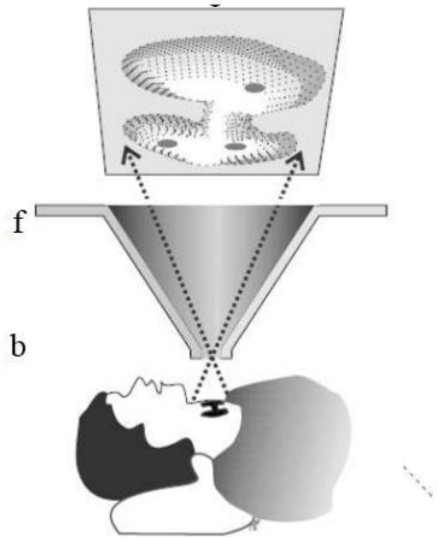

Pinhole
Inverted image, magnified or minified (usually for small objects)

Spatial resolution

<u>Extrinsic</u> spatial resolution : also influenced by linear and angular sampling, reconstruction algorithm (incl. spatial smoothing) and mostly by the *presence of collimators*.

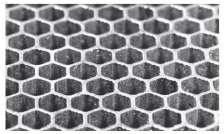

Collimators :

- 👍 improve source distribution localisation by selectively allowing only photons travelling in specific directions to hit the detector (absorptive collimation)
- 👎 degrade spatial resolution (weak link for the camera performance!).

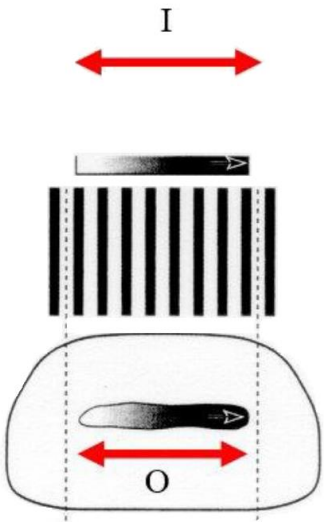

Parallel-hole
Image of the same size and orientation (most common)

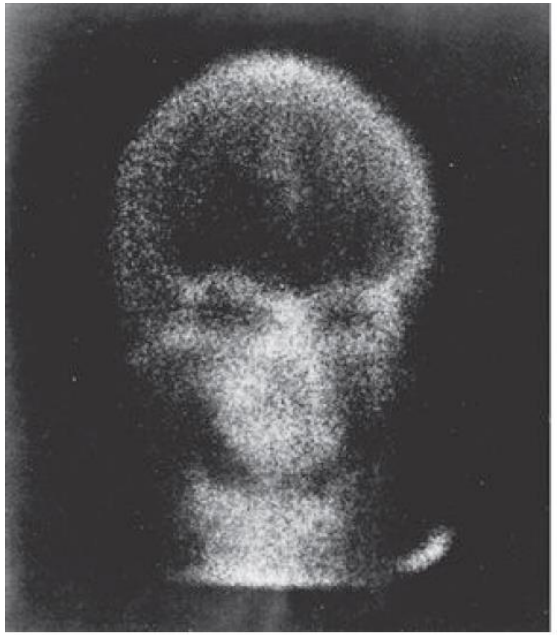

Parallel-hole collimator

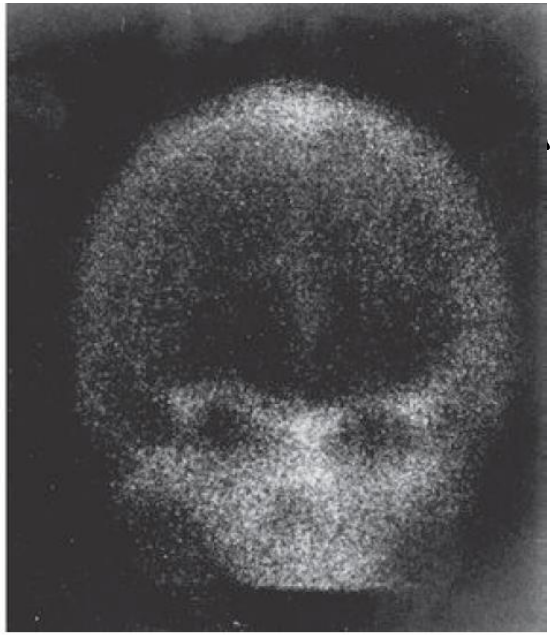

Converging collimator

Spatial resolution

Collimator **efficiency** : fraction of γ striking the collimator that reach the detector.
Collimator **resolution**: sharpness of detail of the object projected on the detector.

Both influenced by **(1) septal penetration** and (2) geometry of the collimator holes:

1) Septal penetration should be reasonably small (< 5%) → thinner septa as possible (better resolution and efficiency) using highly absorbing material (Pb, W, Ta).

⚠ Septa thickness depends on γ energy
→ low- (< 140 keV), medium- (~ 300 keV) & high-energy collimators (> 300 keV) available!

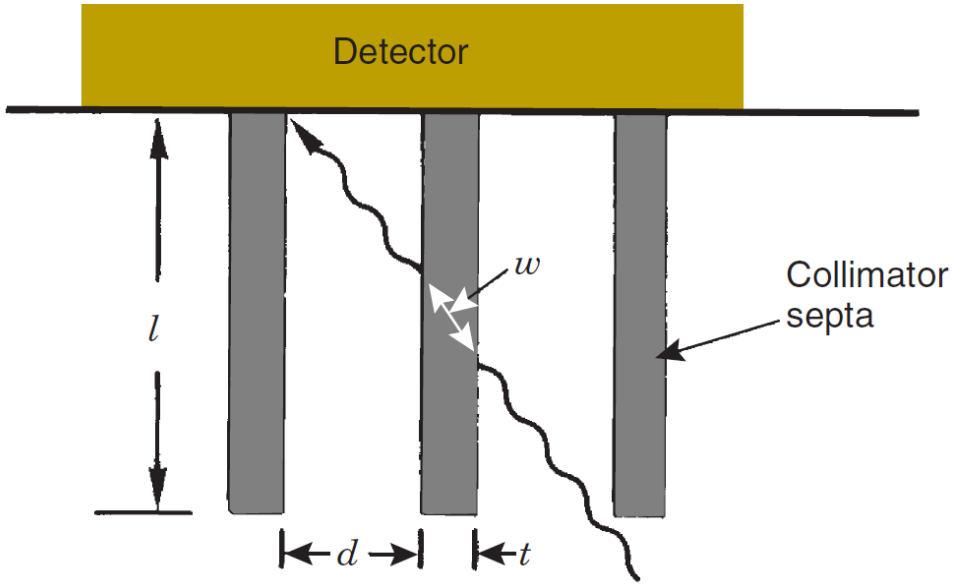

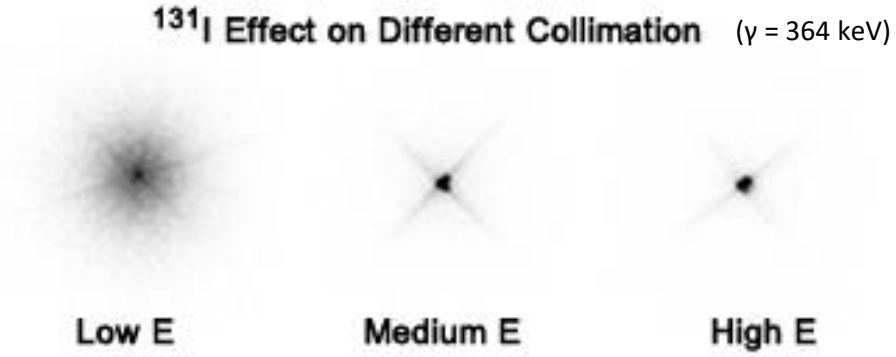

Spatial resolution

Collimator **efficiency** : fraction of γ striking the collimator that reach the detector.
Collimator **resolution**: sharpness of detail of the object projected on the detector.

Both influenced by (1) septal penetration and **(2) geometry** of the collimator holes:

2) Geometry (shape, length, diameter) and distance from the source.

Spatial resolution

Ex: which configuration provides a better spatial resolution?

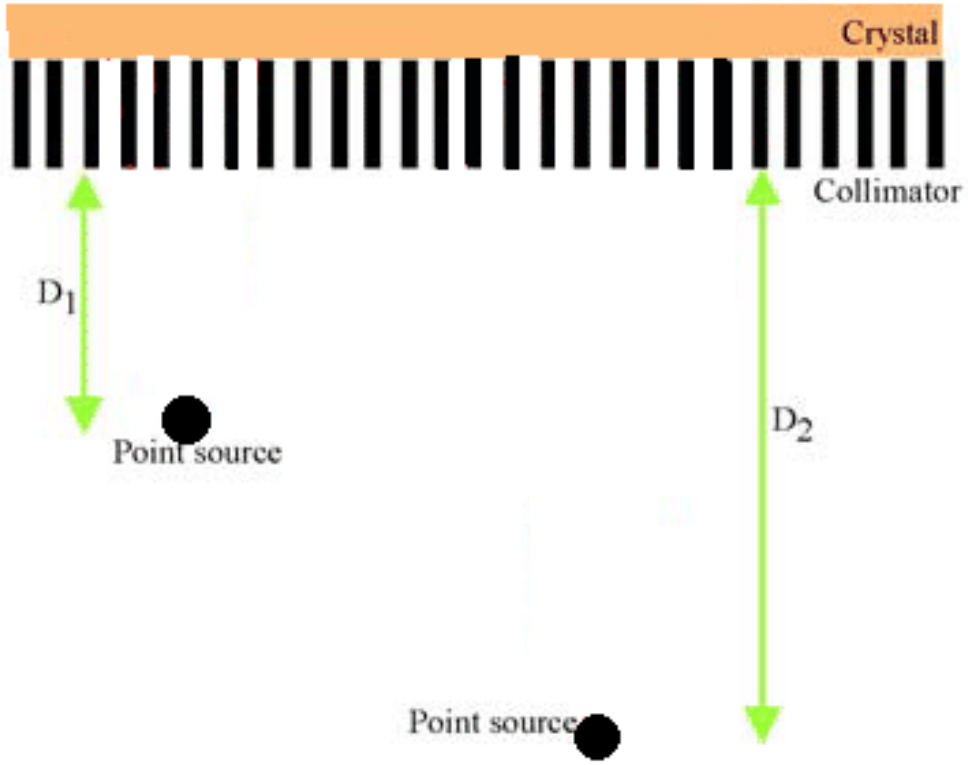

Spatial resolution

Collimator **efficiency** : fraction of γ striking the collimator that reach the detector.
Collimator **resolution**: sharpness of detail of the object projected on the detector.

Both influenced by (1) septal penetration and **(2) geometry** of the collimator holes:

2) Geometry (shape, length, diameter) and distance from the source.

$$R_{coll} \approx d(l+b) \,/\, l$$

Typical R_{coll} ~ **10 mm** (7 – 13 mm)

for a point source @ 10 cm from the collimator surface

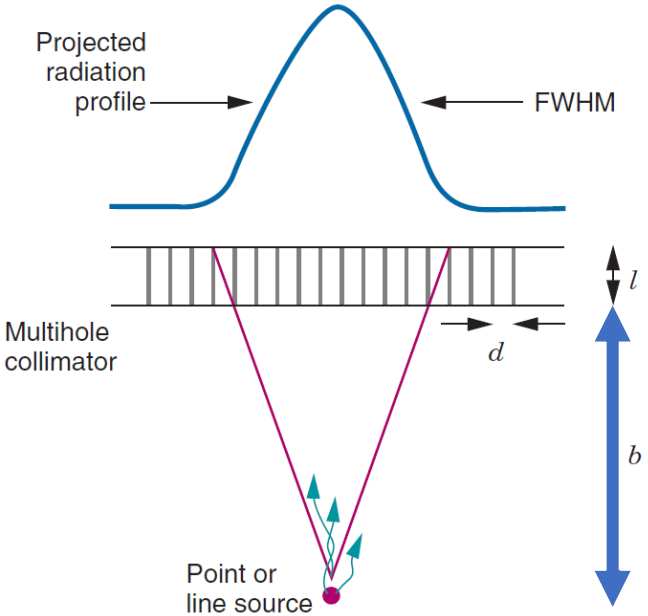

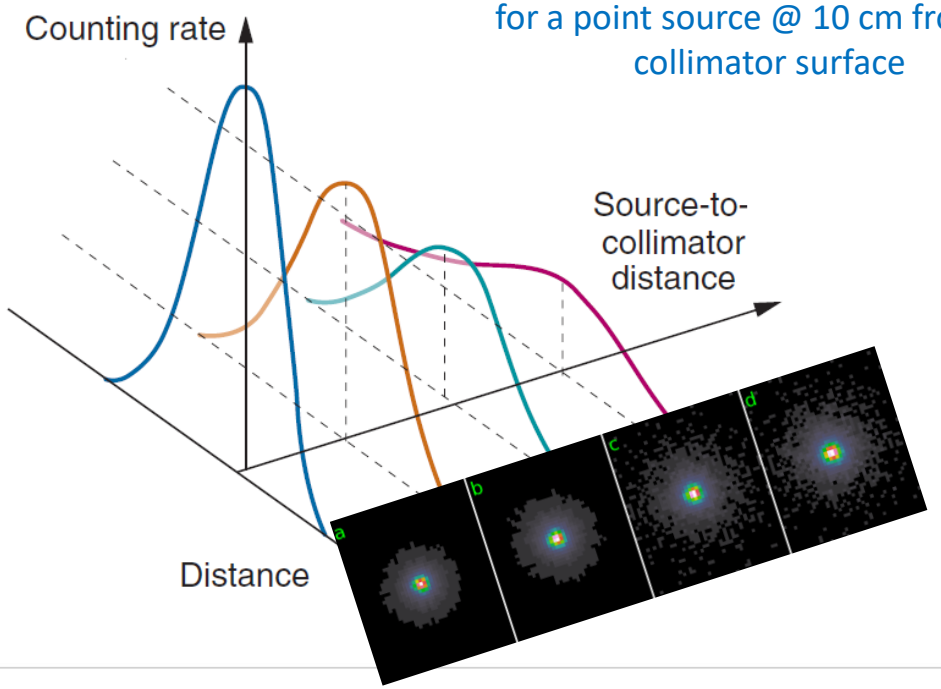

*In equation, l should be the effective length l_{eff} of the collimator holes (slightly smaller than the physical one to take into account the effect of septal penetration, especially higher-energies collimators). Here it is referred as «l» for the sake of simplicity.

Spatial resolution

The gamma camera **total resolution** (or **system** resolution) is mainly influenced by the **intrinsic** resolution (detector and electronics) **and collimator** resolution.

$$R_{sys} = \sqrt{R_{int}^2 + R_{coll}^2}$$

- It provides a metric of the "real" (clinically-significant) resolution.
- It depends on the source-to-collimator distance (R_{coll}).
- For distances of 5-10 cm (typical organ depth), it is governed by R_{coll}.
- It is degraded by scattered radiation.

Q: What is the system resolution of a typical gamma camera ?

$$R_{sys} = \sqrt{(3.5\ mm)^2 + (10\ mm)^2} = 10.6\ mm$$

Finite resolution is partly responsible for partial volume effects :

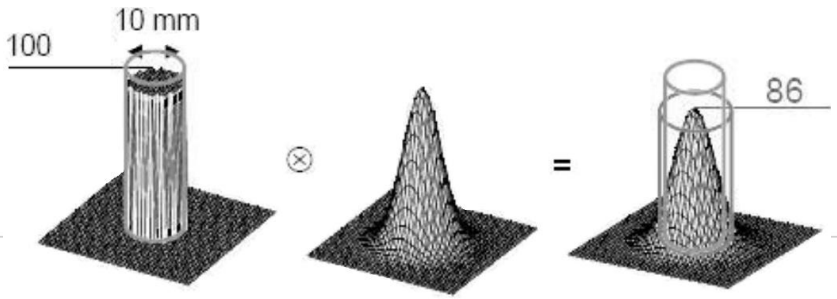

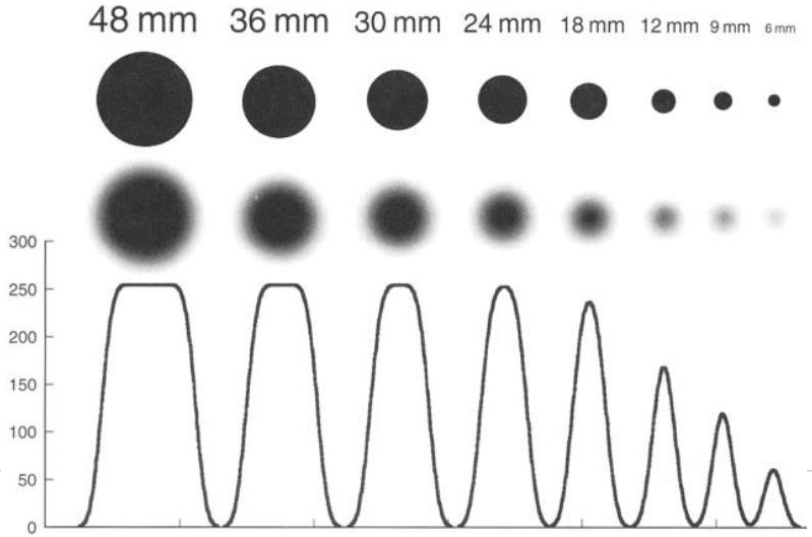

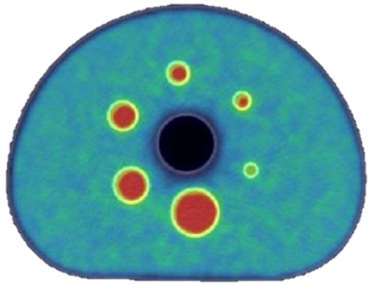

Efficiency

Efficiency: ability to detect incoming radiation. Influenced by **detector** and collimator.

- Thicker detectors have higher intrinsic efficiency (more volume allowing the radiation to deposit energy within the crystal) BUT loss in spatial resolution.
- **Tradeoff**: acceptable detection efficiency and high intrinsic spatial resolution in the energy range of 100 - 200 keV.

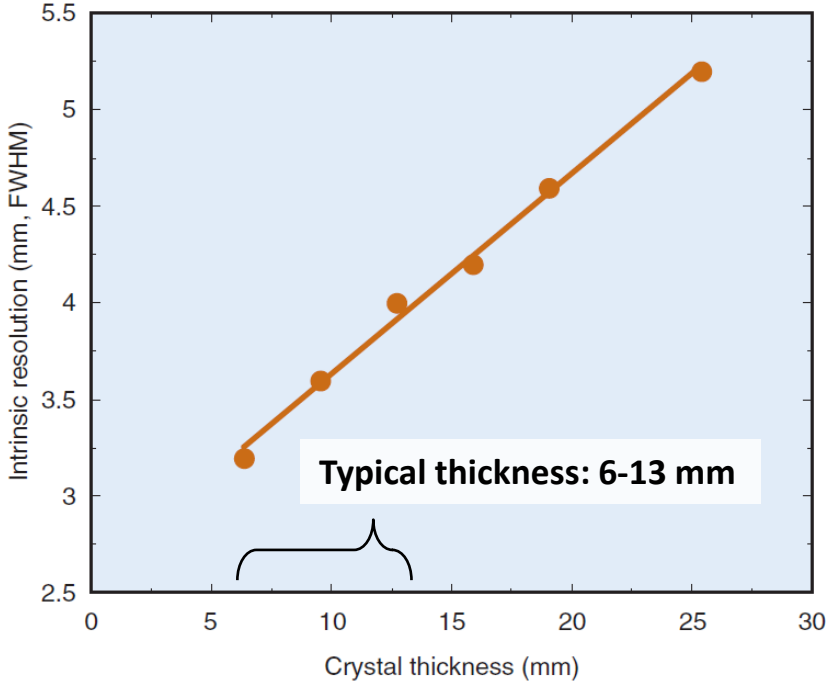

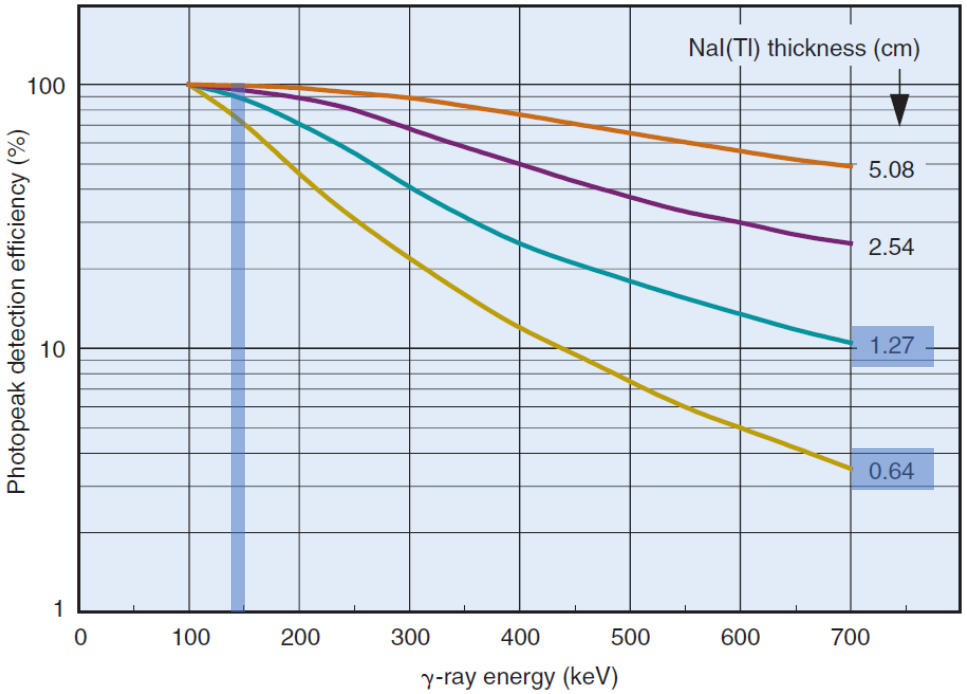

Efficiency

Efficiency: ability to detect incoming radiation. Influenced by detector and **collimator**.

- Fraction of γ rays striking the collimator that pass through it.
- Efficiency (as resolution) is also influenced by the collimator geometry.
- Low-energy collimators have thinner septa and thus increased efficiency.
- **Tradeoff**: high efficiency results in degraded spatial resolution.

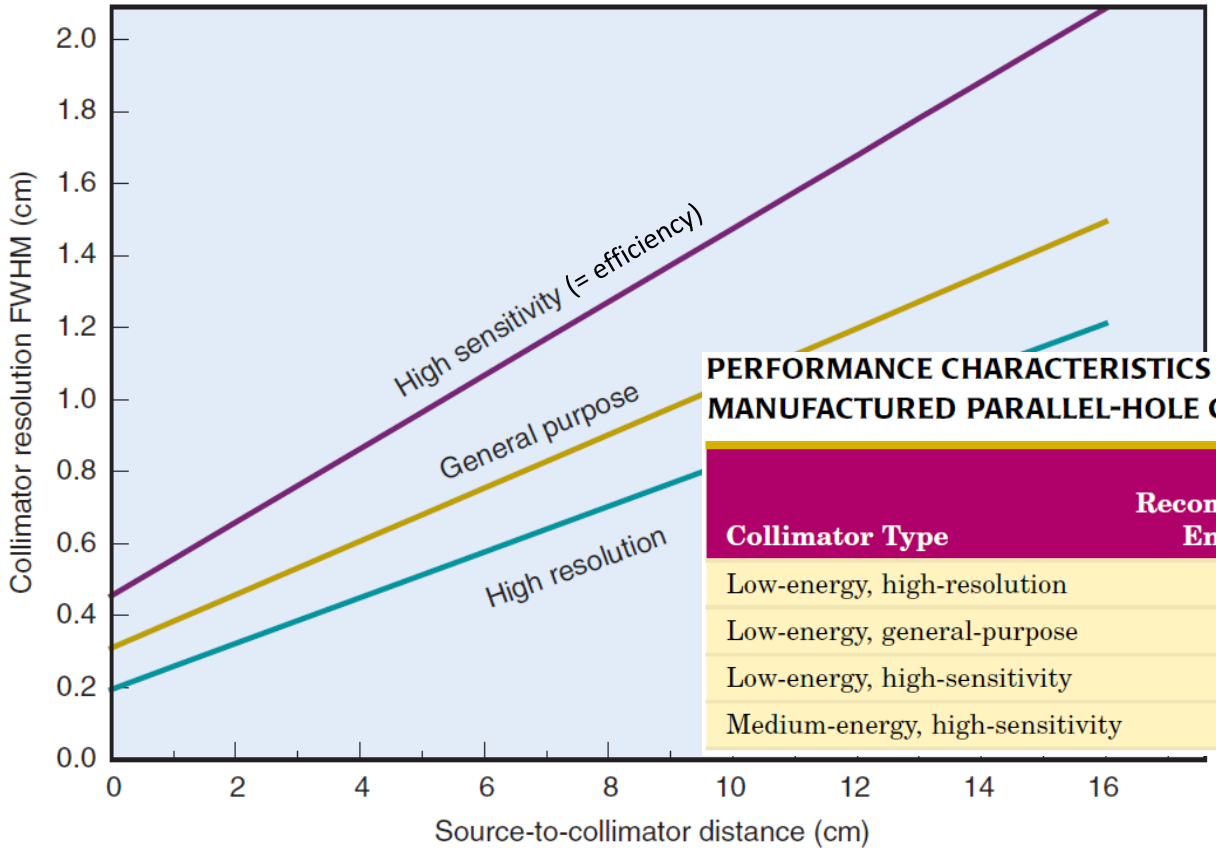

***1 photon out of 10'000**:*
absorptive collimation inherently inefficient!
(cf. with PET next week 😉)

PERFORMANCE CHARACTERISTICS OF SOME TYPICAL COMMERCIALLY MANUFACTURED PARALLEL-HOLE COLLIMATORS

Collimator Type	Recommended Max. Energy (keV)	Efficiency	Resolution R_{coll} (FWHM at 10 cm)
Low-energy, high-resolution	150	1.84×10^{-4}	7.4 mm
Low-energy, general-purpose	150	2.68×10^{-4}	9.1 mm
Low-energy, high-sensitivity	150	5.74×10^{-4}	13.2 mm
Medium-energy, high-sensitivity	400	1.72×10^{-4}	13.4 mm

Spatial resolution & efficiency

The properties of the gamma camera may be either **intrinsic** (due to the detector) or **extrinsic** (due to the influence of the collimators).

*The **collimators are necessary** as they allow for the **correct localisation** of the source distribution within the patient, **but degrade** overall system **efficiency**.*

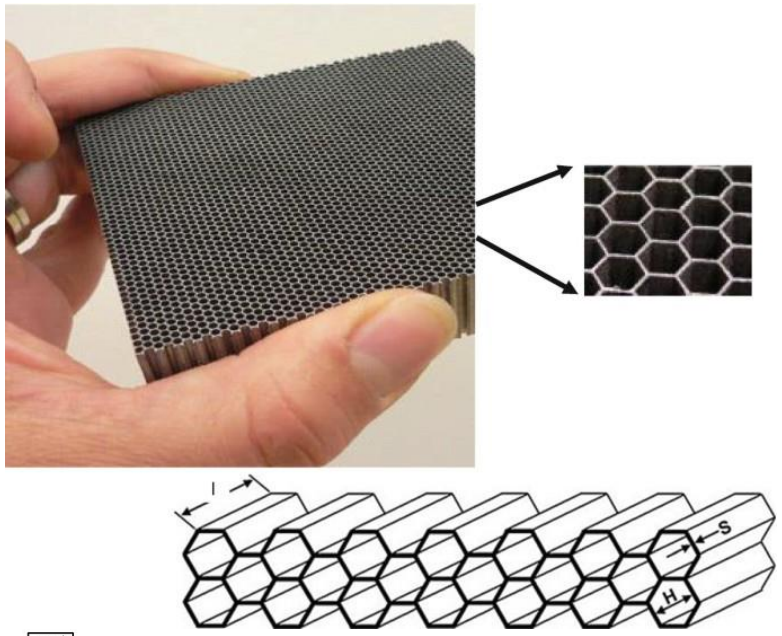

efficiency | **spatial resolution**

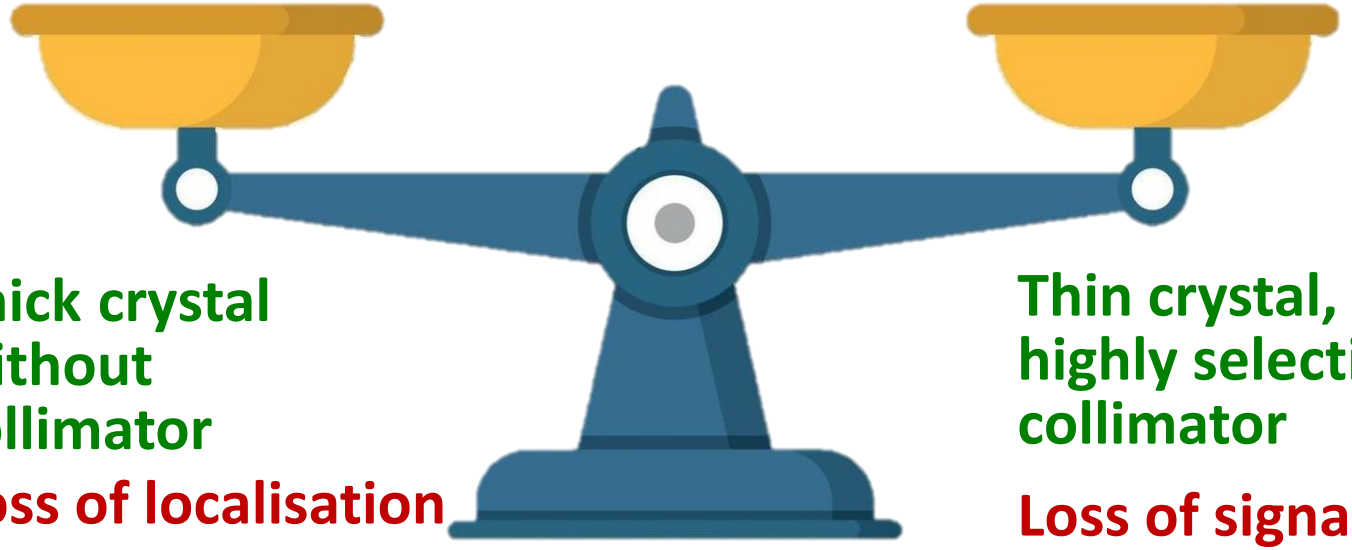

Thick crystal without collimator

Loss of localisation (and spatial resolution)

Thin crystal, highly selective collimator

Loss of signal (loss of efficiency)

From planar scintigraphy to SPECT

- Use the gamma camera detection principle to image activity distribution within the patient.
- **Planar images** can be used for both:
  - **static** studies (activity distribution at a given given time).
  - **dynamic** studies (evolution over time) → e.g. kidney function.

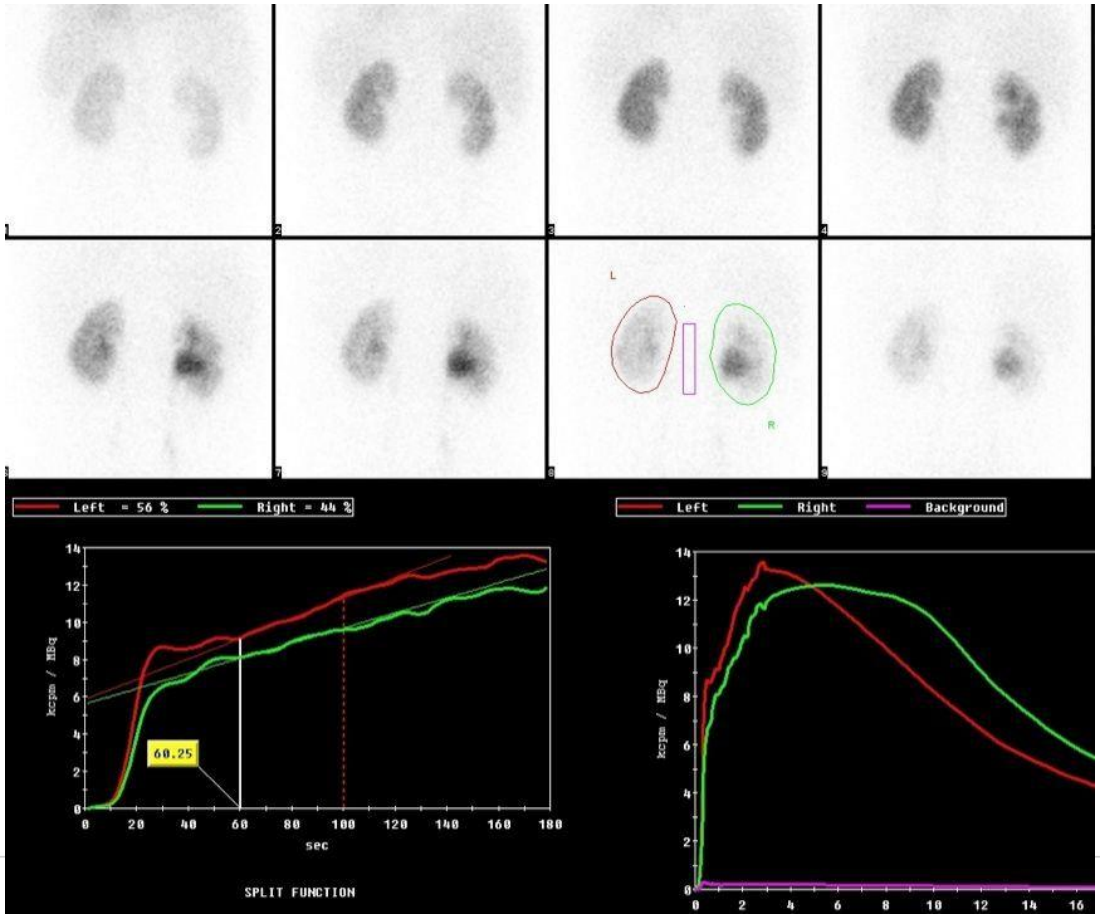

Limitations:

- Signal from overlapping regions
- No 3D information !

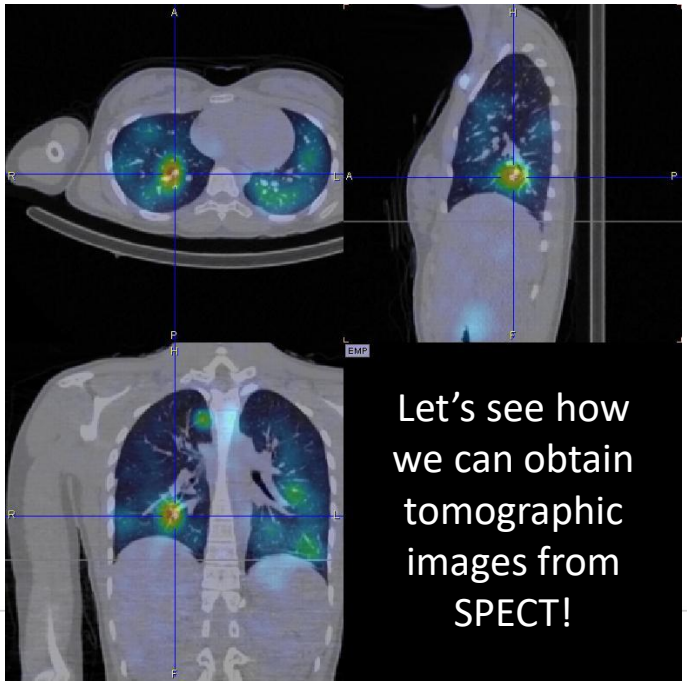

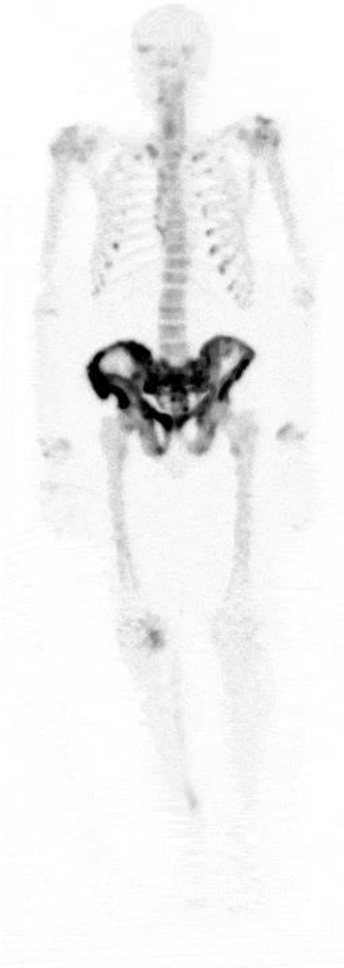

Introduction to tomography in nuclear medicine

CT

TCT: **transmission**
computed tomography

≠

SPECT / PET

ECT: **emission**
computed tomography

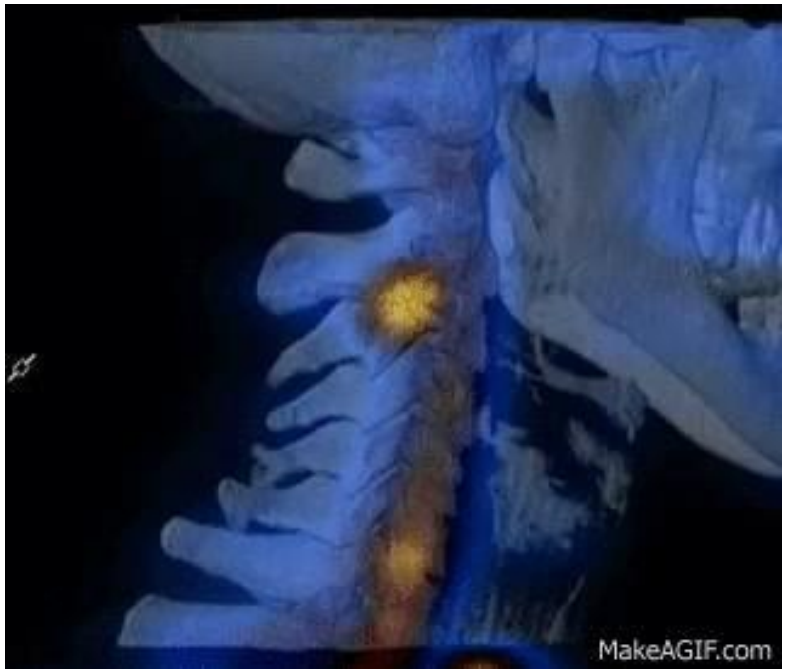

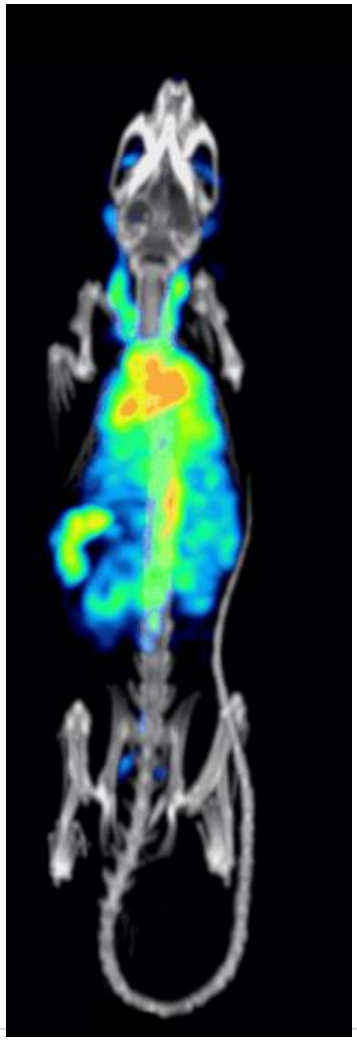

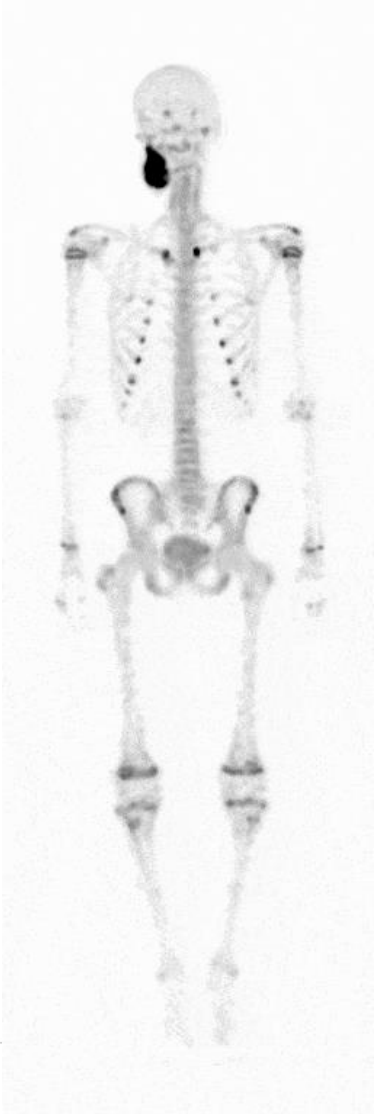

Bases of tomography reconstruction in nuclear medicine

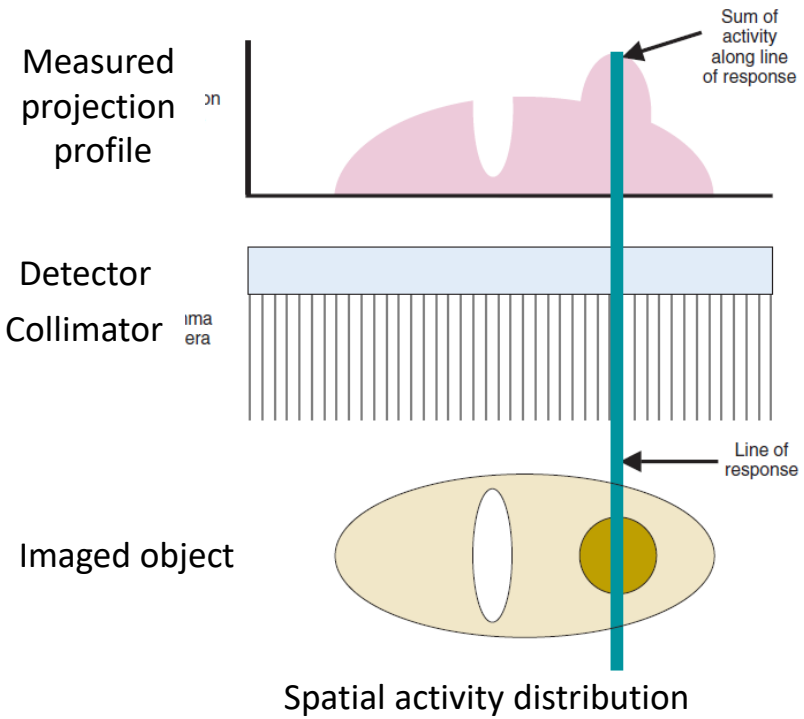

Projections in a simple 1-D detector case

Signal proportional to the summed activity along the line of response (assumption of no attenuation and scatter)

Head rotation around the imaged object

Many projections at different angles are obtained

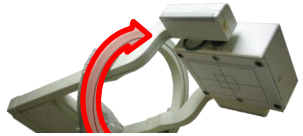

1-D projections of a unknown activity distribution *f(x,y)*

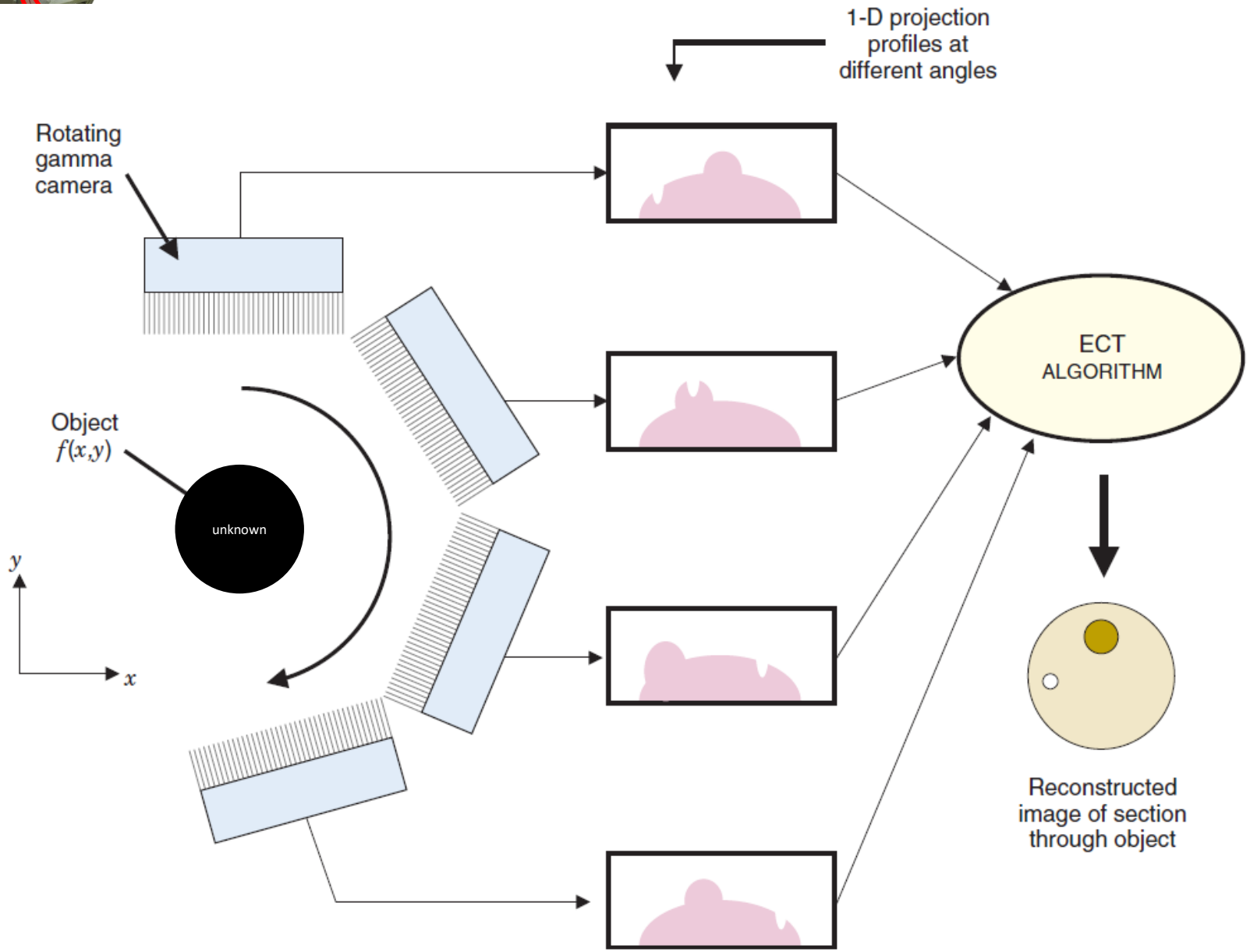

Forward projection

Principle of (forward) projection for one 3×3 slice at angle ϕ= 0 and ϕ = 90°.

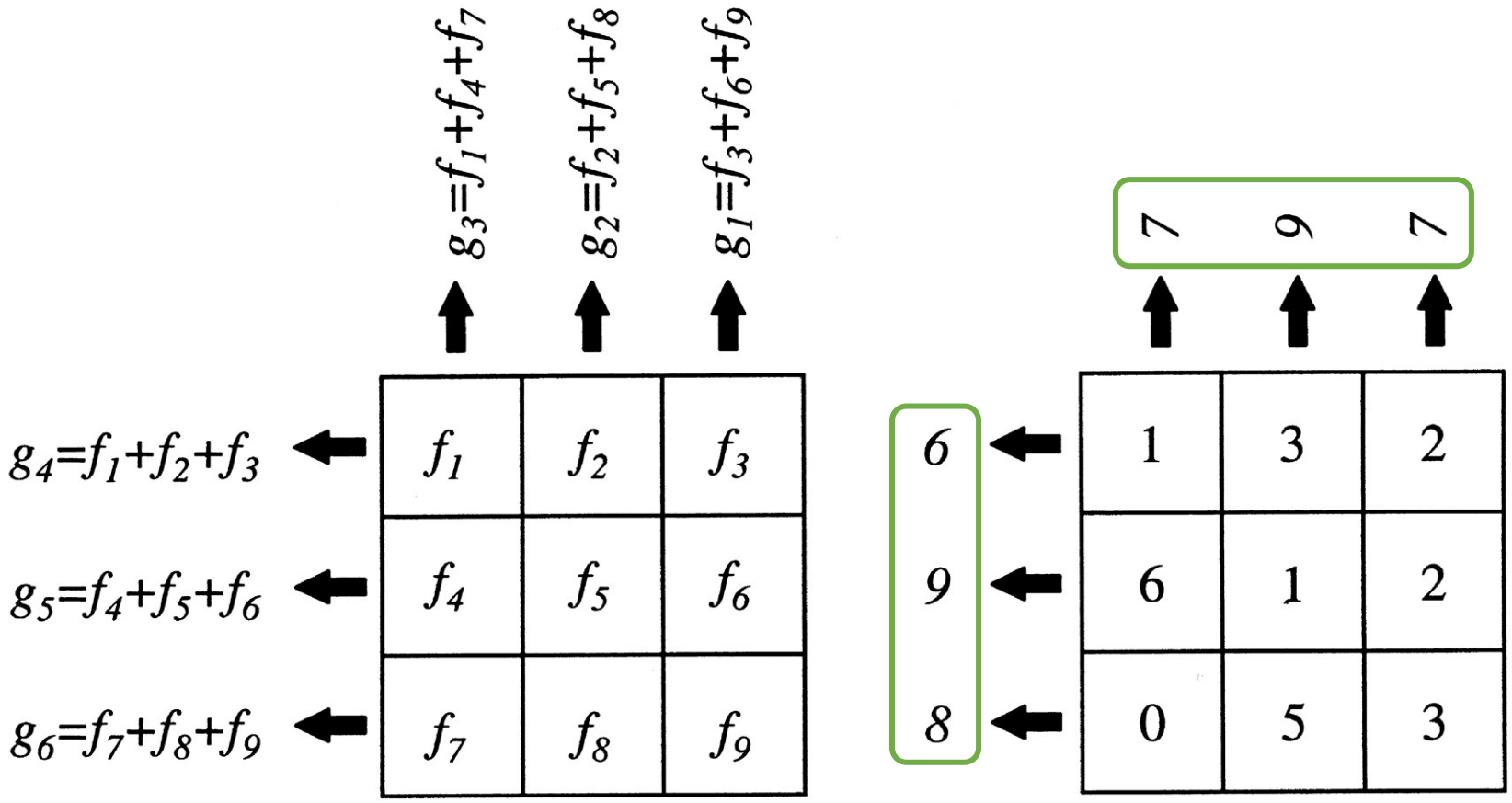

Bruyant et al, JNM, 2002

Forward projection

Principle of (forward) projection for one 3×3 slice at angle ϕ= 0 and ϕ = 90°.

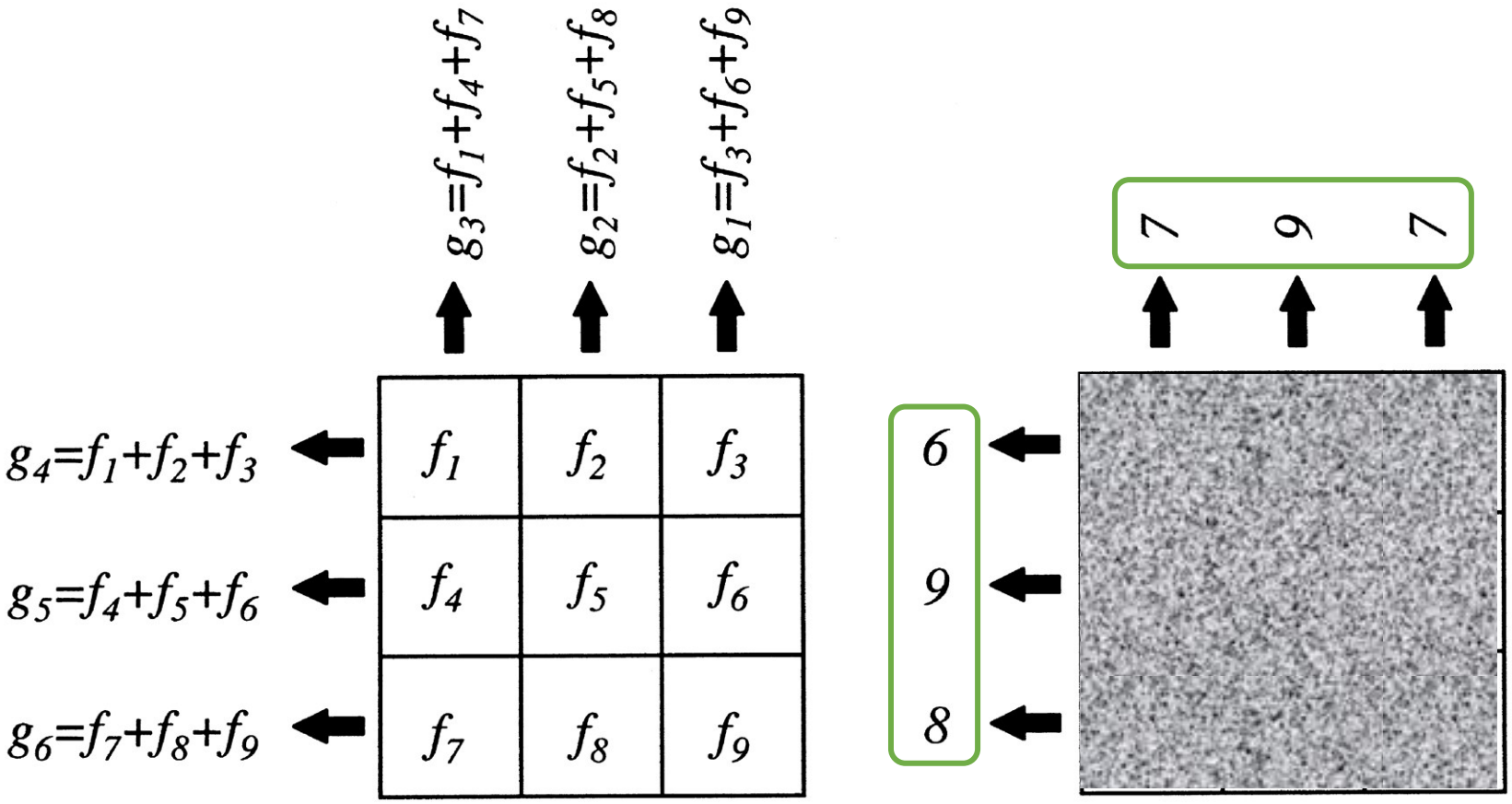

Bruyant et al, JNM, 2002

Obtain an image starting from projections

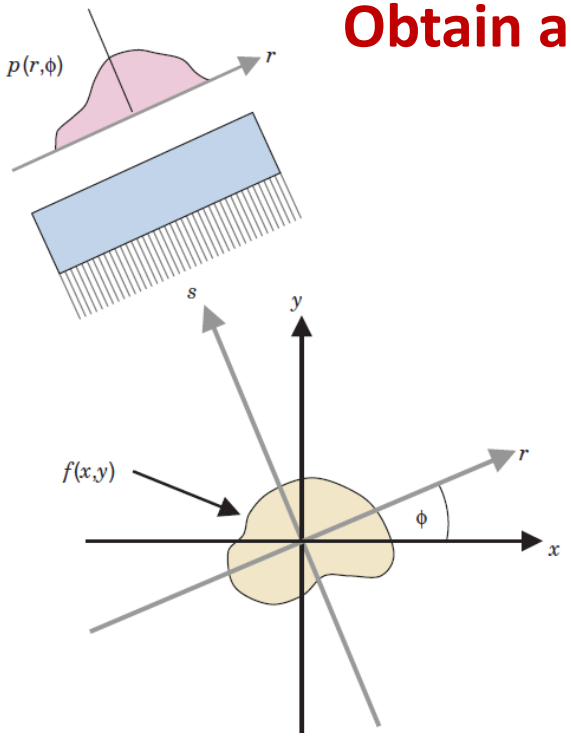

Projection data *p* are arranged in (r, ϕ) coordinate system: tilted of angle ϕ wrt (x,y) and fixed wrt gamma camera

(x,y) → (r,ϕ) } base for **sinogram** representation: set of projection data in the form of a 2D matrix p(r,ϕ)

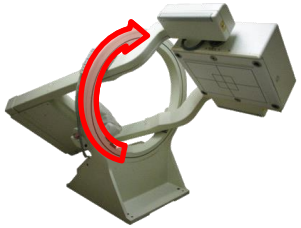

N projections are recorded around the emitting object (0-360 deg)

N projections p(r,ϕ)

Angular spacing is A_s = 360/N deg

Typically A_s = 3 deg for N = 120 projections

Dual-head camera → 60 acquisition steps

15 sec per step → 15 minutes image acquisition

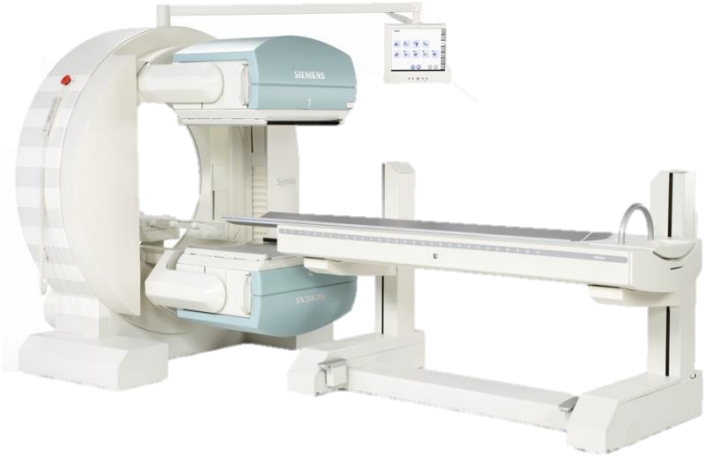

dual-head camera = 2 projections per step

1D Projection data are arranged in a 2D (r,ϕ) **sinogram representation**

Each row (ϕ) in the sinogram displays the intensity profile measured in the corresponding projection

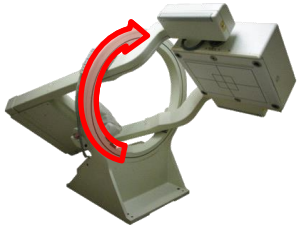

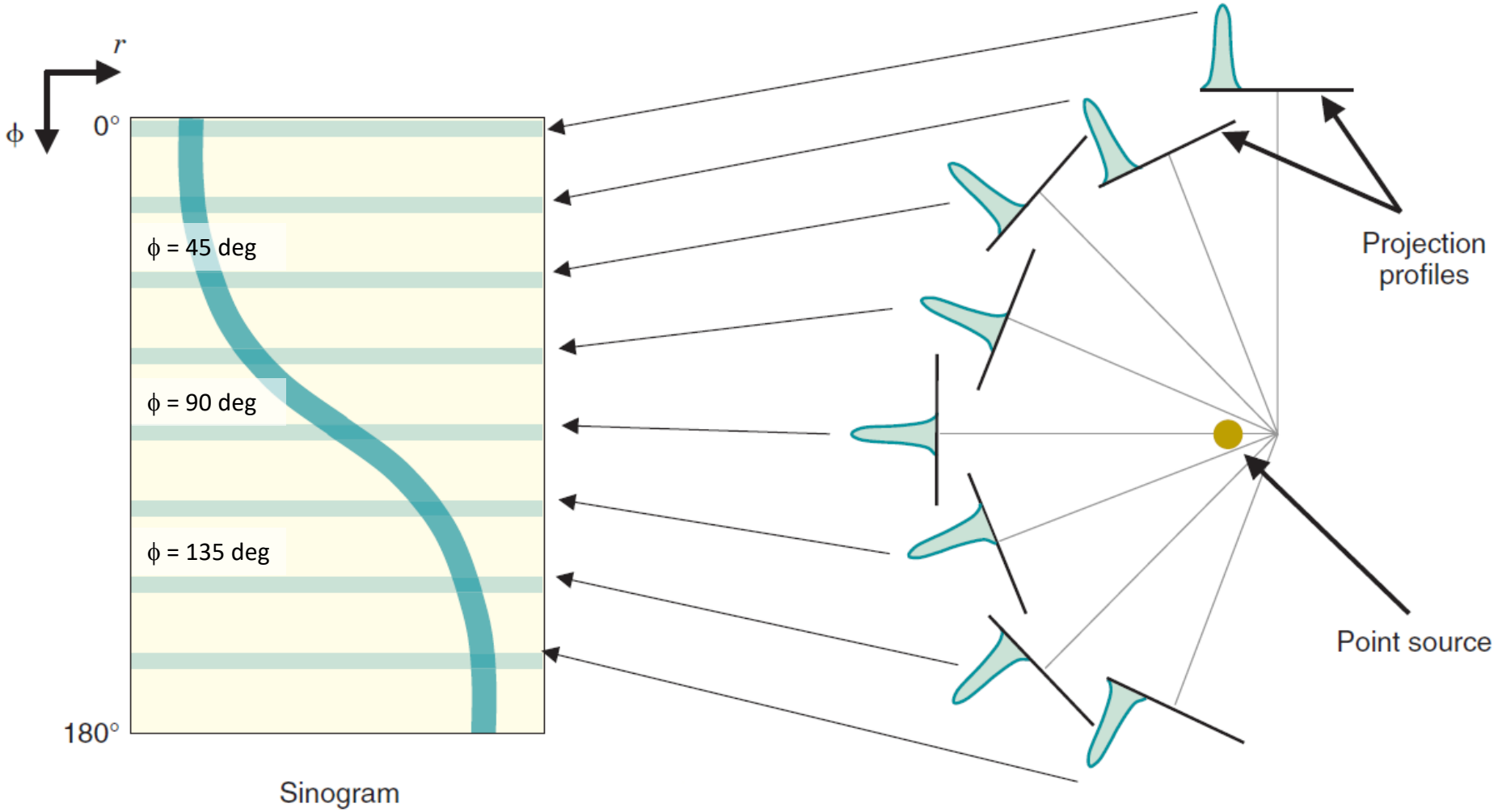

Each **row** (ϕ) corresponds to each projection angle

Each **column** (r) corresponds to the position on the camera

1 slice = N projections ↔ N angular samples ↔ N sinogram lines

1D Projection data are arranged in a 2D (r,ϕ) **sinogram representation**

Each row (ϕ) in the sinogram displays the intensity profile measured in the corresponding projection

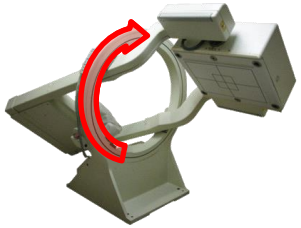

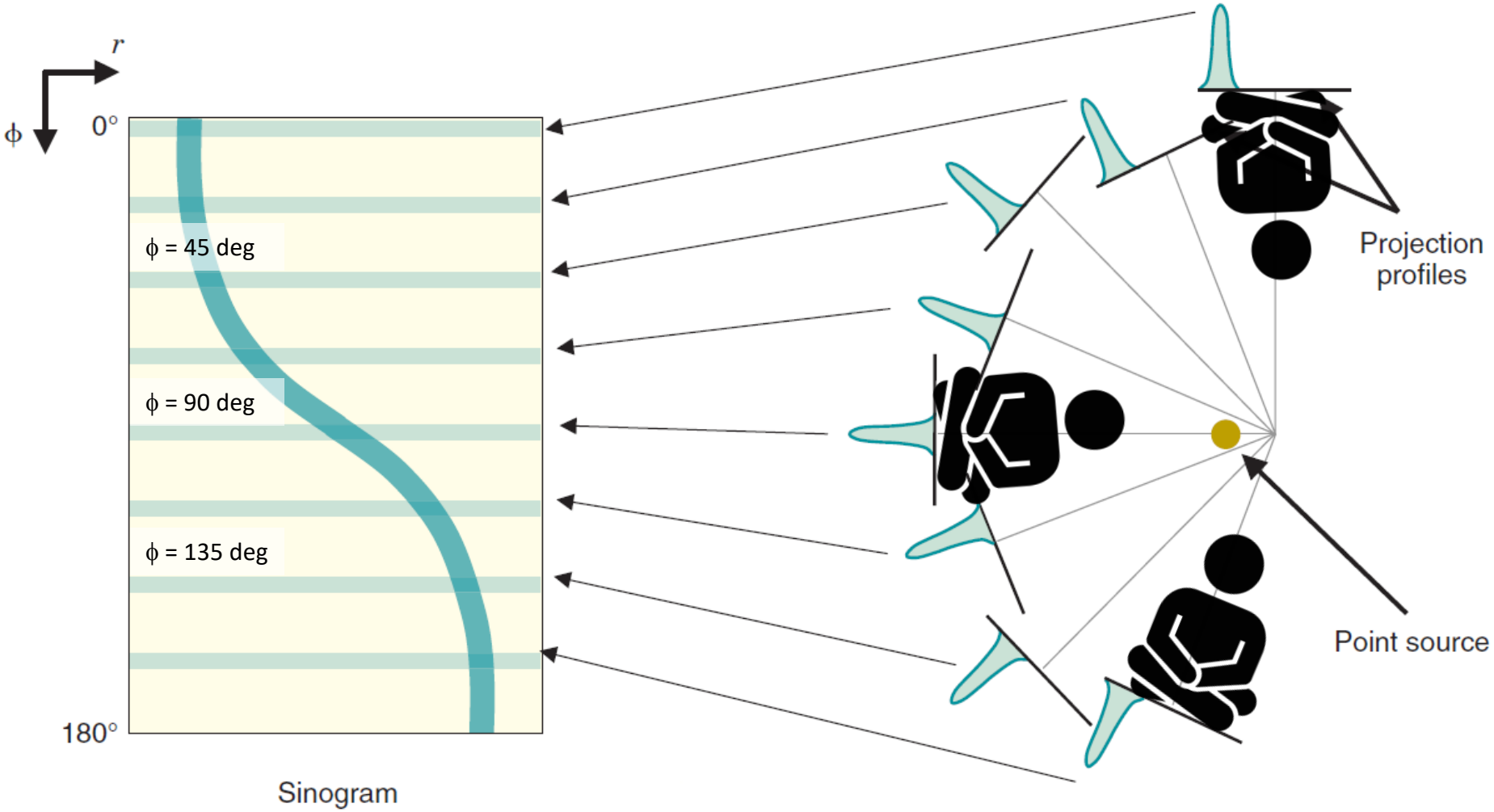

Each **row** (ϕ) corresponds to each projection angle

Each **column** (r) corresponds to the position on the camera

1 slice = N projections ↔ N angular samples ↔ N sinogram lines

1D Projection data are arranged in a 2D (r,ϕ) **sinogram representation**

Each row (ϕ) in the sinogram displays the intensity profile measured in the corresponding projection

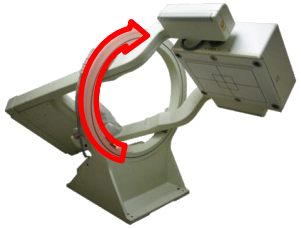

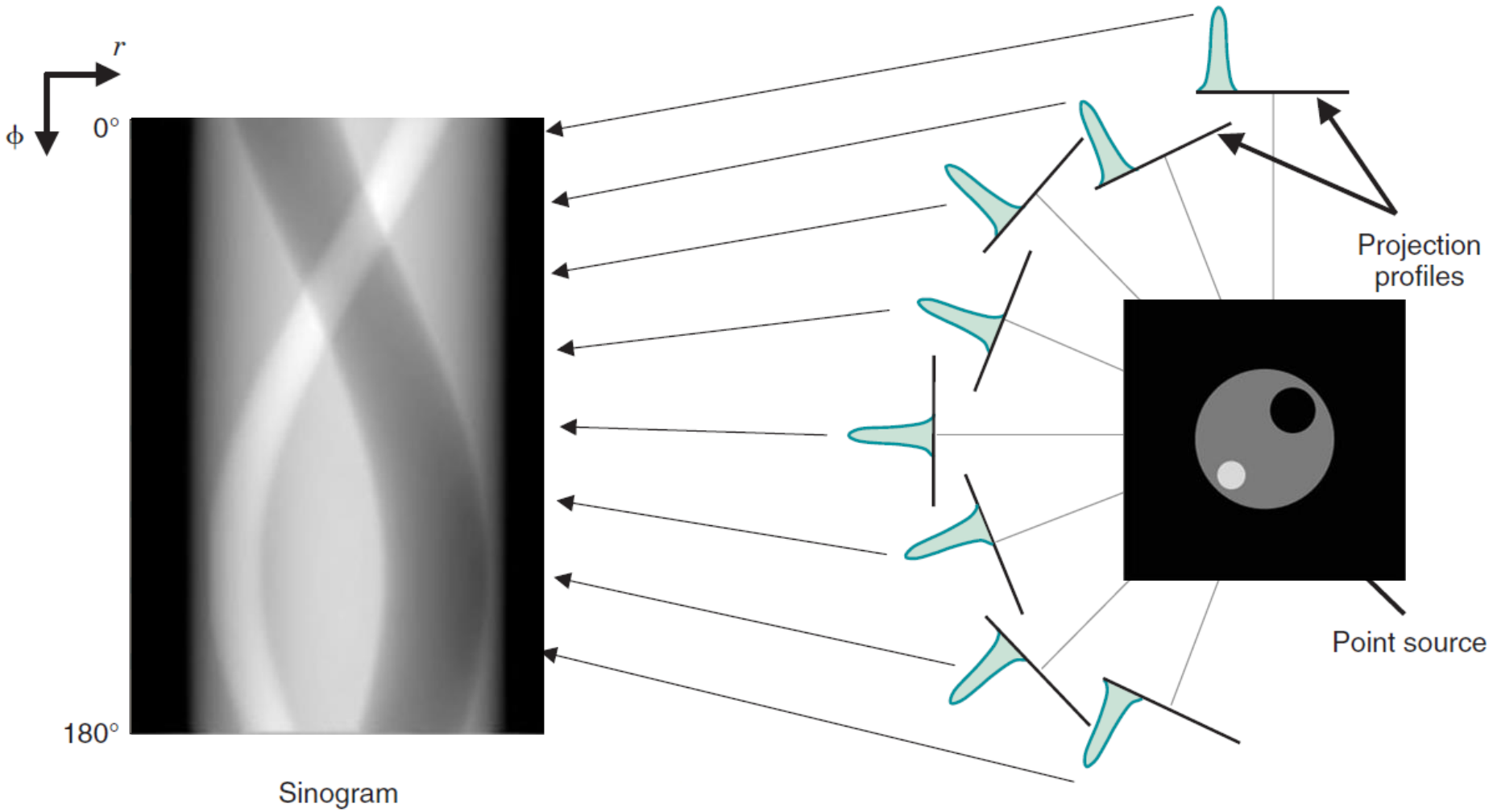

Each **row** (ϕ) corresponds to each projection angle

Each **column** (r) corresponds to the position on the camera

each slice has its own sinogram

1 slice = N projections ↔ N angular samples ↔ N sinogram lines

Reconstruction

What we have:
a discrete number of measured projections p(r,ϕ) arranged in a sinogram

What we want: Recover the unknown (true) activity distribution f(x,y) !

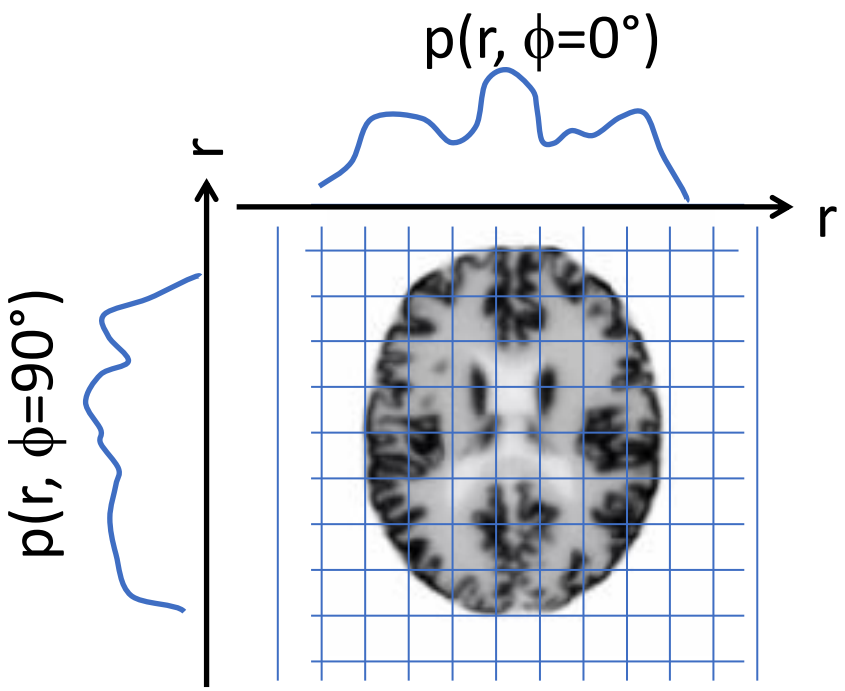

By reconstructing our image, we can access the activity distribution f'(x,y) in a 2D plane of discrete pixels.

Matrix dimension in SPECT is typically 128 x 128

Simple backprojection

the unknown activity distribution is reconstructed by spreading the measured intensity back across the (pixelized/finite) construction plane.

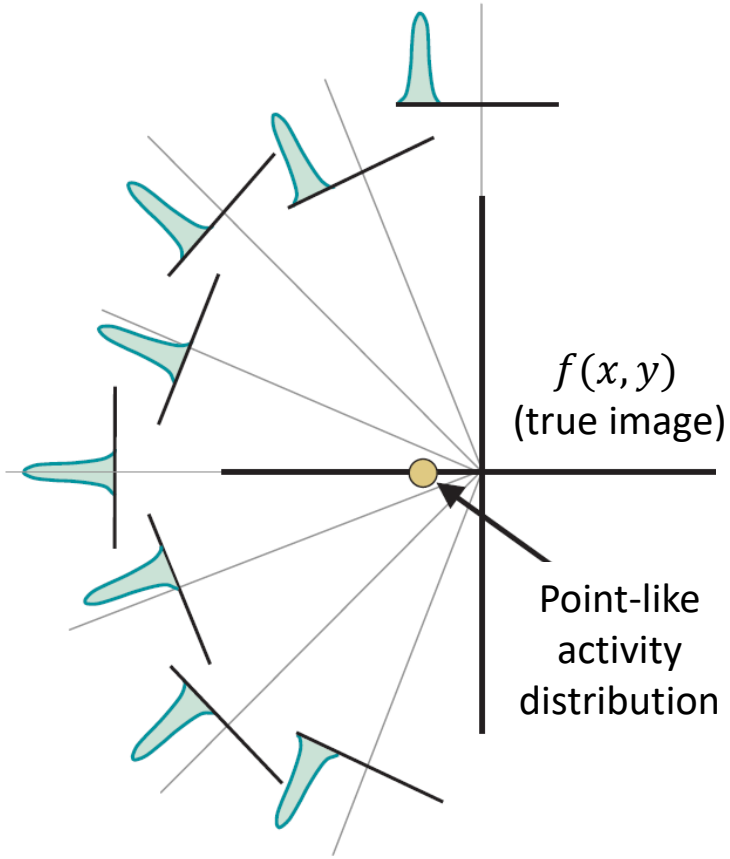

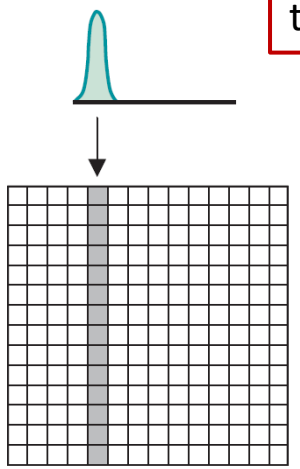

Backprojection of intensity profile at ϕ = 0° across the reconstruction plane

Backprojection after

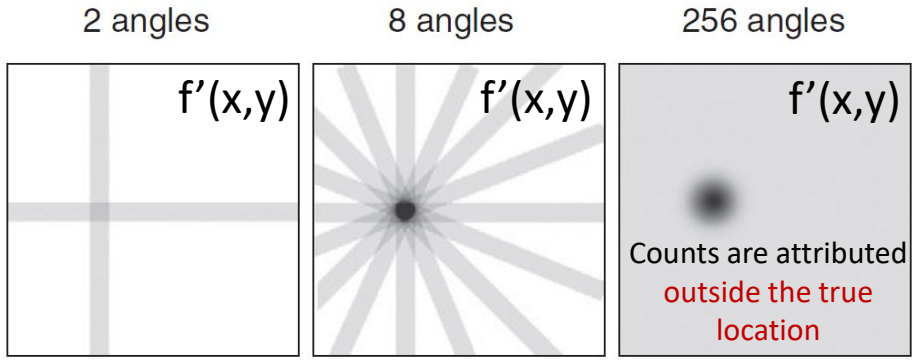

Simple backprojection results in a blurred reconstructed image

1/r blurring

(blurring reduces radially from the centre of the source)

$$f'(x, y) = f(x, y) * (1/r)$$

reconstructed source distribution

original (true) source distribution

Simple backprojection

the unknown activity distribution is reconstructed by spreading the measured intensity back across the (pixelized/finite) construction plane.

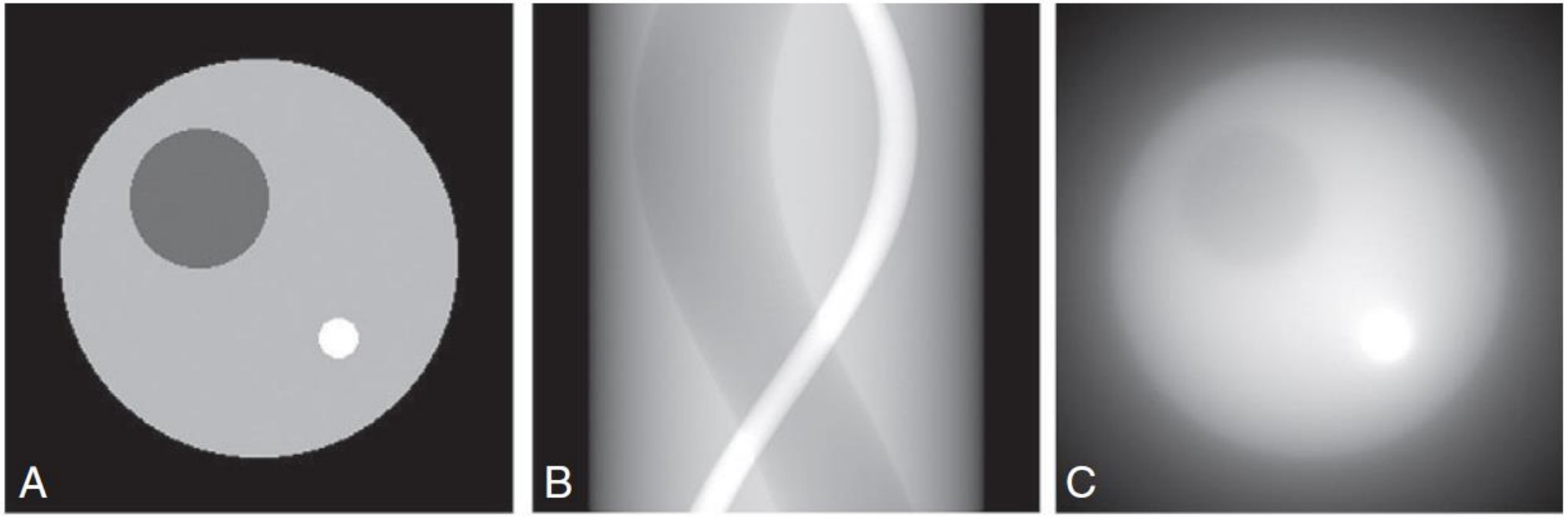

Phantom to test reconstruction algorithms (simulated).

Simulated sinogram (256 projection angles).

Simple backprojection reconstruction.

1/r blurring
- degradation of sharper details (edges).
- degradation of contrast.

Simple backprojection

Simple backprojection of an activity distribution in brain

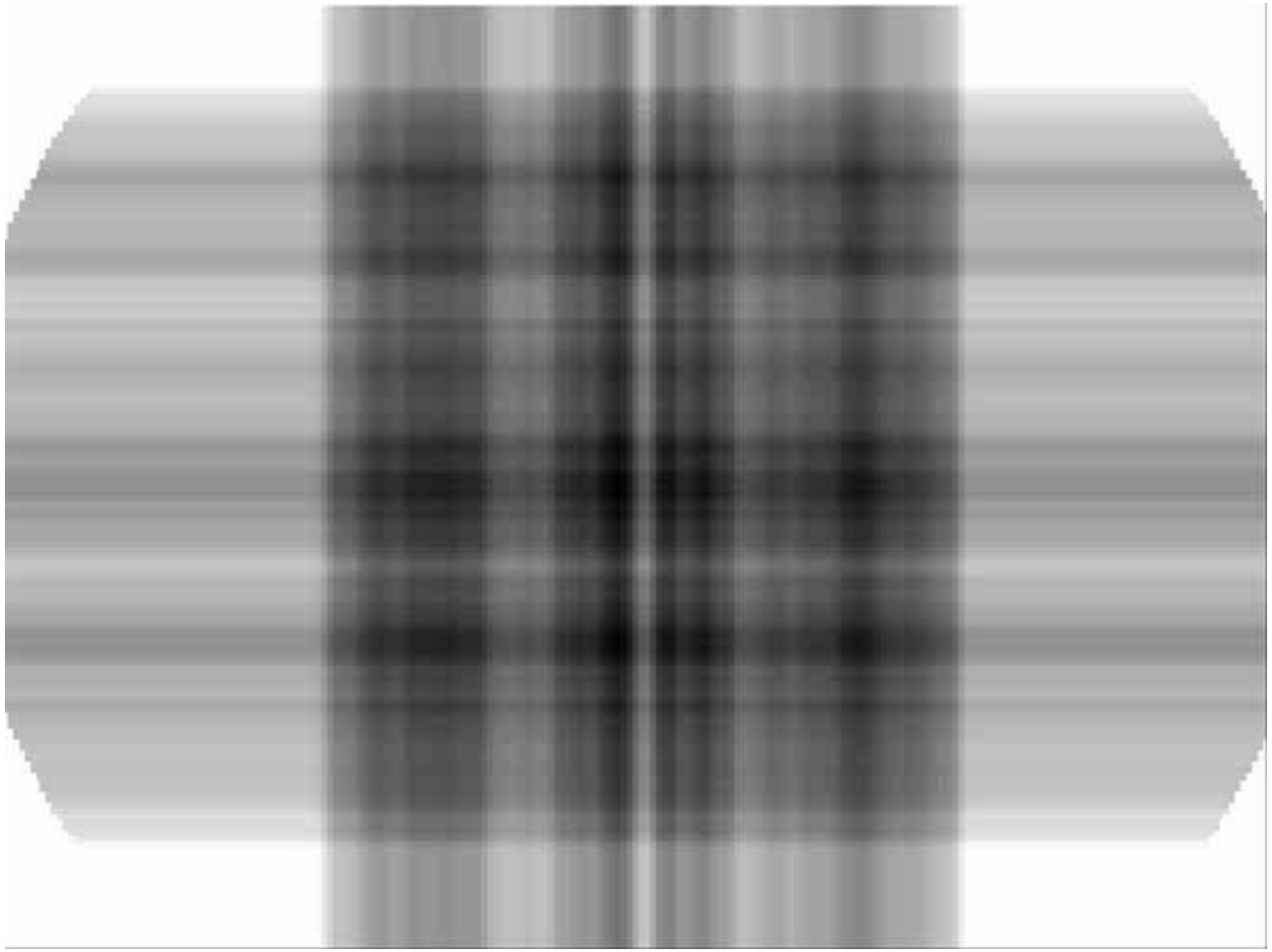

Simple backprojection results in a blurred reconstructed image

Filtered backprojection (FBP)

- Image (real) and frequency space are related by the Fourier transform (FT).
- FT provides another method to represent spatially varying data:
  - 1D image profile can be represented as Σ of cos and sin with ≠ spatial frequencies k.

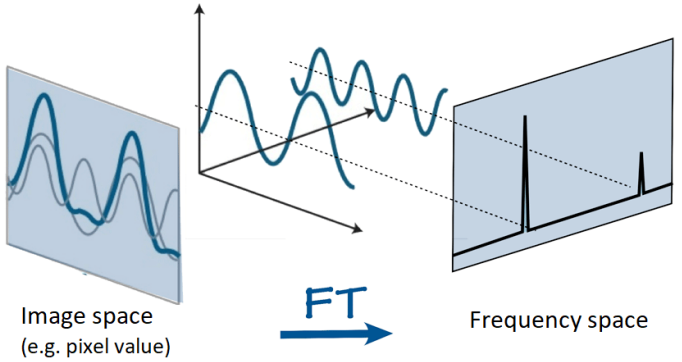

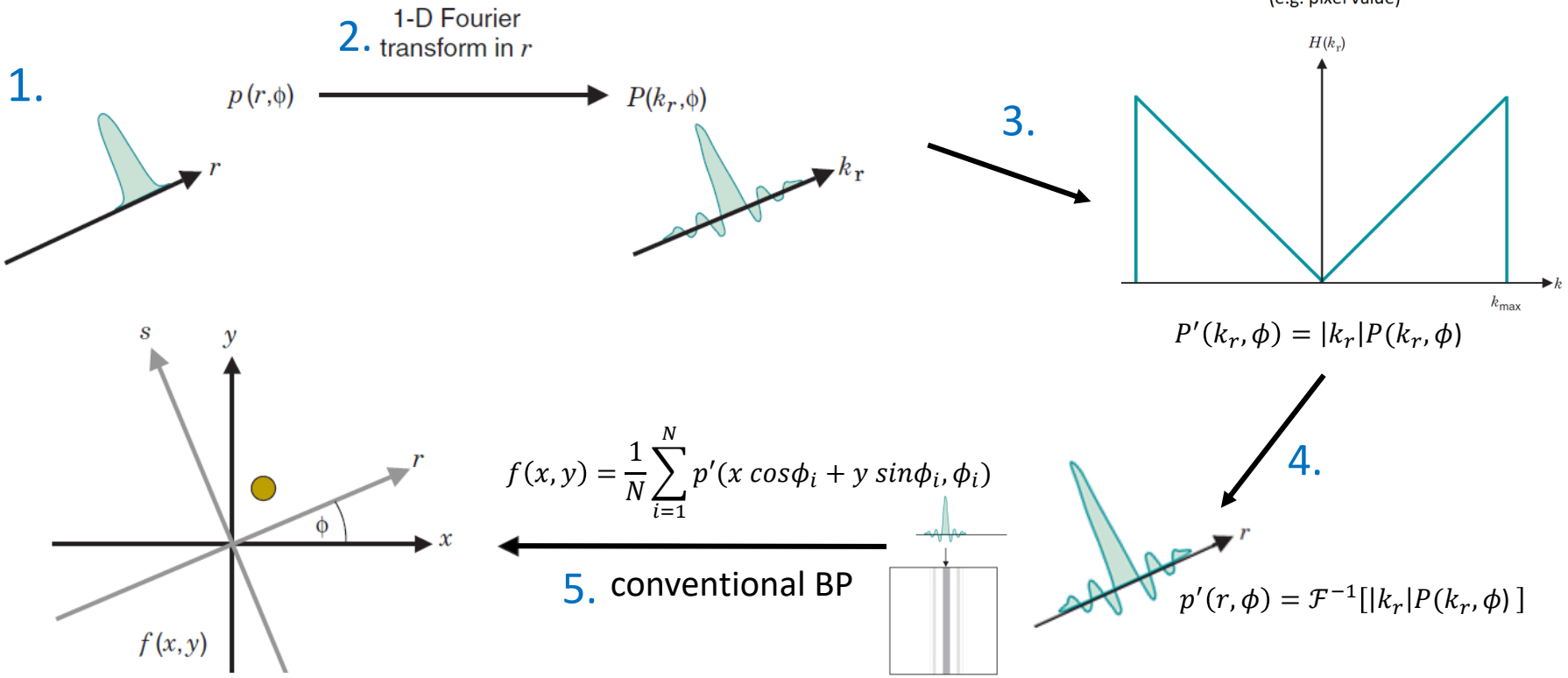

1. Acquire N projection profiles p(r, ϕ) (sinogram).
2. Compute the FT of each profile (sinogram row).
3. Apply a filter to each profile in frequency k-space → $|k_r|$.
4. Compute the inverse FT of each filtered profile to obtain a modified projection profile.
5. Perform conventional backprojection with the new (filtered) profiles to compute the image.

Filtered backprojection (FBP)

- Filtering in k-space precedes backprojection into object (image) space.
- Ramp filter
  - ✓ Low frequency damping
  - ✓ Removes 1/r blurring + sharpens detail.
  - • High frequency selected
  - ✗ High frequency noise amplified.
  - ✗ Degradation of signal to noise ratio (SNR).
- FBP images appear sharper but noisier than simple BP.
- Other filters can be used to mitigate this effect (“rounded shape” filters).

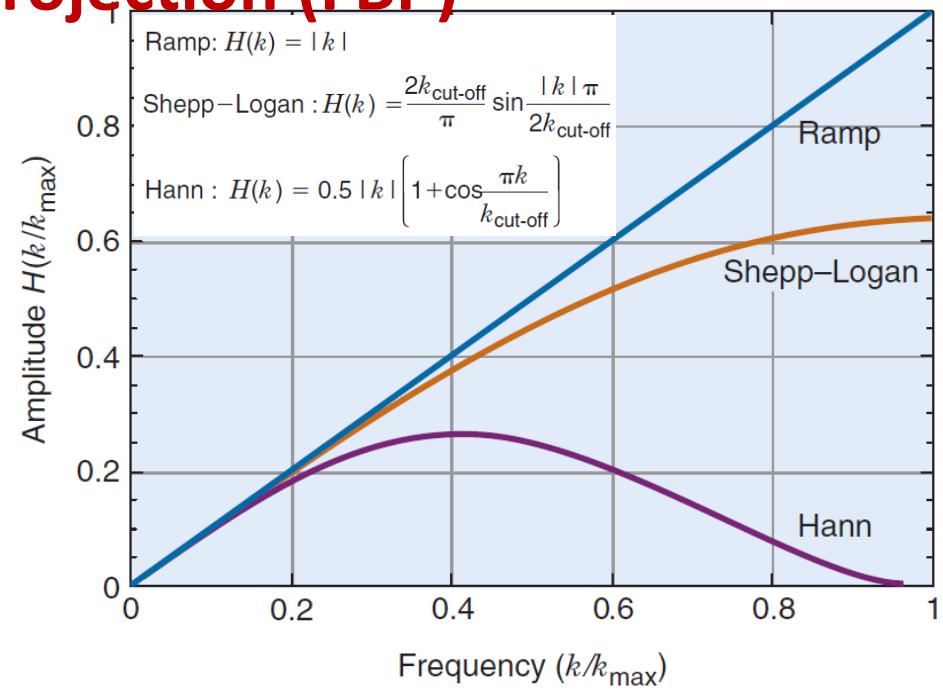

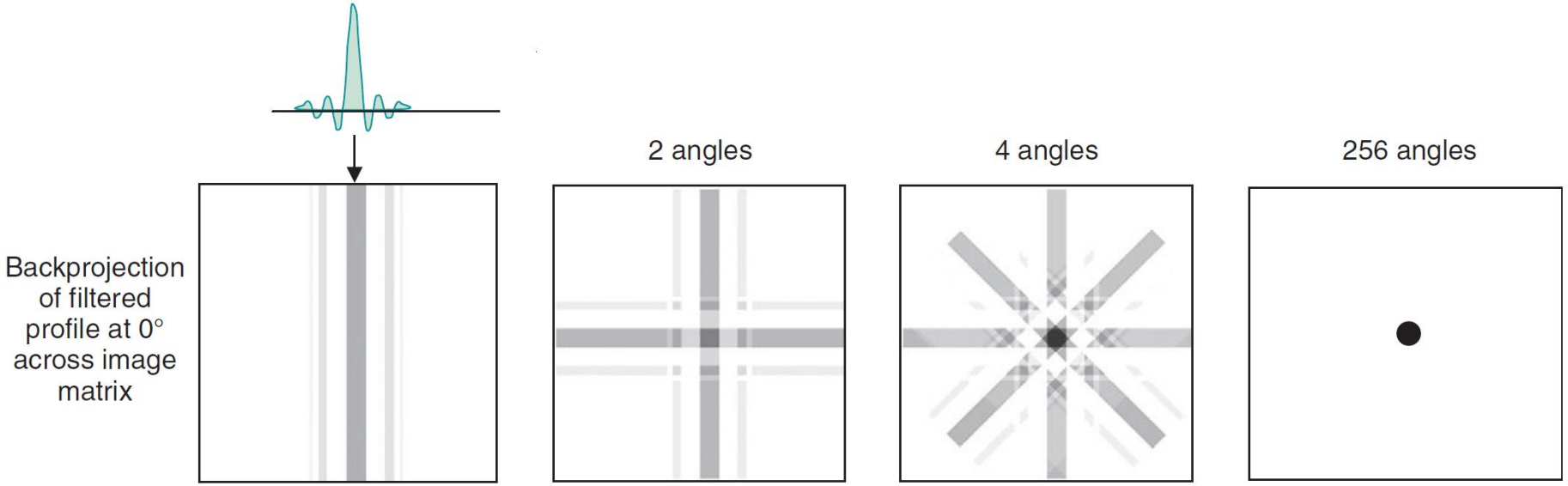

Filtered backprojection (FBP)

Fitered Backprojection (FBP) of an activity distribution in brain

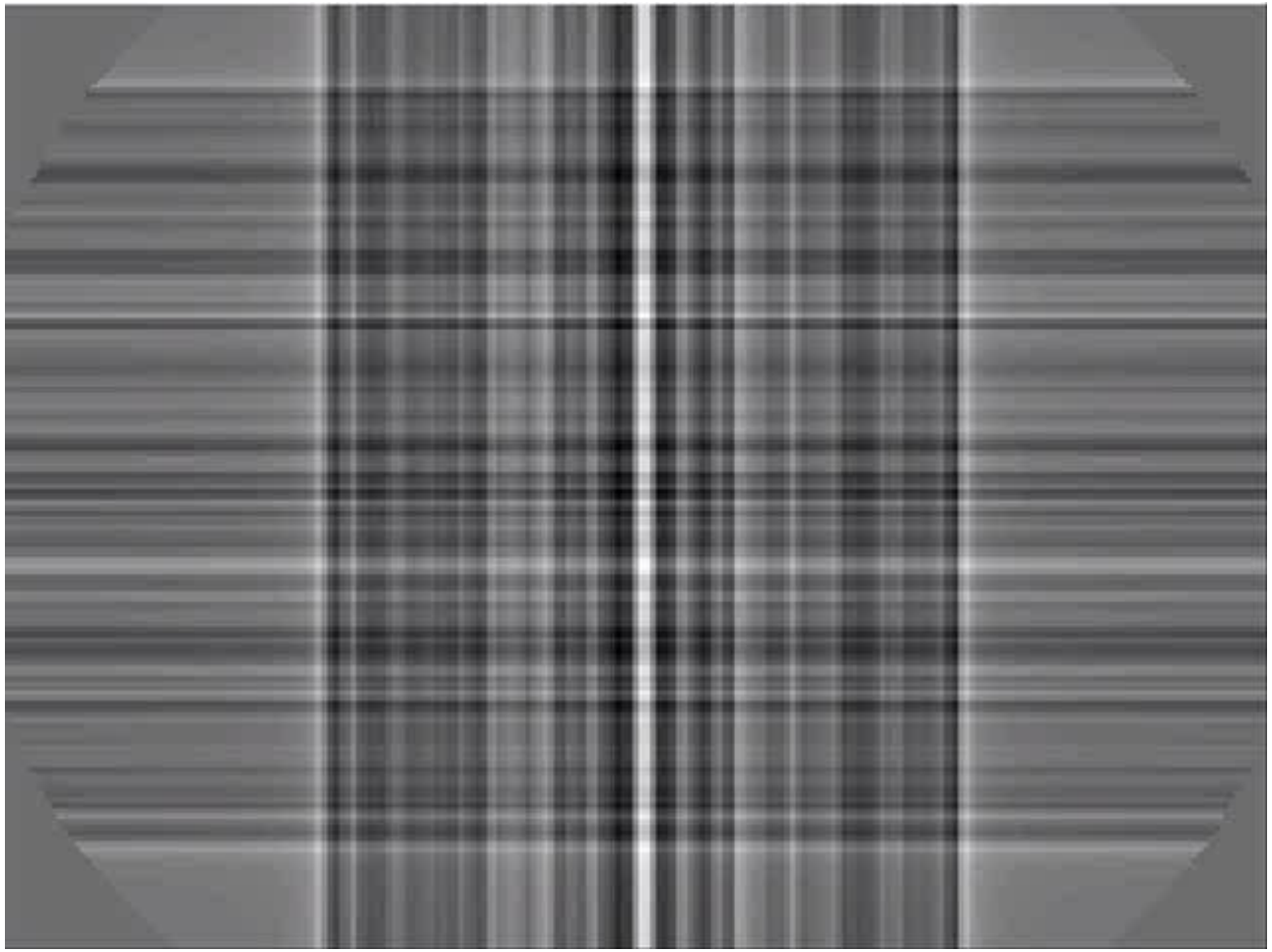

If noiseless projections and virtually infinite angles views are available

Quantitative true activity distribution reconstruction

Filtered backprojection (FBP)

Advantages :

- Accurate if noise-free measurements and completely sampled data.
- Fast and easy to implement.

Limitations :

- Major artifacts if data is measured incompletely.
- Still noisy → can only be partially mitigated by filters.
- No natural way to implement corrections for:
  - Spatial resolution
  - Scattering
  - Attenuation

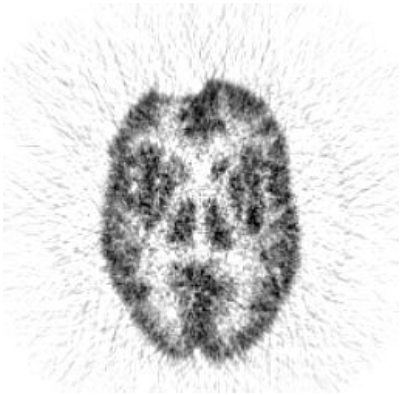

iterative reconstruction techniques !

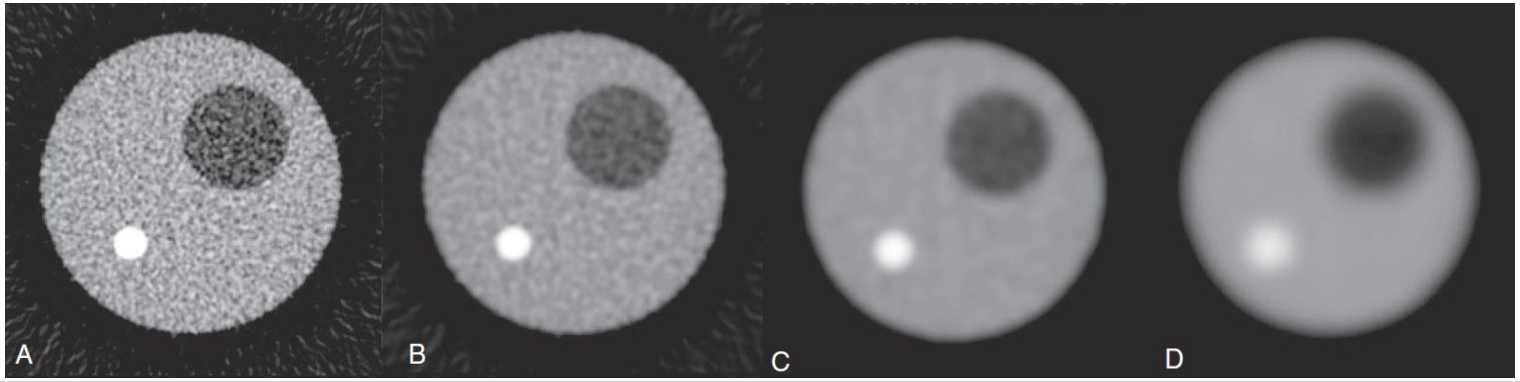

Example: FBP with Shepp-Logan filter and different cutoffs → tradeoff between SNR and image sharpness/detail.

Iterative reconstruction

more computationally intensive than FBP, but standard nowadays.

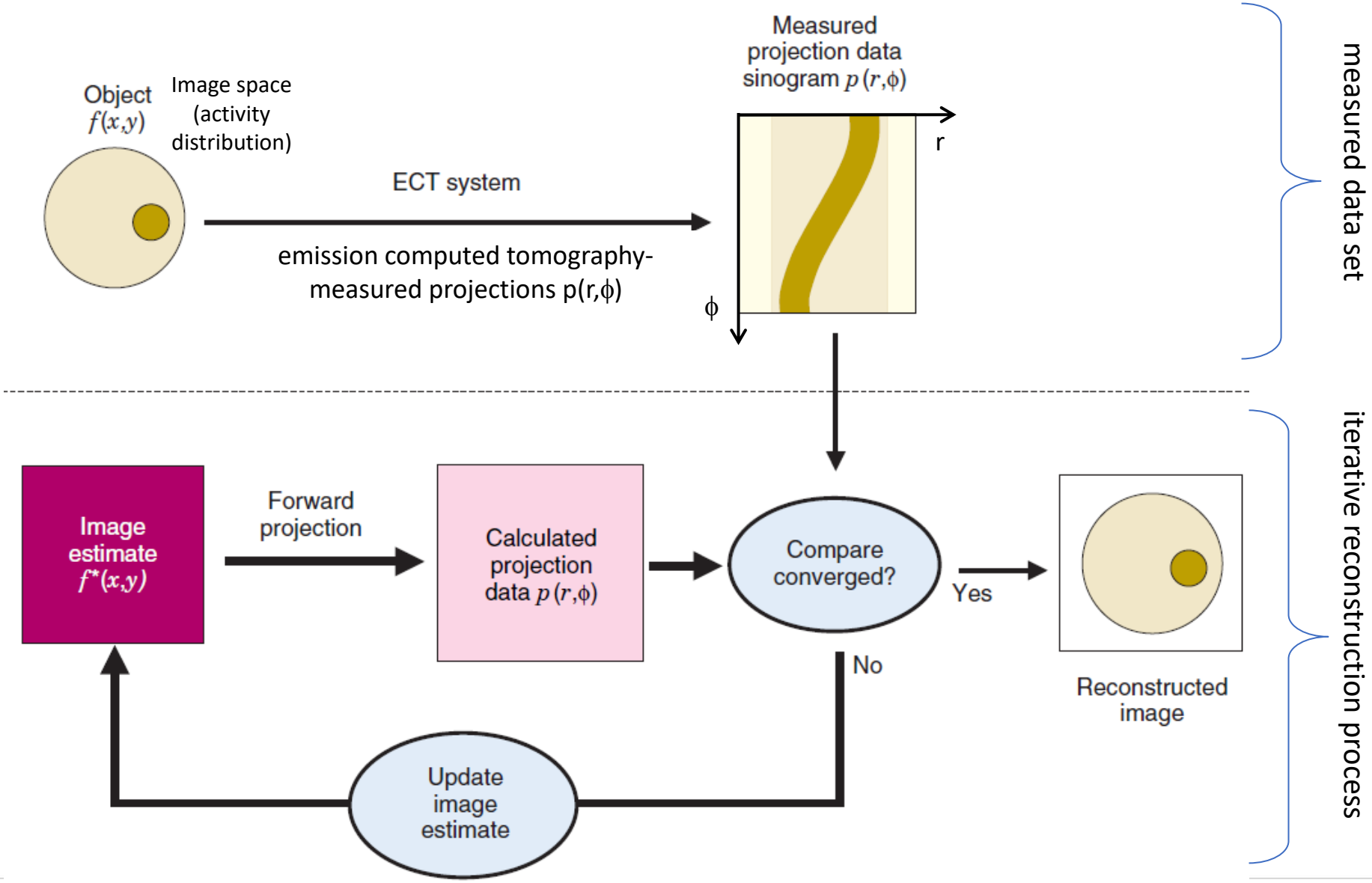

Iterative reconstruction

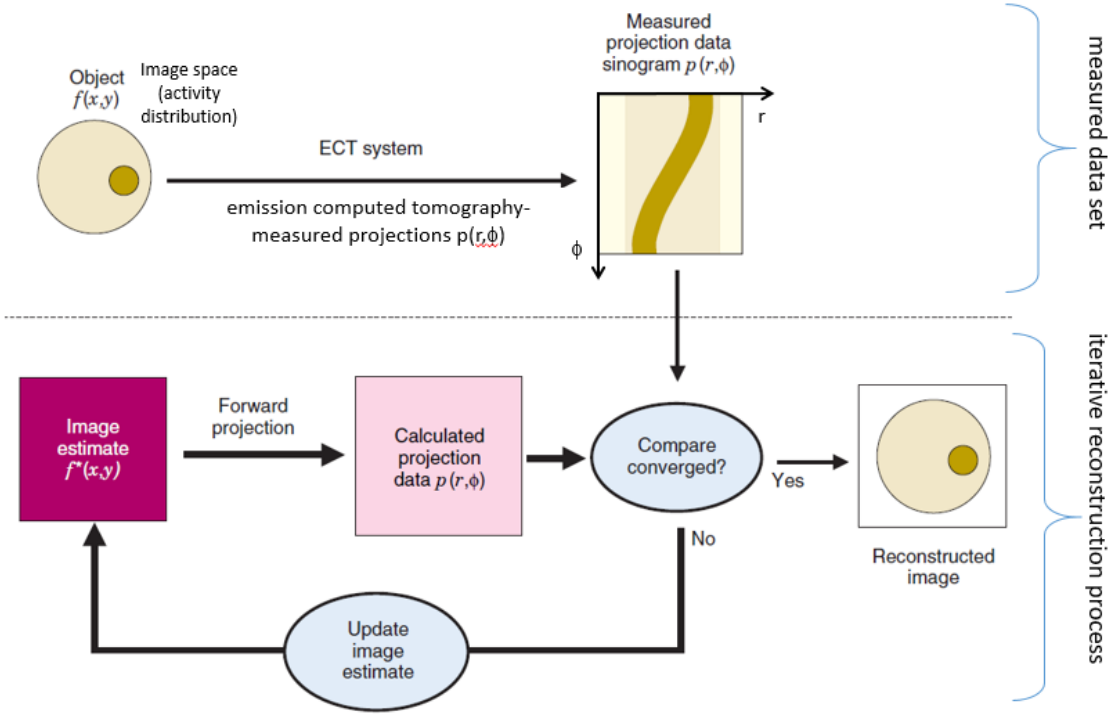

True activity distribution f(x,y) is estimated by successive approximations f(x,y):*

1. Start with a simple initial image estimation *f*(x,y)* *(e.g. uniform activity distribution in the FOV or FBP).*
2. Compute (forward) projections to calculate estimated sinogram.
3. Compare measured and computed sinogram.
4. If no convergence is reached, compute correction factors.
5. Refresh the image estimate and continue iterating until convergence.

Iterative reconstruction

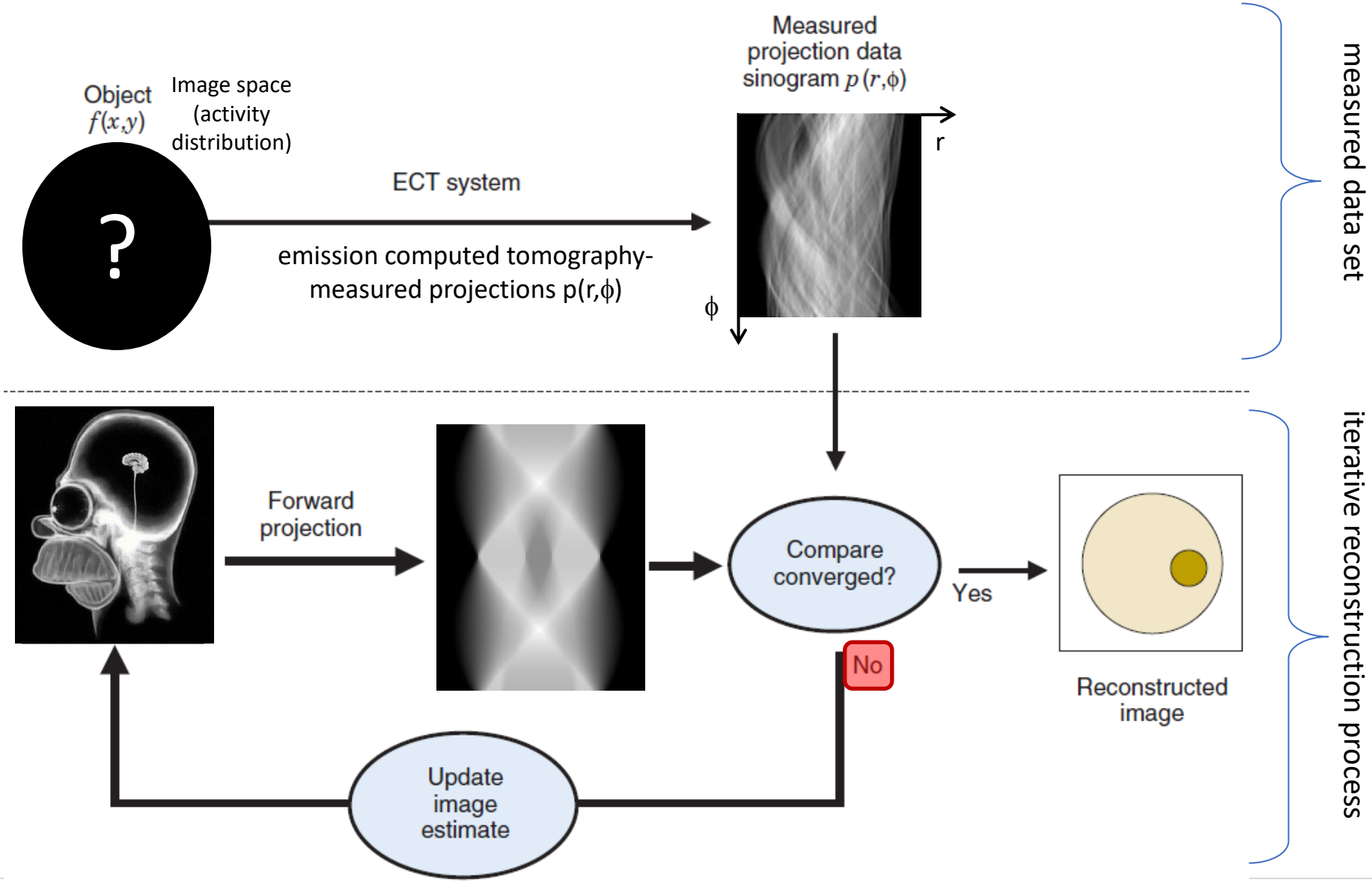

Iterative reconstruction

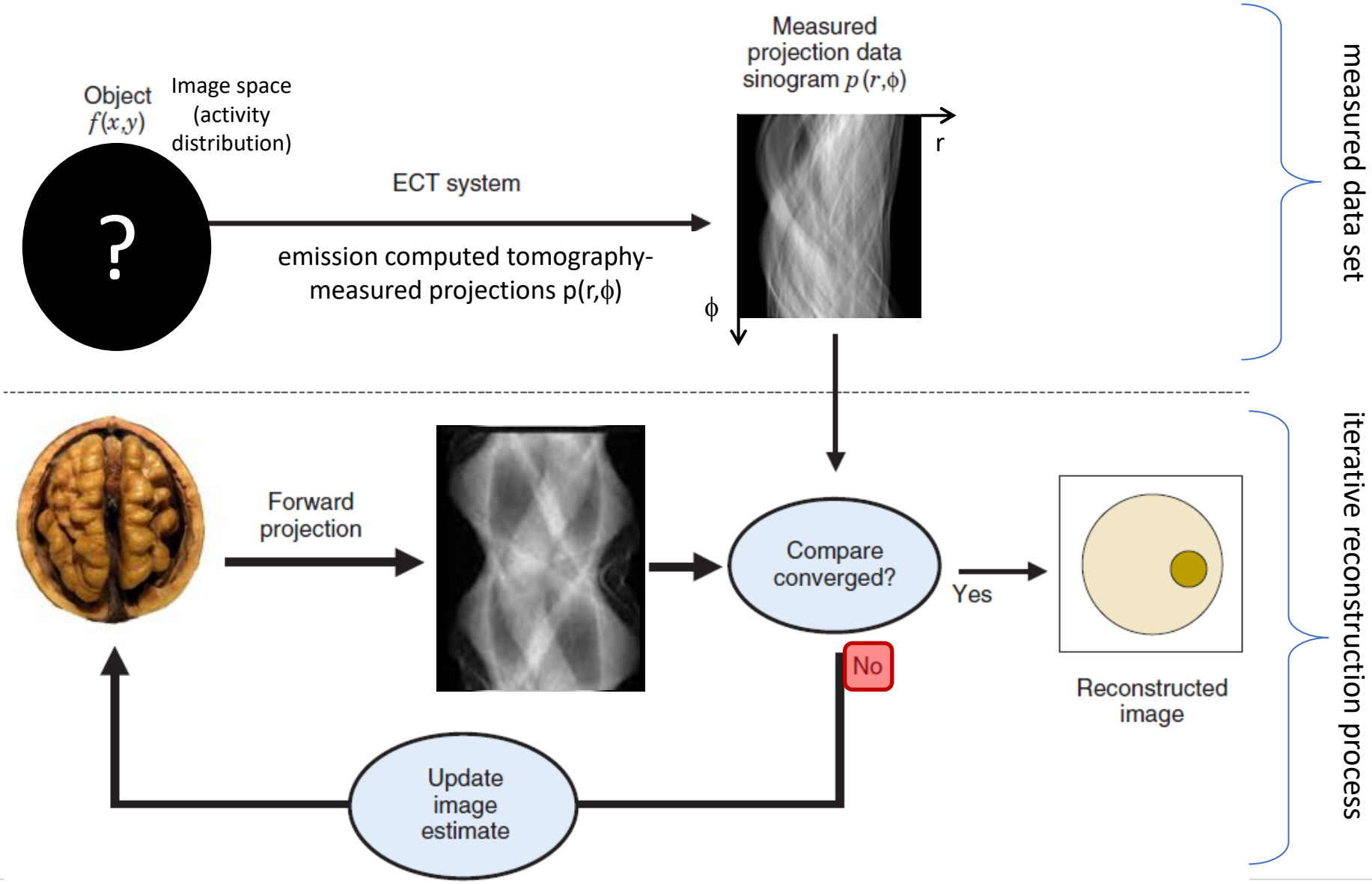

Iterative reconstruction

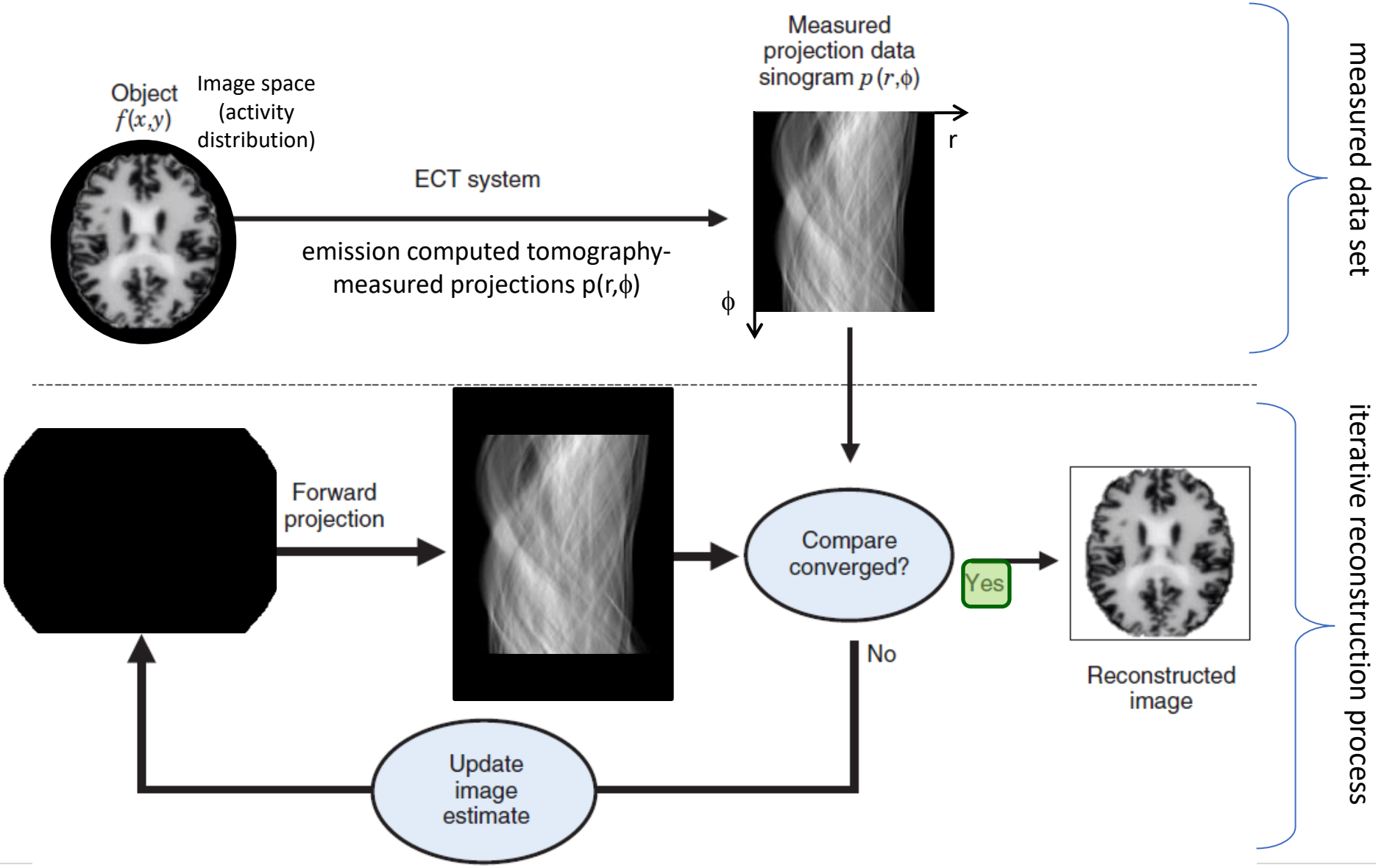

Animations from:
Floris HP van Velden, PhD

Iterative reconstruction

Iterative reconstruction is based on:

1. Comparing estimated vs. measured data

2. Updating the image estimate

→ ***Maximum-likelihood expectation maximization algorithm (MLEM)***
Compute the maximum-likelihood source distribution that would result in the measured projection data (sinograms).

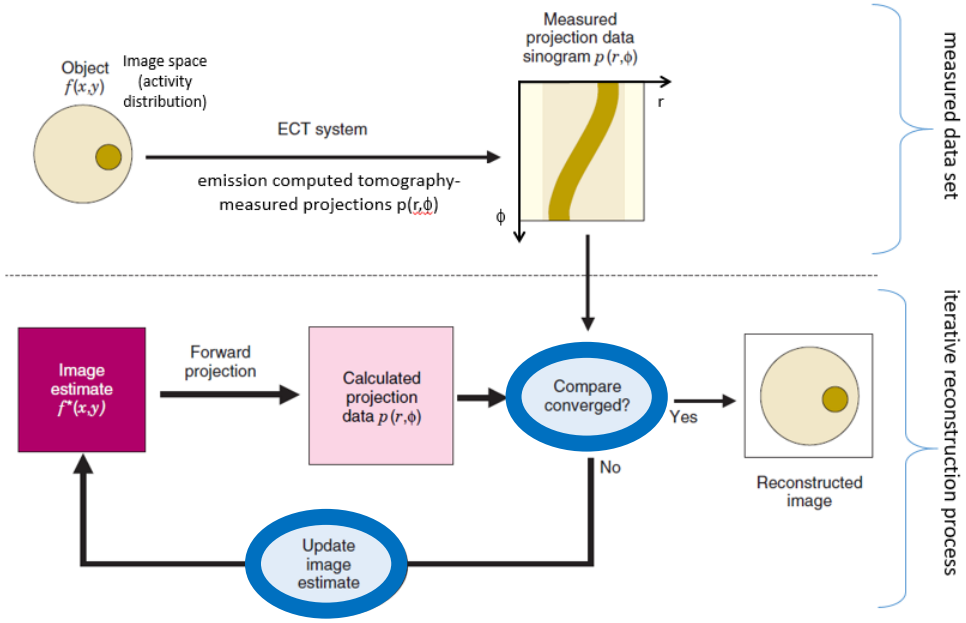

Iterative reconstruction is more computationally intensive than FBP:

- Needs several iterations to converge (FP needs to be done several times).
- Reconstruction algorithms allow to include specific characteristics of the imaging modality:
  - attenuation,
  - scatter,
  - finite resolution, system geometry.
- Speed-up solution → ordered subsets (OSEM) : only a small number of projections (angles) are used in the first iteration steps (time per iteration ∝ # projection profiles to compute).

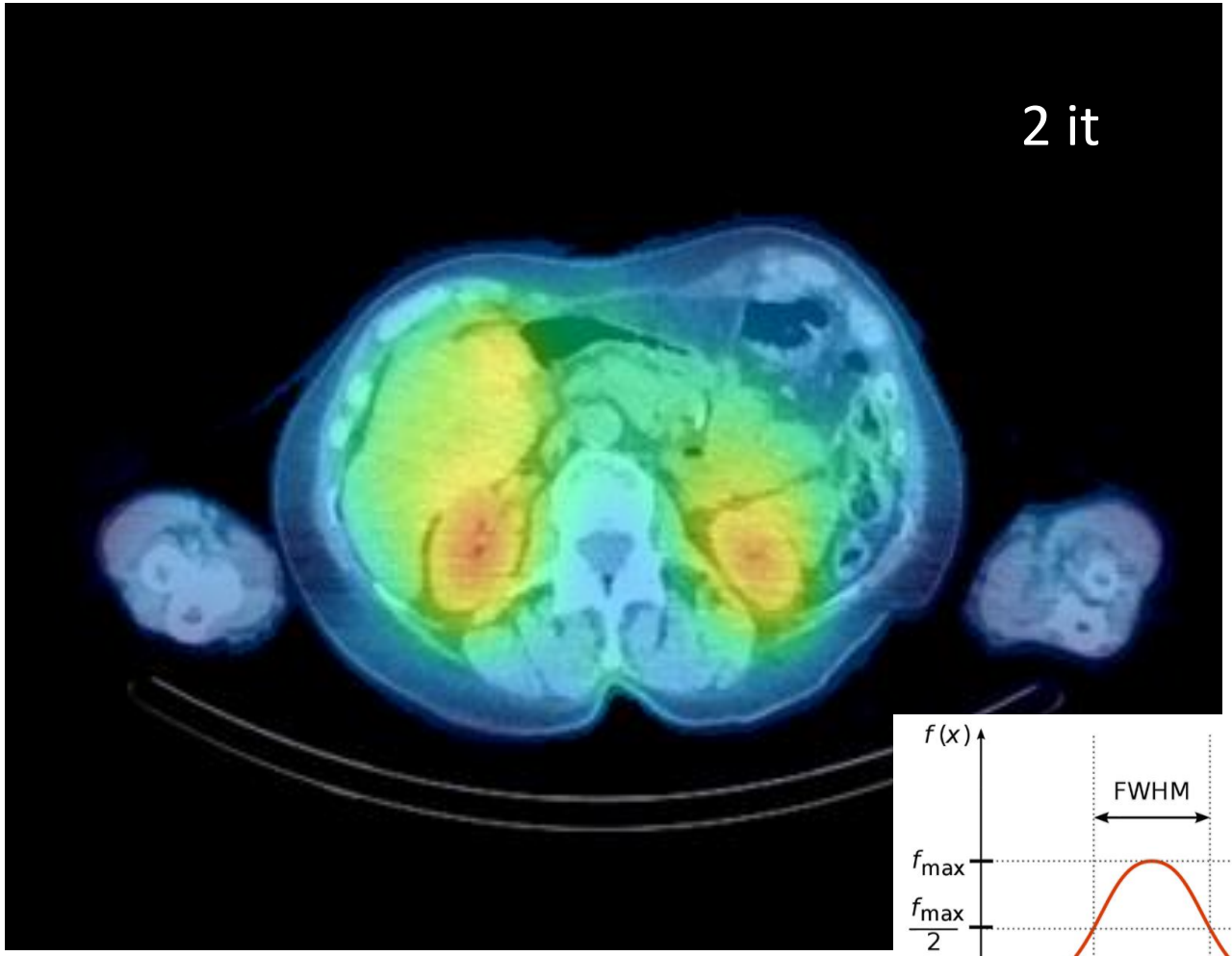

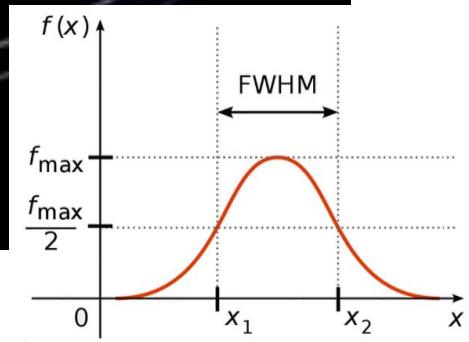

FLASH3D 16it
4ss G4

Translation =

- iterative algorithm
- using 16 iterations
- 4 subsets
- post-processing (smoothing) filter with a Gaussian shape and full width at half maximum (FWHM) of 4 mm.

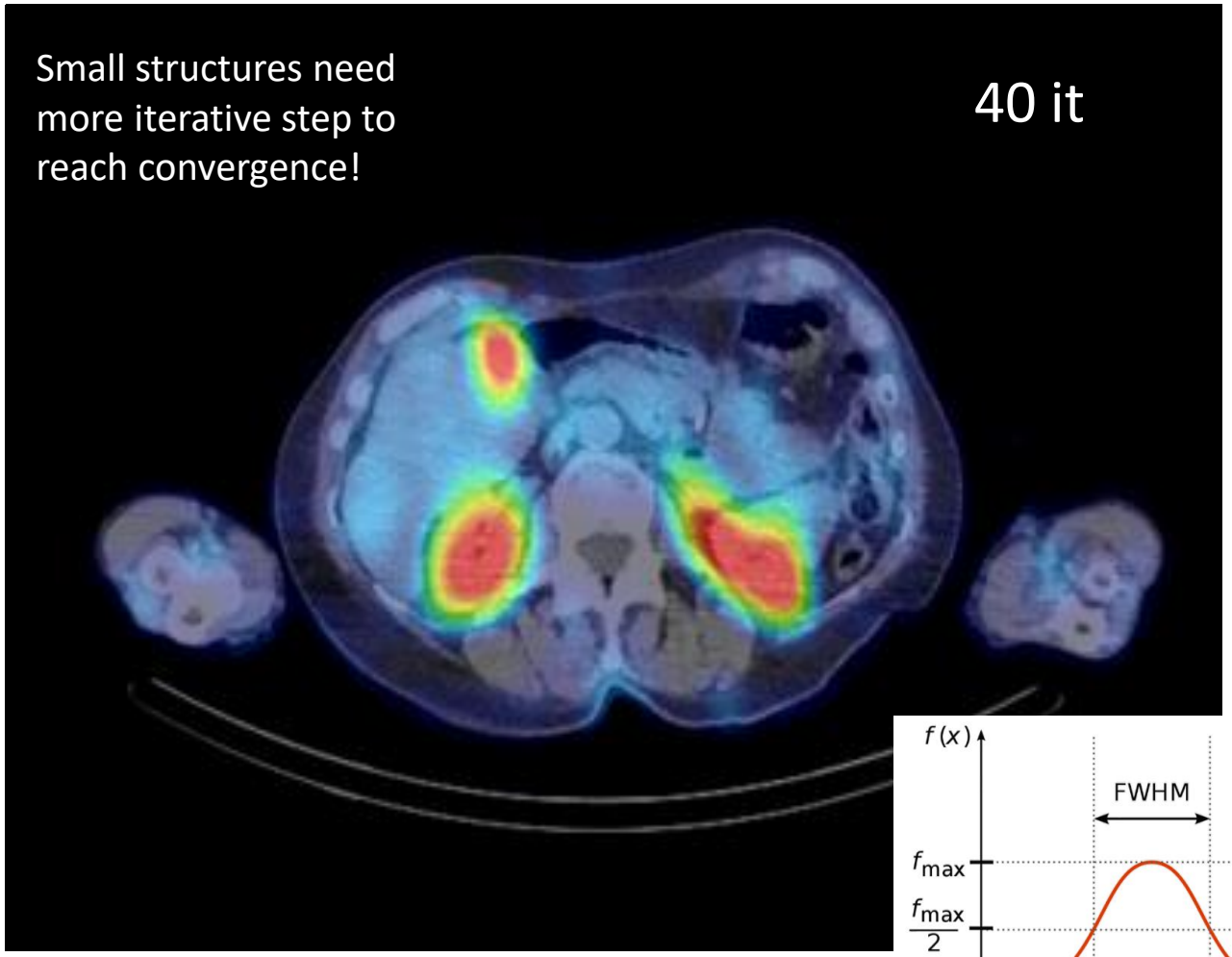

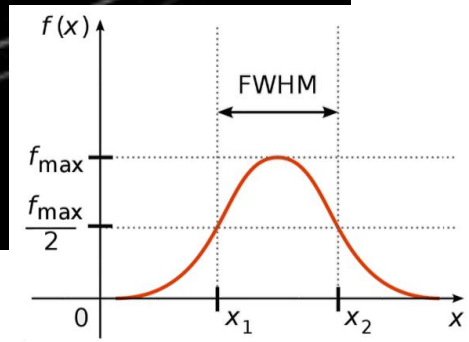

FLASH3D 16it
4ss G4

Translation =

- iterative algorithm
- using 16 iterations
- 4 subsets
- post-processing (smoothing) filter with a Gaussian shape and full width at half maximum (FWHM) of 4 mm.

Protocol optimization in SPECT

- Patient receiving a therapeutic administration (~6 GBq) of Lu-177 DOTATATE.
- Signal recovery was assessed at organ and lesion level by varying the number of iterations
- Signal recovery (and convergence) depends on the size of the considerate lesion/tissue.
- Protocol optimization has a direct impact on organs and lesion dose assessment.

Ex: *What number of iterations would you chose?*

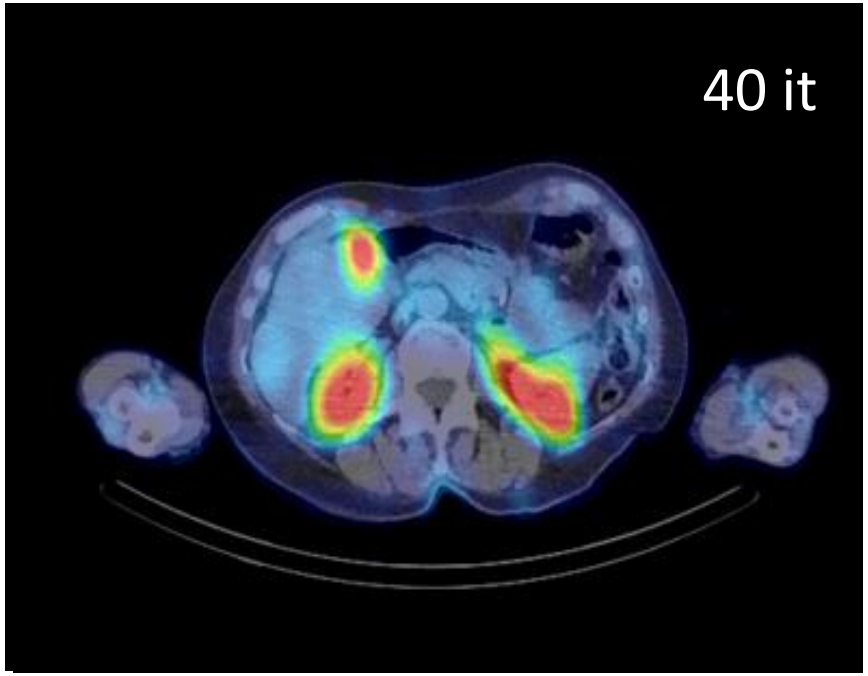

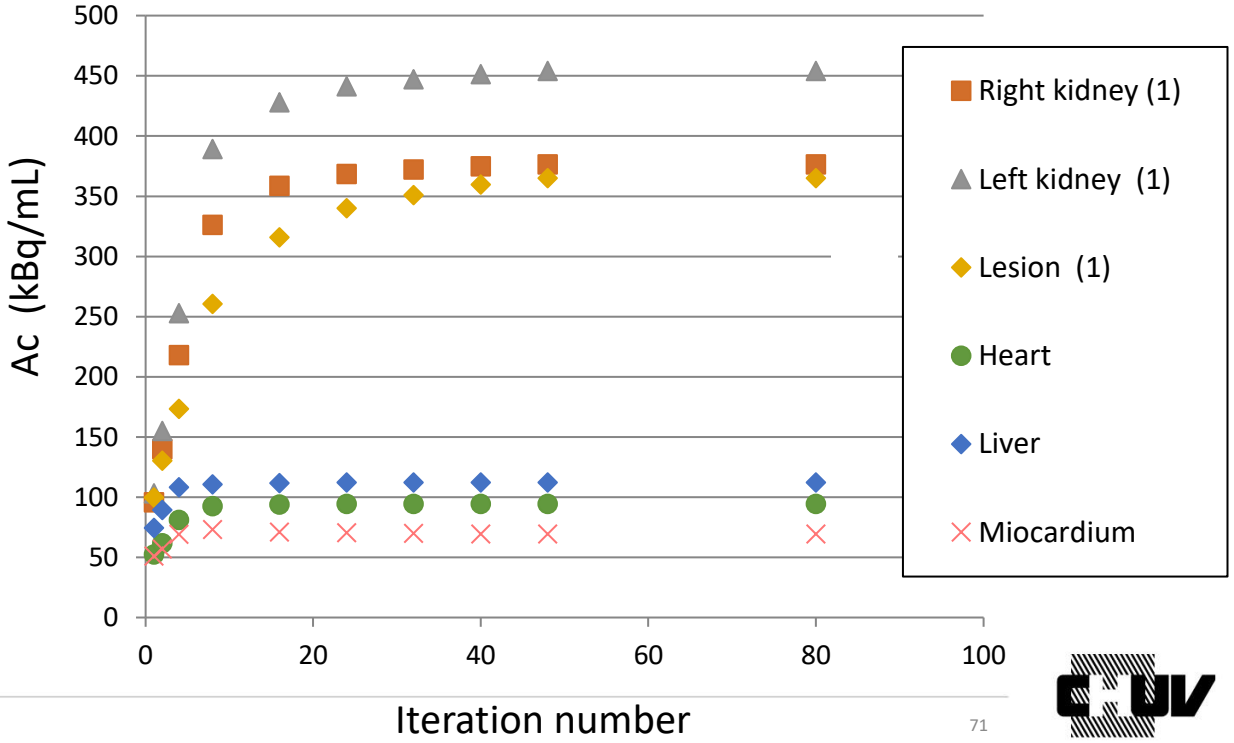

Single Photon Emission Computer Tomography: SPECT

(some of its characteristics)

Single Photon Emission Computer Thomography: SPECT

Single head

Double head

Triple head

Acquisition: 2D array of 1D-projections
→ 2D planar image

Tomographic reconstruction

2D axial slices
stacked in a 3D array
(3D volume image)

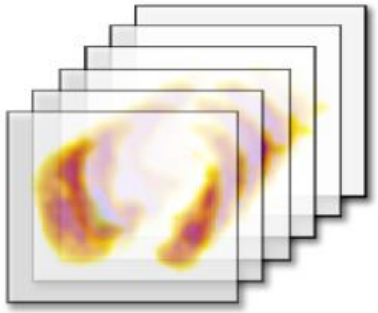

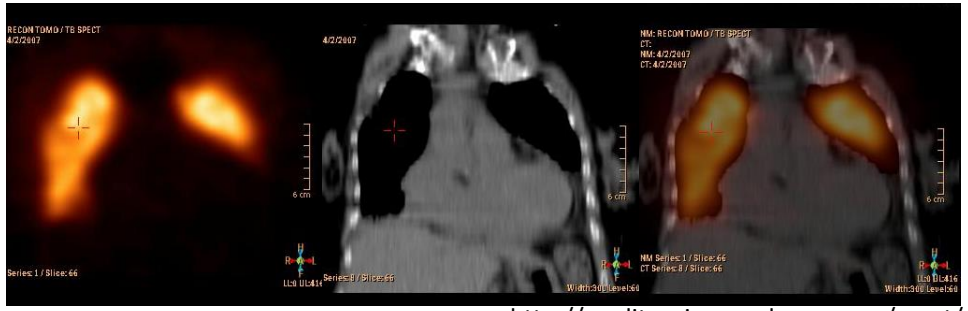

http://meditronics.wordpress.com/spect/

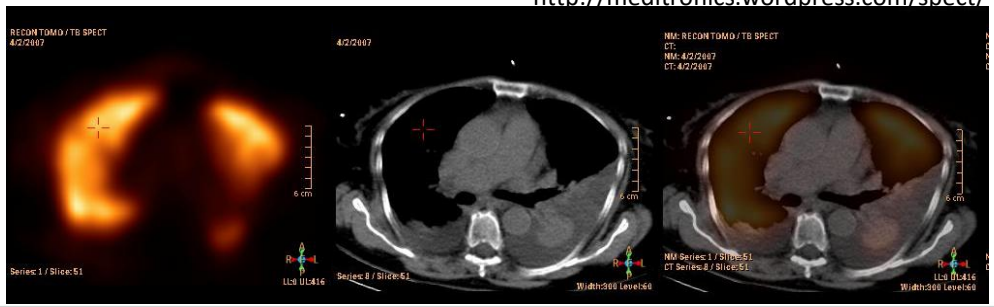

Multiple detection heads

→ increased detection sensitivity

→ reduced acquisition time

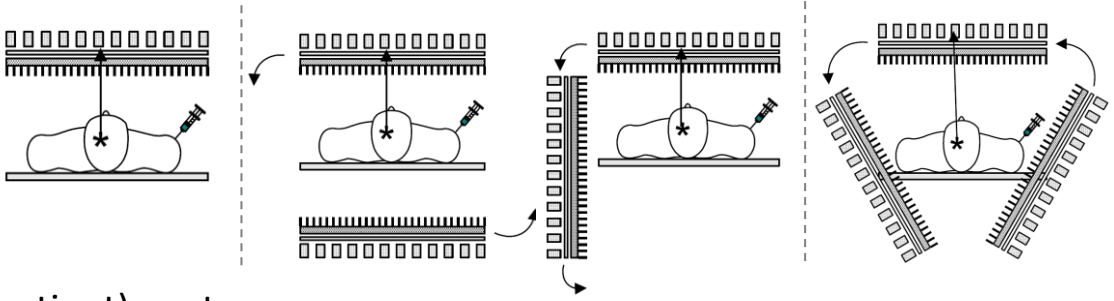

Acquisition orbit

→ as close as possible to the objet (patient) contour

→ minimize resolution degradation with distance

Automatic patient detection systems

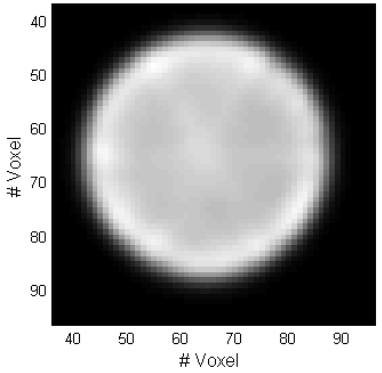

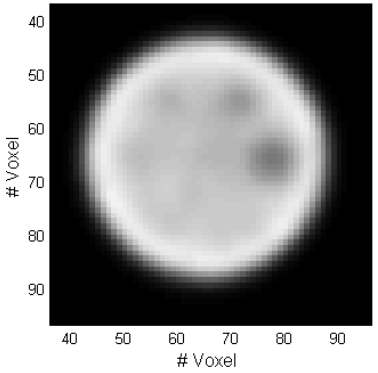

fixed circular orbit

Ø ~ 60 cm

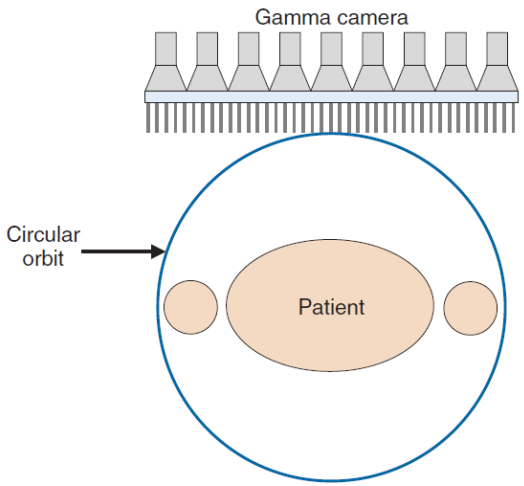

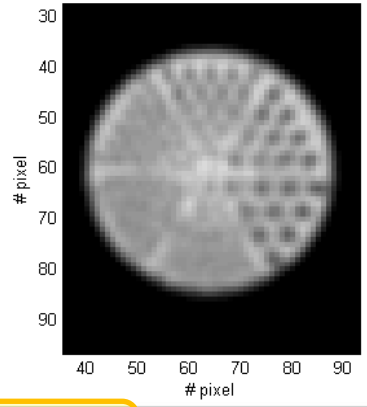

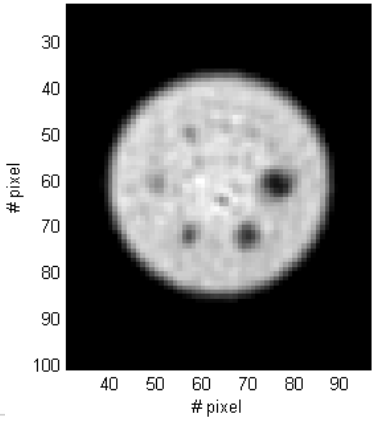

automatic adaptative orbit

Ø ~ 34 cm

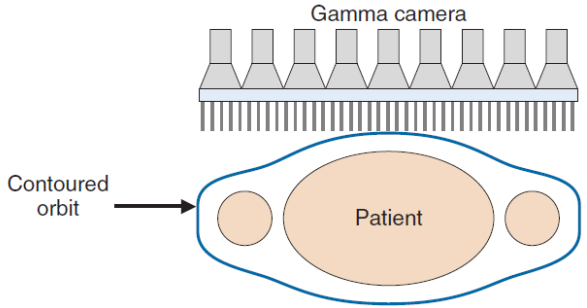

SPECT

Special designs: **neuro**, **cardiac** and **preclinical imaging**

Multiple detection heads
→ increased detection sensitivity
→ reduced acquisition time

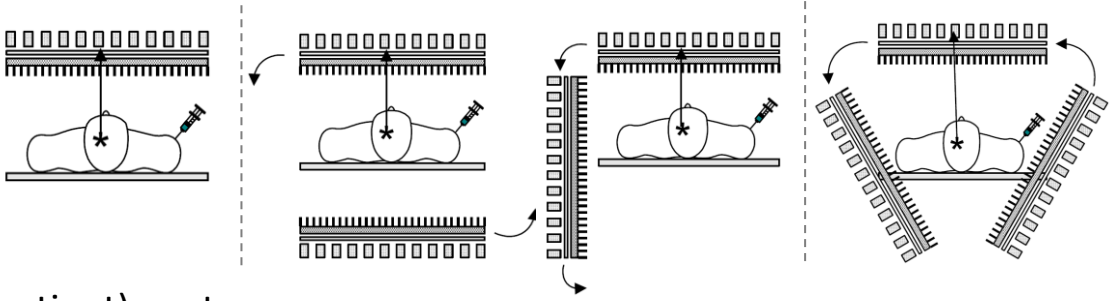

Acquisition orbit
→ as close as possible to the objet (patient) contour
→ minimize resolution degradation with distance

Special cases: **neuro** and **cardiac** imaging

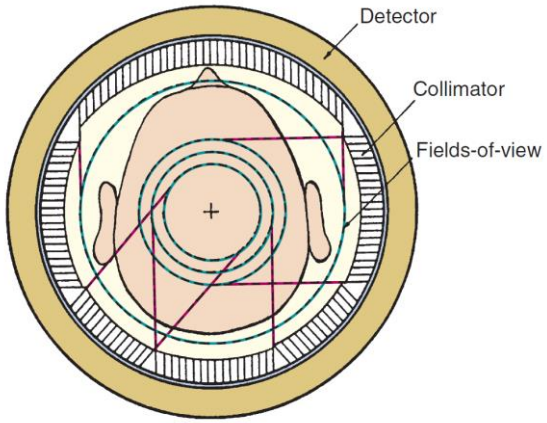

smaller FOV

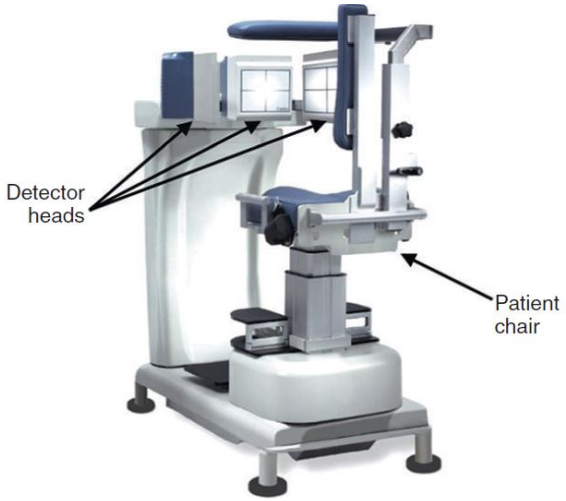

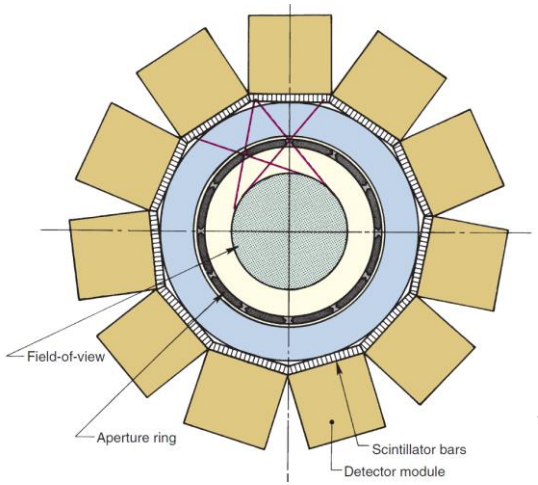

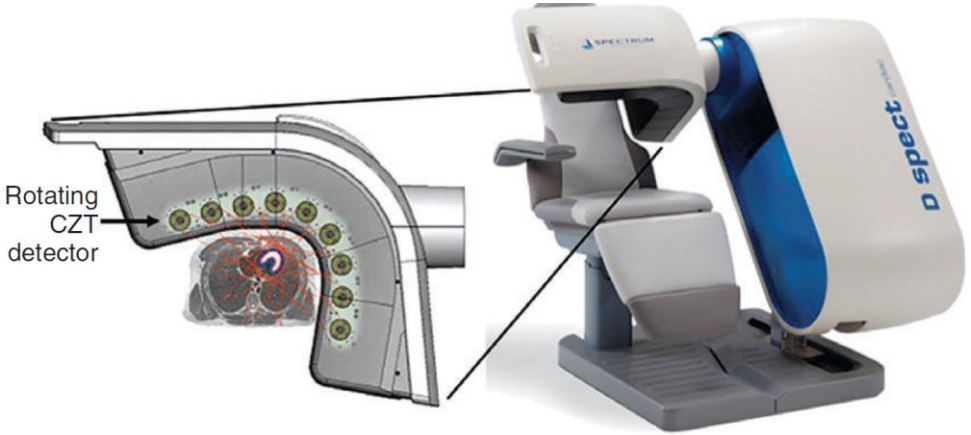

Special designs: preclinical studies (small animals)

Small animal SPECT/-PET/-CT

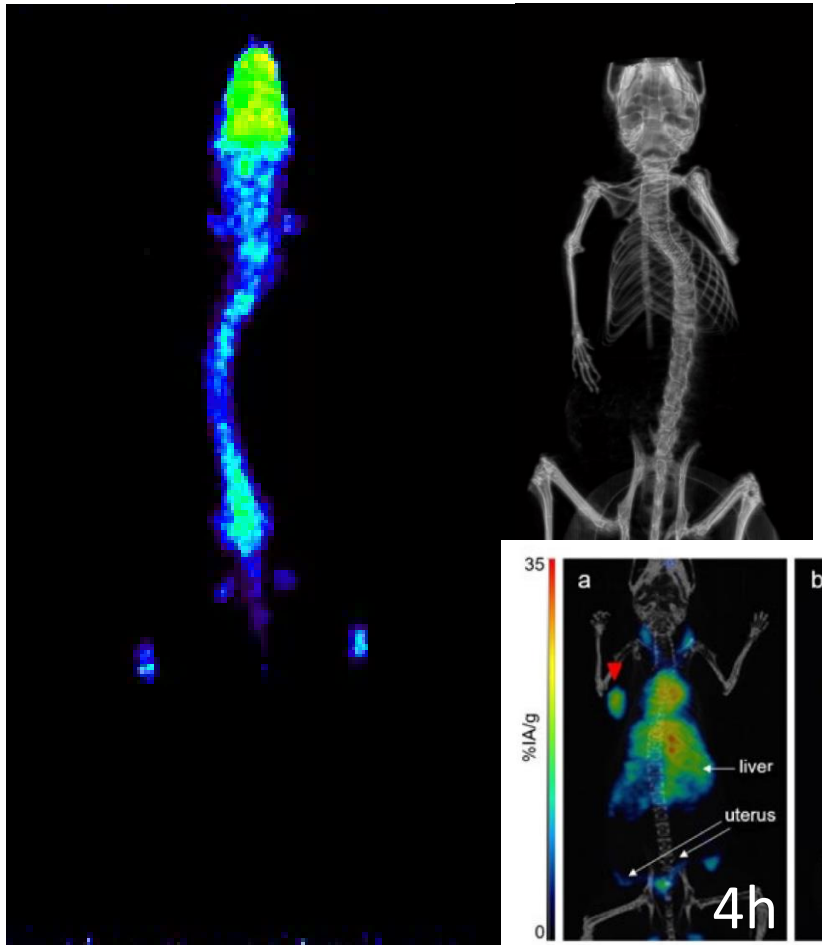

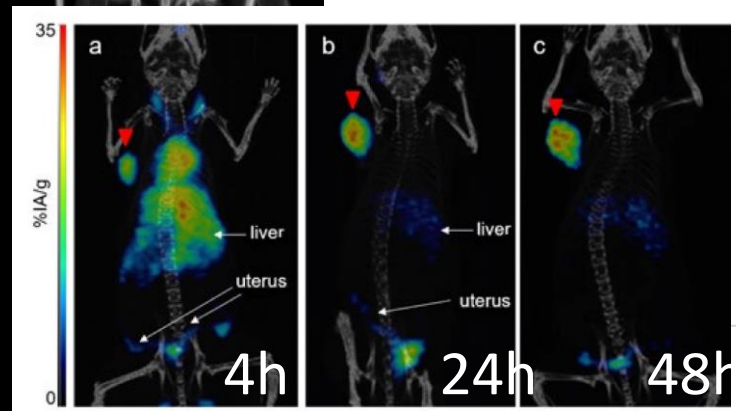

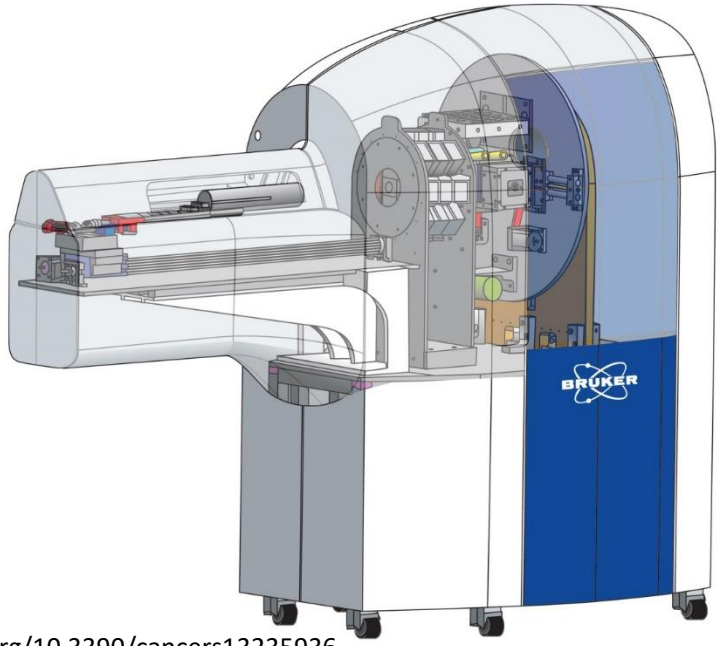

From Delage et al. https://doi.org/10.3390/cancers13235936

Sampling

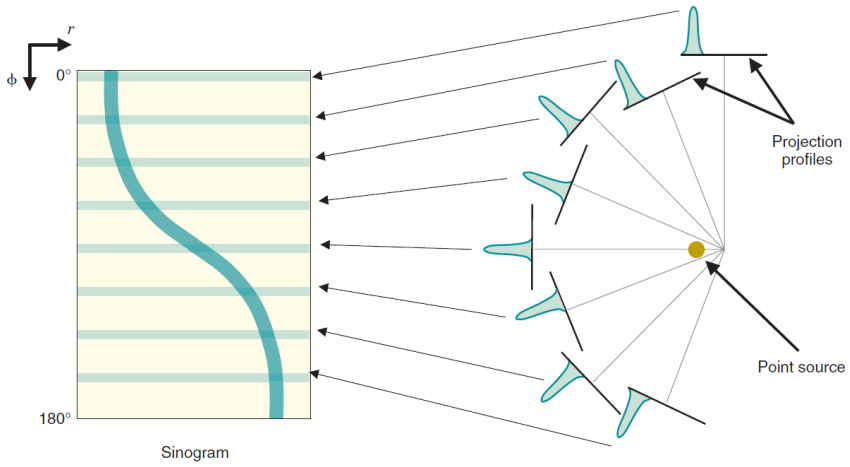

Projections are *discrete* data-sets.

1) Linear sampling distance Δr: distance between sample points.

2) Angular sampling interval N_{view}: finite number of sampled angles.

Image quality of reconstructed image depends on : system resolution, reconstruction, filters and choice of linear an angular sampling.

1) *Sampling theorem:*

The discrete representation of a signal requires samples that are evenly spaced at a sampling rate greater than twice the maximum frequency present in that signal:

$$f_{sampling} \geq 2f_{max} \quad \rightarrow \quad \frac{1}{f_{sampling}} \leq \frac{1}{2f_{max}} \quad \rightarrow \quad \Delta r \leq \frac{1}{2f_{max}}$$

limit f_{max} is also known as the Nyquist frequency

Δr defines a limit to the spatial resolution (higher frequencies contain fine image details, but also noise).

$\Delta r \xleftrightarrow{\text{tradeoff}}$ resolution & signal-to-noise ratio. If lower frequency filters cutoffs are used to improve SNR → degrading spatial res!

Sampling requirement (rule of 👍) :

$$\Delta r \leq FWHM/3$$

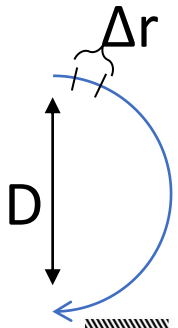

2) Angular sampling (angle between projections):

The minimum # of angular views N_{views} for a FOV with diameter D should be ~ the length of the 180-degree arc where projections are acquired ($\pi D/2$) divided by the linear sampling distance, Δr :

$$N_{views} \geq \pi D/2\Delta r$$

Artefacts

linear and angular sampling: how projections should be acquired ?

Linear undersampling (distance between sampling points) → image blurring + aliasing artifacts.

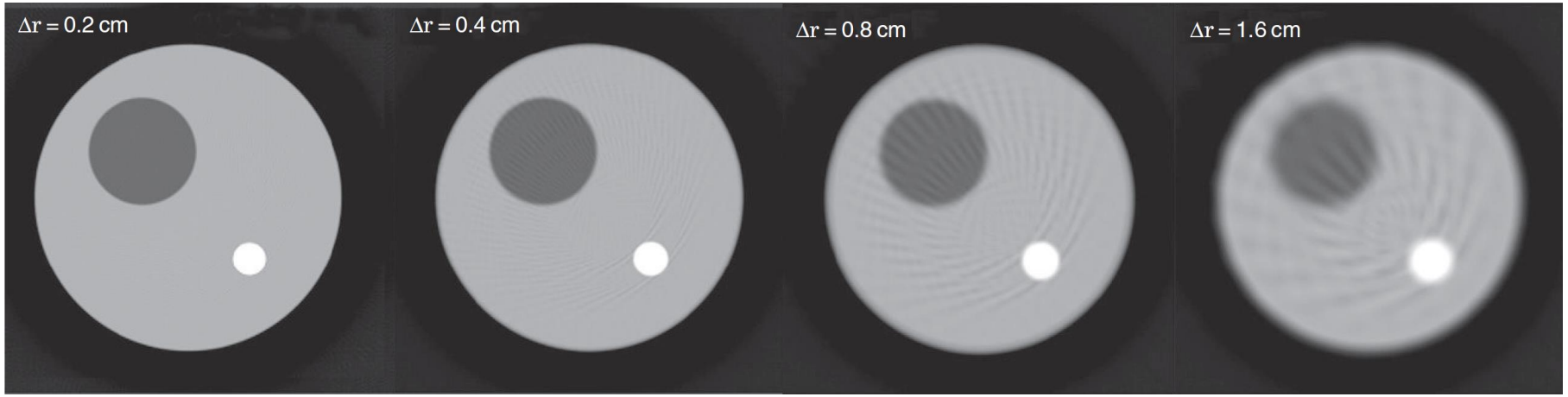

Angular undersampling (number of sampled angles) → streak-like artifacts.

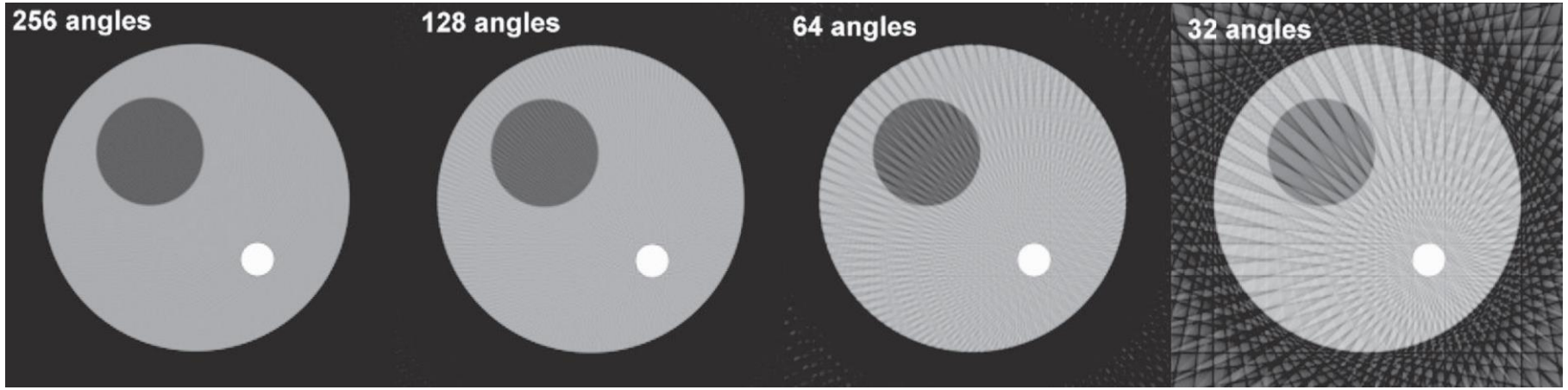

SPECT

Artefacts

linear and angular sampling: how projections should be acquired ?

Projections acquired over less than 180° → artifacts.

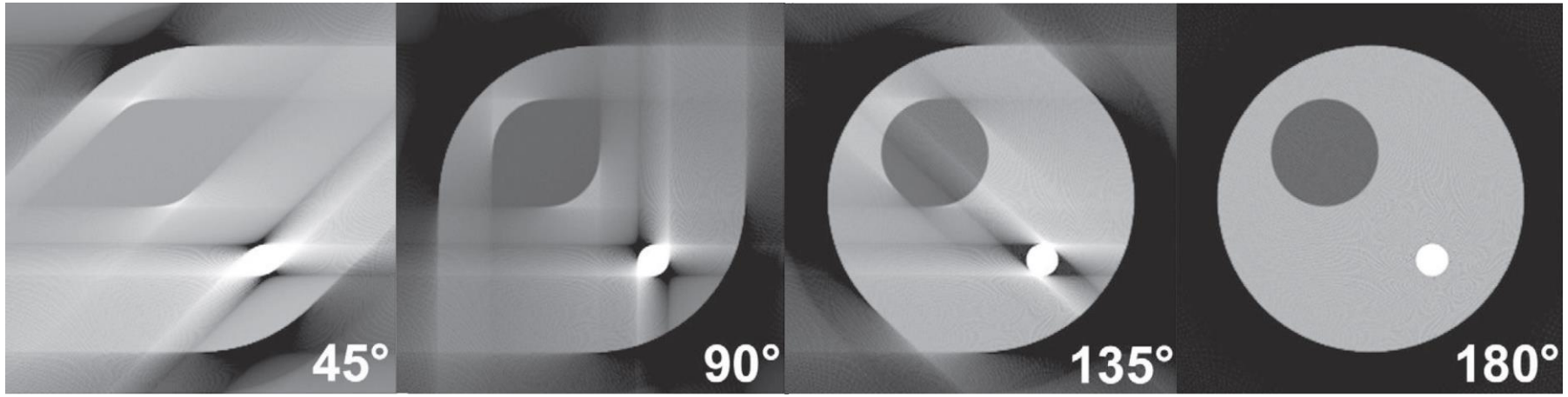

Projections not covering the whole object → artifacts

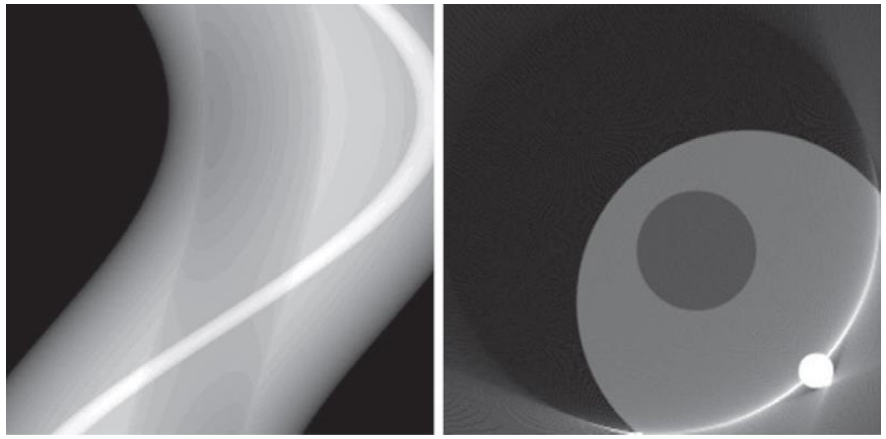

Missing projection (part of detector kaputt) → artifacts

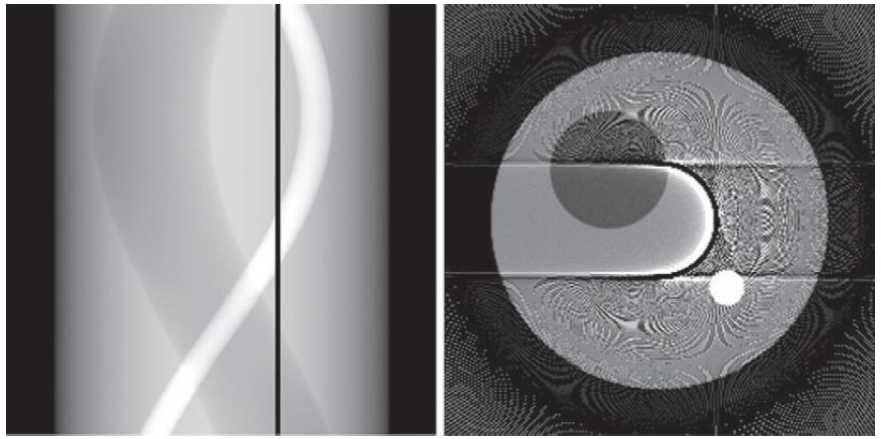

SPECT

How many projections are needed ?

Ex. :

A SPECT has FOV of 30 cm and a system spatial resolution of 1 cm.

- What are the linear sampling distance that will support this system resolution and thus the resulting pixel number?
- What is the angular sampling interval?

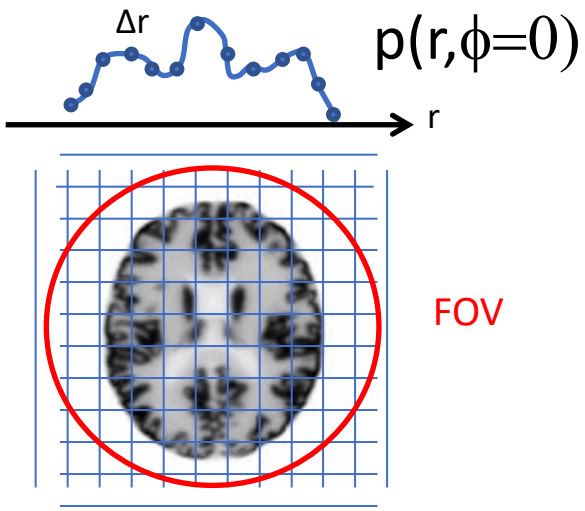

SPECT

Attenuation correction

Expected *Measured (NAC)*

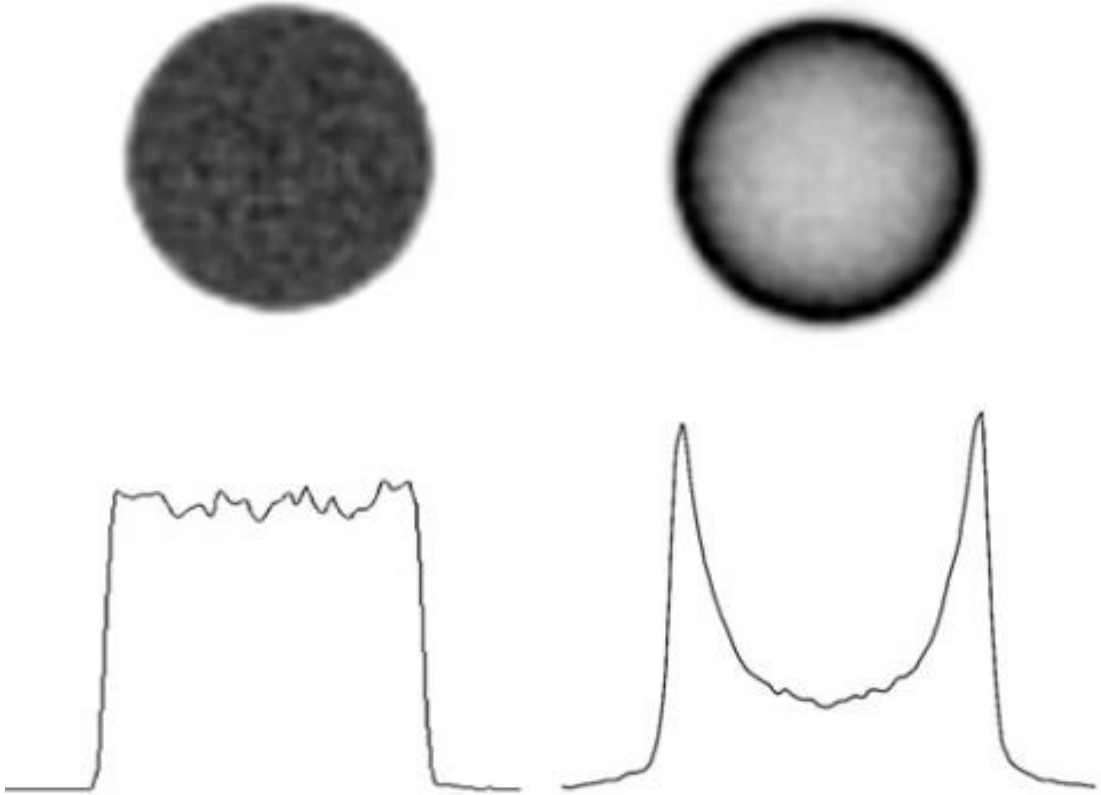

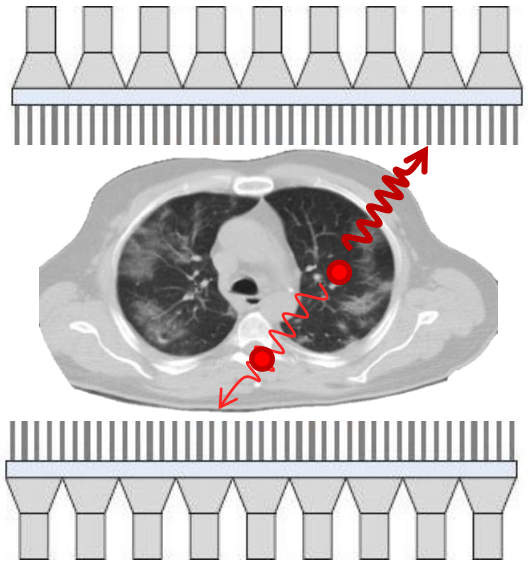

The attenuation correction is influenced by:

- the energy of the photons
- the size/density of the structure to be crossed

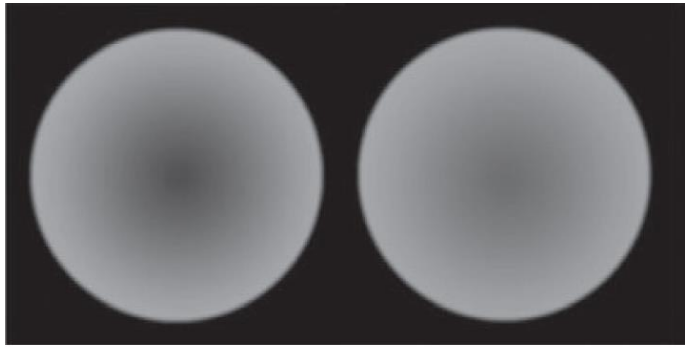

^{99m}Tc ^{131}I

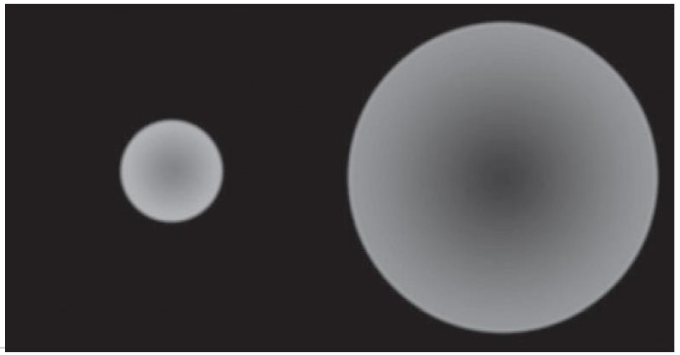

10 cm 30 cm

Attenuation correction :

- Corrects (brings back) the pixel values according to the attenuation that the photons experience on their way.

Attenuation

- Attenuation is the inverse of transmission.
- It depends on the distance the photons need to travel through the tissue.
- Attenuation coefficient $\boldsymbol{\mu}$ depend on **density**, atomic number **Z** and **energy**.

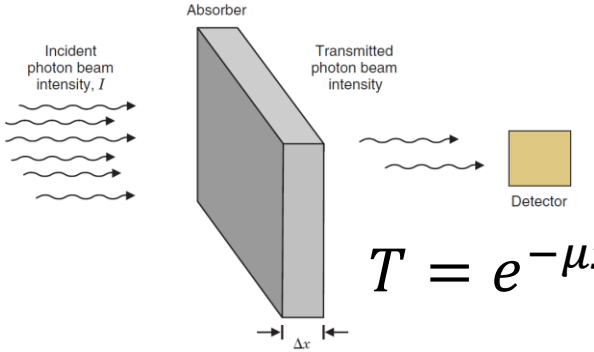

$$T = e^{-\mu x}$$

μ: linear attenuation coefficient (in cm^{-1})

$\mu_{\text{soft tissue}}(140\ keV) = \ 0.155\ cm^{-1}$

$\mu_{\text{bone}}(140\ keV) = \ 0.25\ cm^{-1}$

Effect of attenuation :

*^{99}Tc-line source response in **air***

↓ degradation of spatial resolution due to source-to-collimator distance

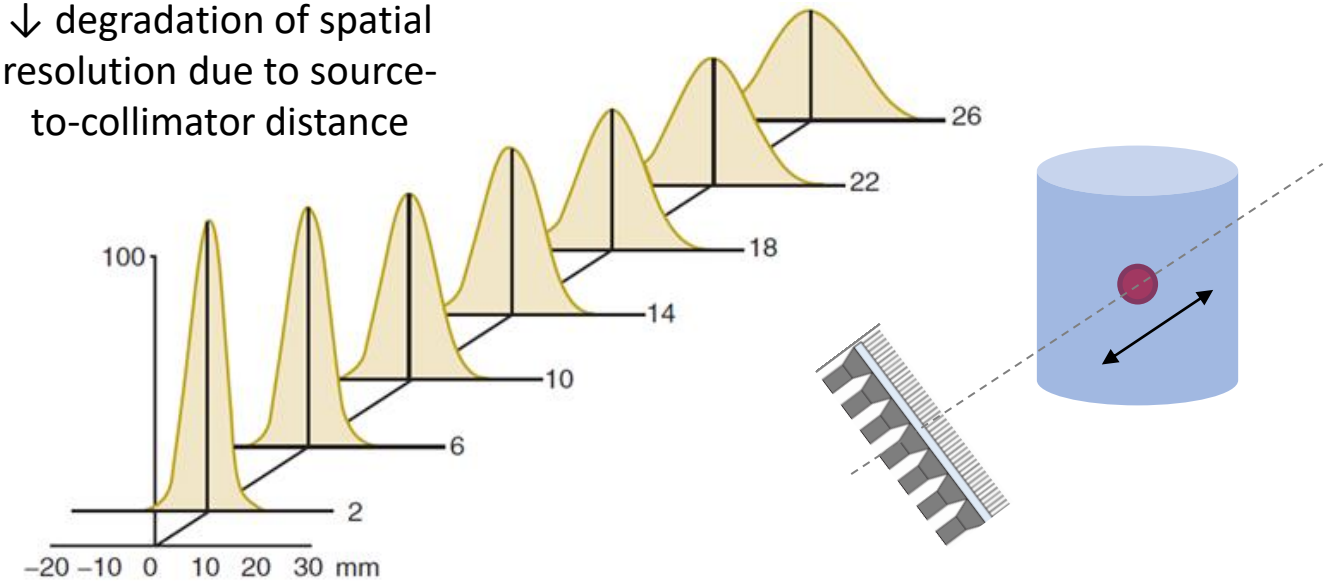

*^{99}Tc-line source response in **water***

↓ degradation of spatial resolution due to source-to-collimator distance **and attenuation**

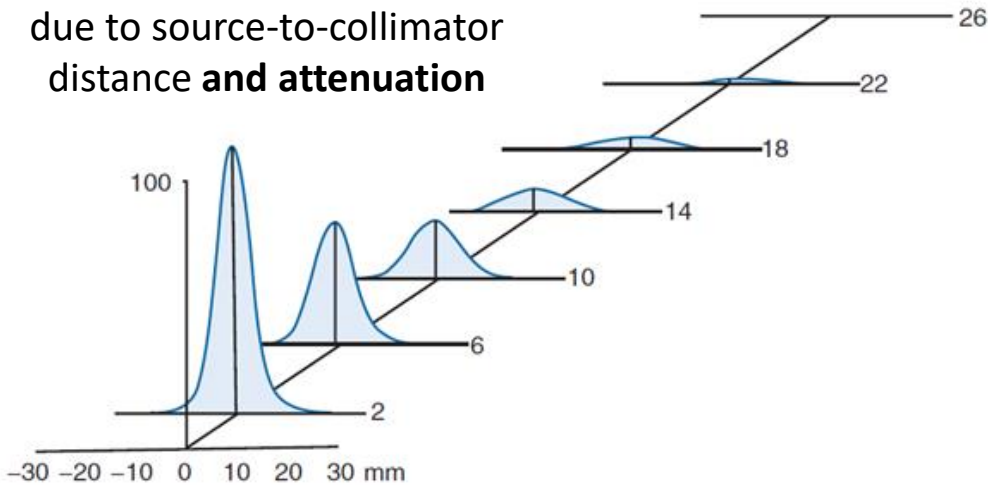

Attenuation correction in SPECT

- Attenuation is the inverse of transmission.
- It depends on the distance the photons need to travel through the tissue.
- Attenuation coefficients depend on density, atomic number Z and energy.

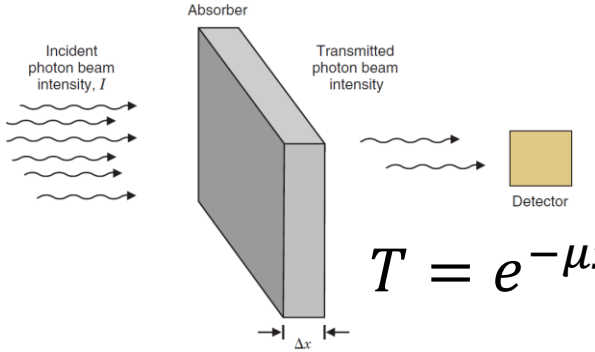

$$T = e^{-\mu x}$$

μ: linear attenuation coefficient (in cm^{-1})

$\mu_{tissue}(140\ keV) = \ 0.155\ cm^{-1}$

$\mu_{bone}(140\ keV) = \ 0.25\ cm^{-1}$

Conjugate counting :

reduce effects of line of response & tissue attenuation by acquiring profiles from directly opposing views.

Projections acquired over 360° and then combined

→ *but how? Arithmetic mean? Geometric mean?*

$$\overline{C_A} = \frac{(C_1 + C_2)}{2} = \frac{k}{2}\left(e^{-\mu d_1} + e^{-\mu d_2}\right)$$

$$\overline{C_G} = \sqrt{C_1 \times C_2} = k\sqrt{e^{-\mu(d_1+d_2)}} = k\sqrt{e^{-\mu(D)}} = ke^{-\mu D/2}$$

$C_1 = k\ e^{-\mu d_1}$

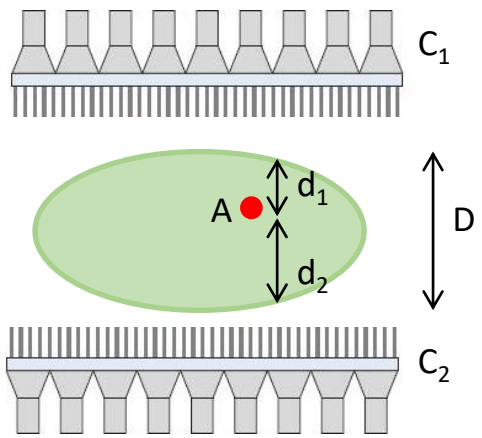

$C_2 = k\ e^{-\mu d_2}$

Geometric mean

- independent on source depth.
- only depends on total tissue thickness (*D*).

SPECT

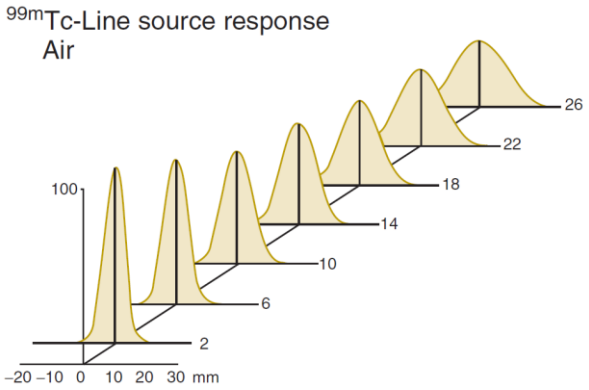

single detector

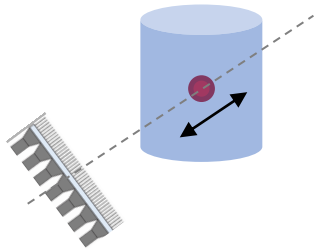

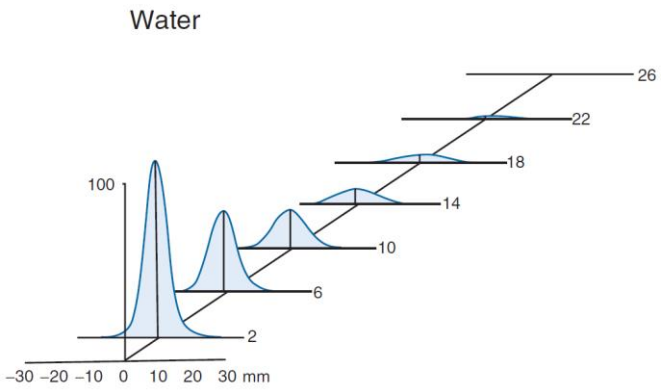

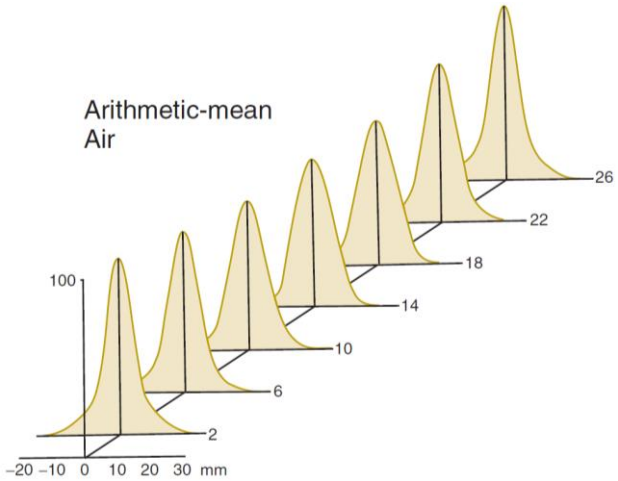

double detector
(conjugate counting, arithmetic mean)

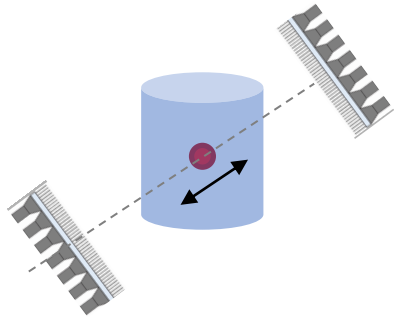

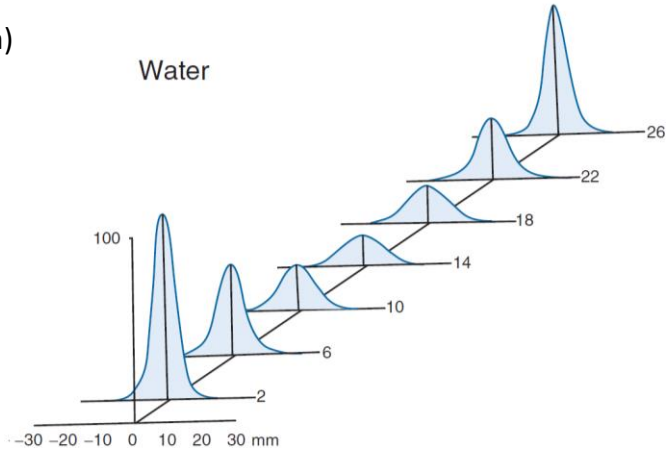

$$\overline{C_A} = \frac{(C_1 + C_2)}{2} = \frac{k}{2}\left(e^{-\mu d_1} + e^{-\mu d_2}\right)$$

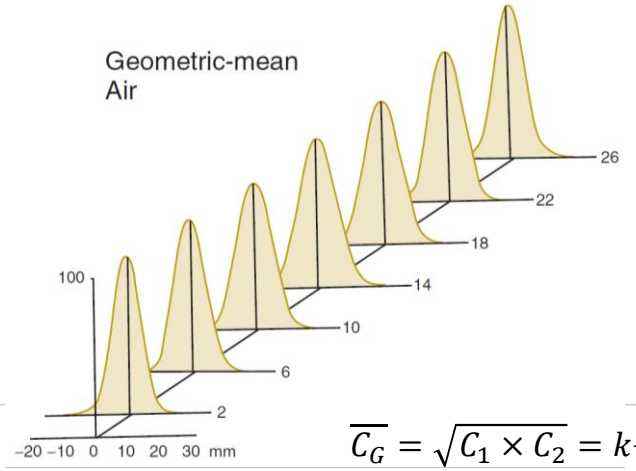

double detector
(conjugate counting, geometric mean)

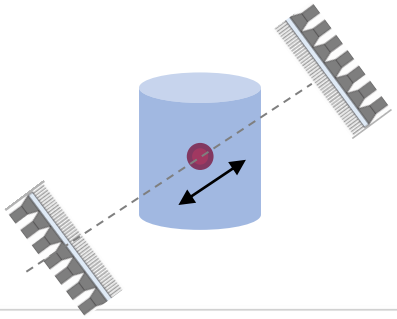

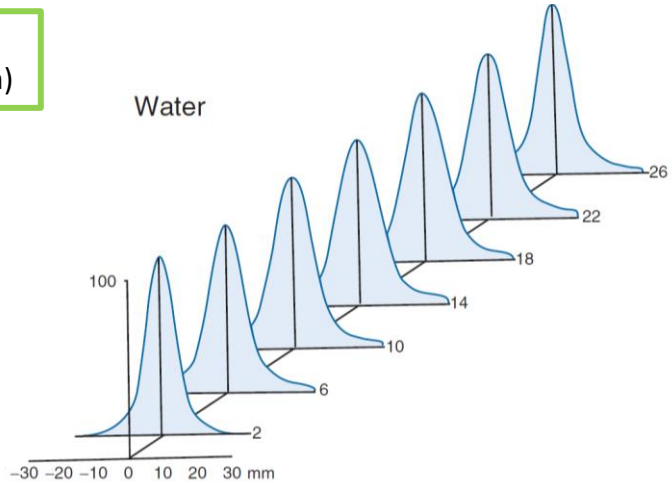

$$\overline{C_G} = \sqrt{C_1 \times C_2} = k\sqrt{e^{-\mu(d_1+d_2)}} = k\sqrt{e^{-\mu(D)}} = ke^{-\mu D/2}$$

Attenuation correction in SPECT

What about multiple sources ?

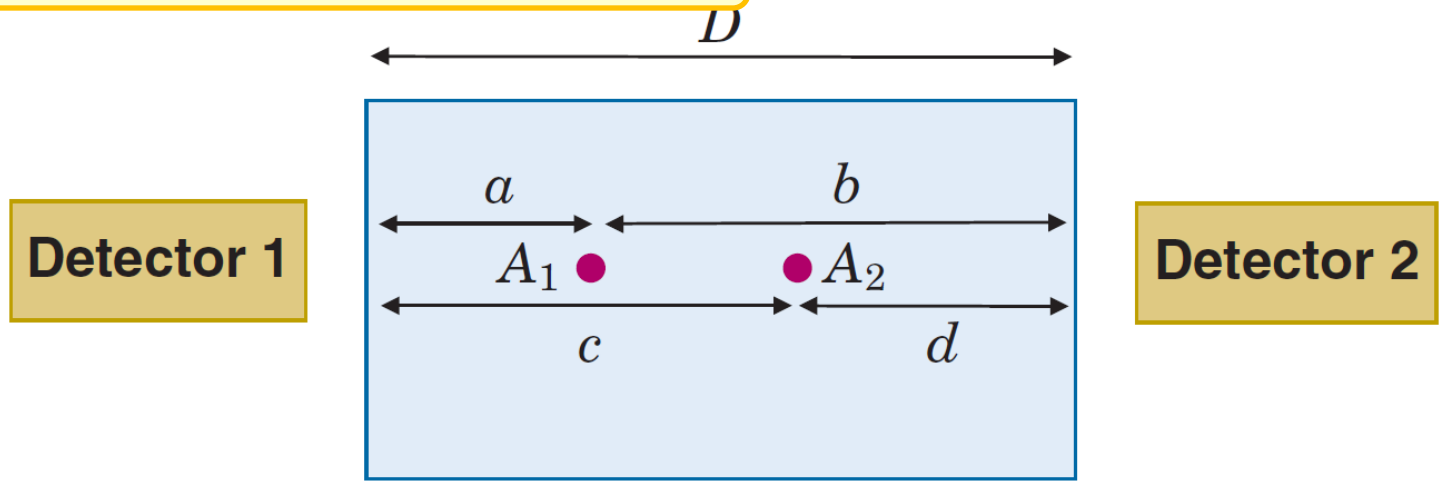

$$a + b = D$$
$$c + d = D$$

$$D_1 = k_1 e^{-\mu a} + k_2 e^{-\mu c} \qquad D_2 = k_1 e^{-\mu b} + k_2 e^{-\mu d}$$

$$\bar{C}_G = \sqrt{C_1 \times C_2} = k_1^2 e^{-\mu \overbrace{(a+b)}^{=D}} + k_2^2 e^{-\mu \overbrace{(c+d)}^{=D}} + k_1 k_2 e^{\mu(a+d)} + k_1\, k_2 e^{-\mu(c+b)}$$

$$\bar{C}_G = \left(k_1^2 + k_2^2\right) e^{-\mu D} \underbrace{+ k_1 k_2 e^{\mu(a+d)} + k_1\, k_2 e^{-\mu(c+b)}}_{\text{depend on actual depth of the source!}}$$

Attenuation correction in SPECT

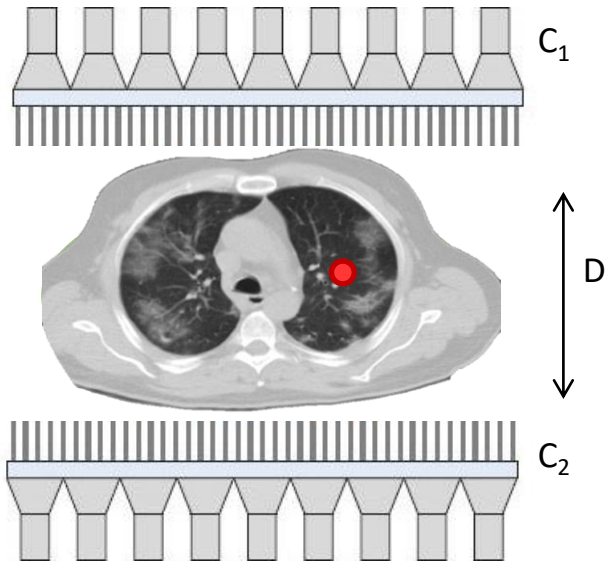

Limitations of conjugate techniques :

- Inaccurate for arbitrary source distribution in FOV.
- Assumption of uniform linear attenuation throughout the objet.

Conjugate counting with geometric mean:

Can reduce variations in amplitude, but there are scaling factors $\left(\propto e^{-\mu D/2}\right)$ that contribute to **loss of signal**.

Compensate for this by estimating the tissue thickness D, assuming a constant linear attenuation μ and multiply the projection profiles by an attenuation correction factor (ACF) → $f(x,y) = f'(x,y) \times ACF$

<u>Chang's multiplicative method:</u>

- A first image *f'(x,y)* is obtained through conventional FBP (no attenuation correction).
- Image contours used to estimate D.
- ACF for each pixel (x,y) in the reconstructed image is computed as:

$$ACF(x,y) = \frac{1}{\frac{1}{N}\sum_{i=1}^{N} e^{-\mu d_i}}$$

d_i: attenuation path length for the pixel at projection view i

Attenuation correction in SPECT

No attenuation correction

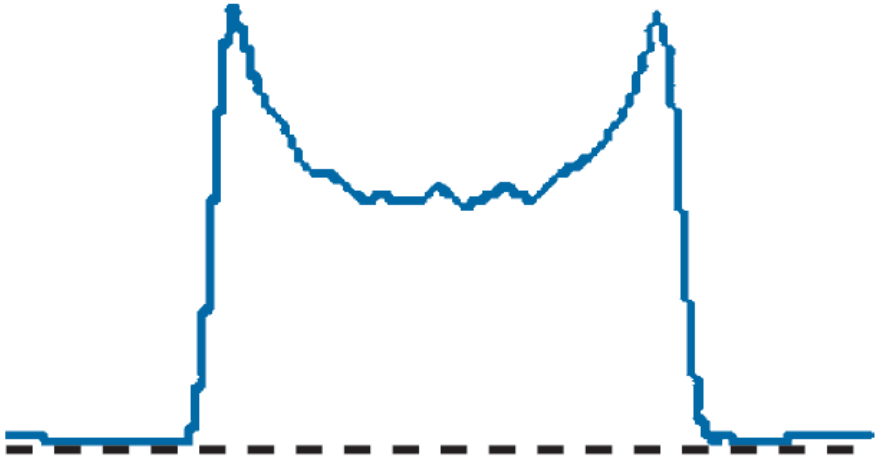

Attenuation correction approaches based on the Chang method are used in commercial SPECT systems where no other information concerning the attenuation are available.

Constant linear attenuation approximation

acceptable for:

- *brain*
- *abdomen*

not acceptable for:

- *thorax*
- *pelvic region*

Attenuation correction in SPECT

Ideal attenuation correction

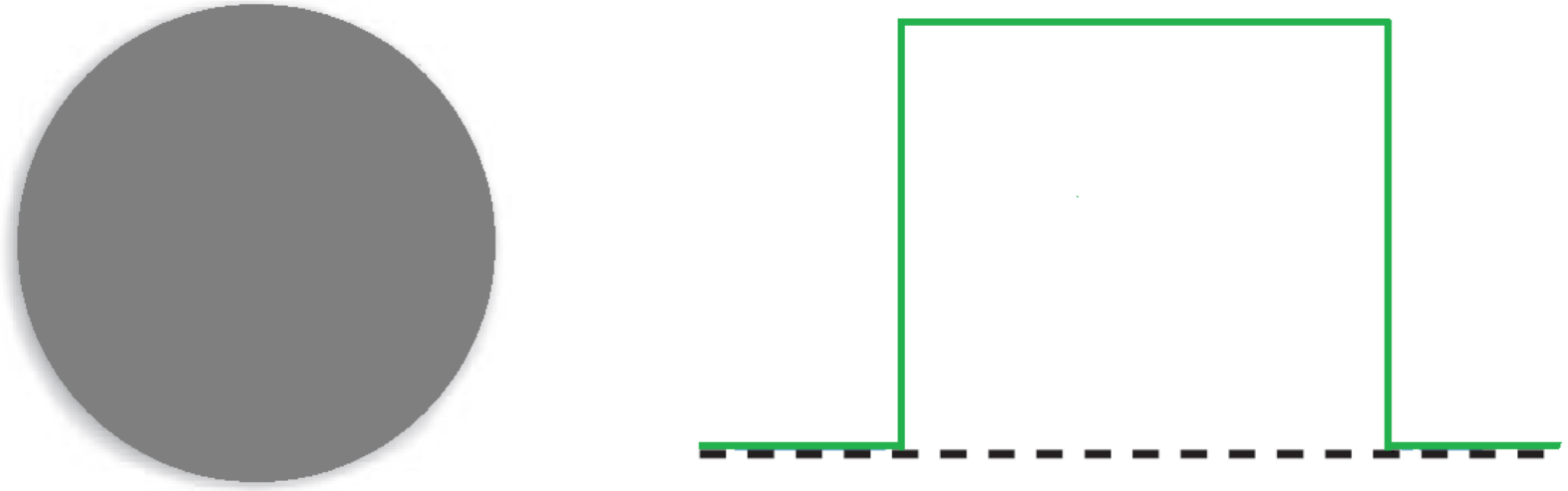

Attenuation correction approaches based on the Chang method are used in commercial SPECT systems where no other information concerning the attenuation are available.

Constant linear attenuation approximation

acceptable for:

- *brain*
- *abdomen*

not acceptable for:

- *thorax*
- *pelvic region*

Attenuation correction in SPECT

Chang correction ($\mu = 0.15\ cm^{-1}$)

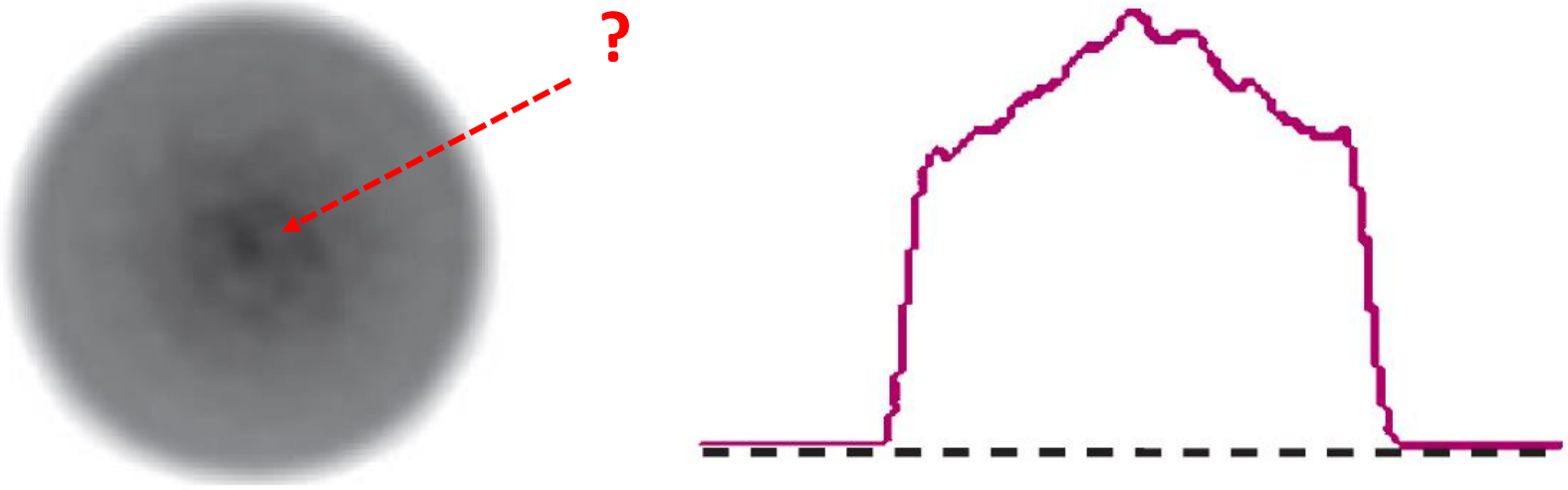

Attenuation correction approaches based on the Chang method are used in commercial SPECT systems where no other information concerning the attenuation are available.

Constant linear attenuation approximation

acceptable for:

- *brain*
- *abdomen*

not acceptable for:

- *thorax*
- *pelvic region*

Hybrid systems and attenuation correction (AC)

Concept : use more reliable attenuation values for better AC correction.

Measure tissue attenuation from transmission scan (CT).

⚠ CT for AC purposes are low-dose! ☢

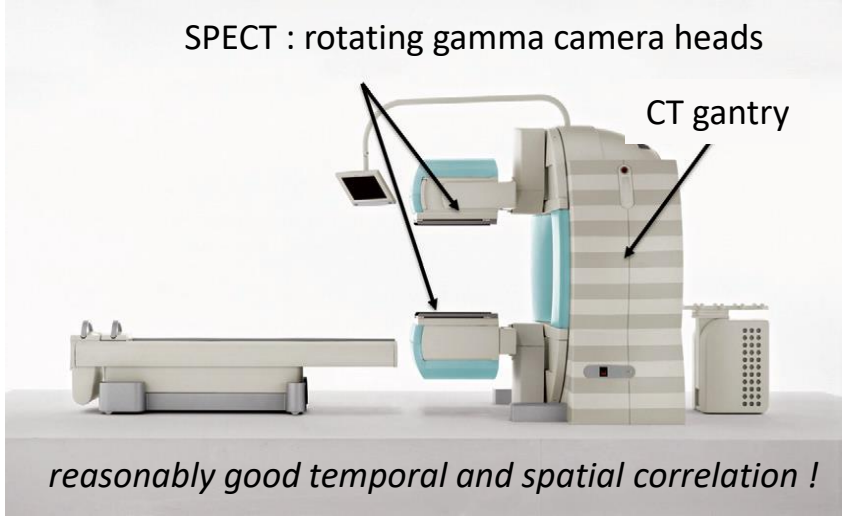

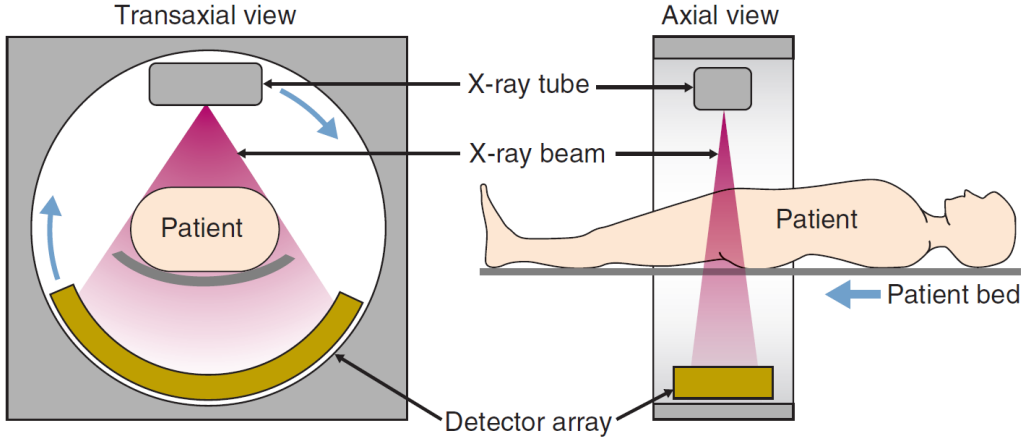

CT-based attenuation map is used for attenuation correction of SPECT data

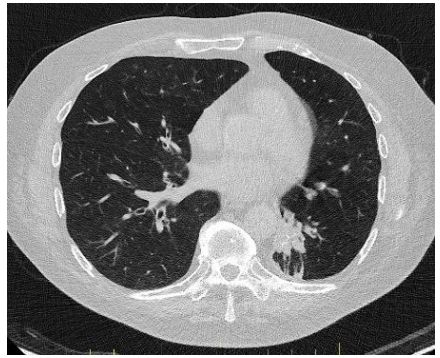

CT-AC is <u>standard</u> in modern hybrid SPECT/CT devices

Hybrid systems and attenuation correction (AC)

Vacuum tube with cathode (filament heated through an electrical current).

e- are liberated and accelerated by a bias voltage towards the anode (generally, rotating tungsten plate).

Production of continuous Bremmstrahlung radiation + discrete characteristic X-rays (anode material).

Tube current → # of emitted e-

Voltage → energy spectrum of X-rays (max =kVp) and #

X-ray beam collimated and filtered.

CT provide a map of the attenuation coefficient μ within the body

Conversion of the map of μ acquired with the **CT** transmission photon **energy** (e.g. effective energy 90 keV) **to the SPECT** emission photon **energy** (e.g. 140 keV for ^{99m}Tc).

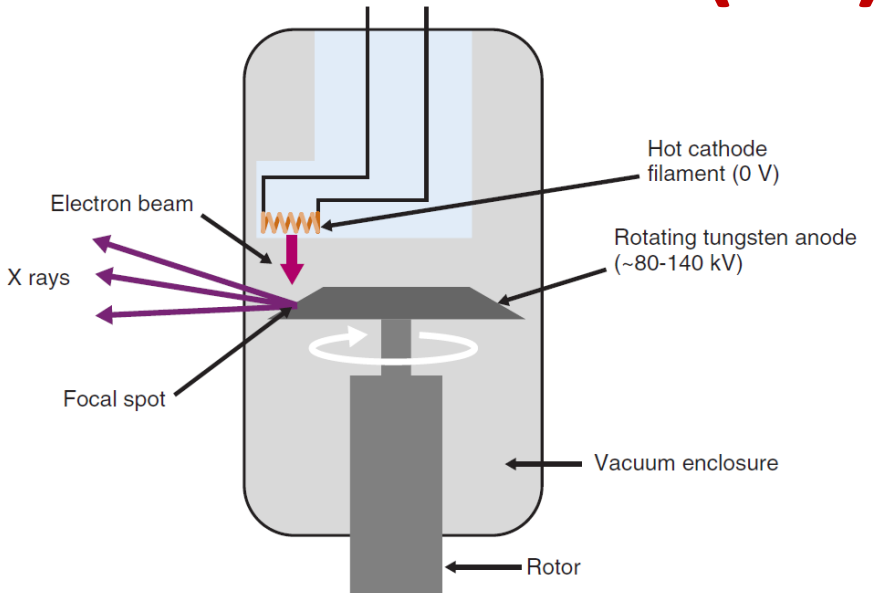

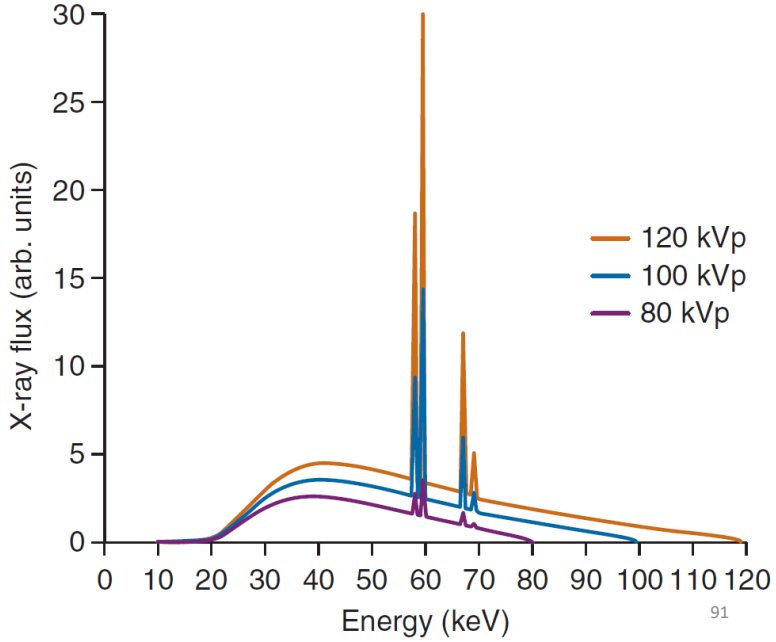

What about AI (CT-free attenuation correction)?

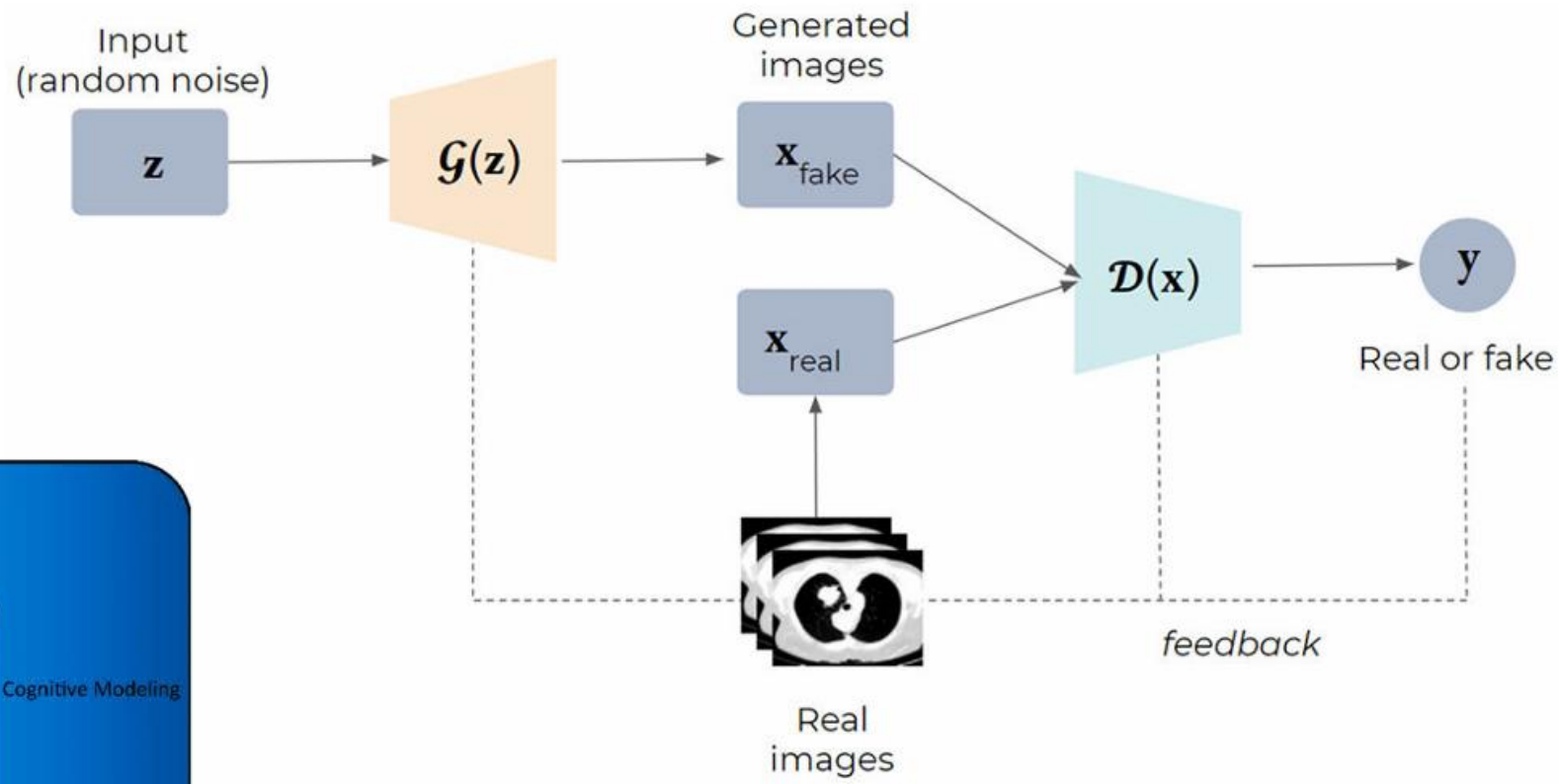

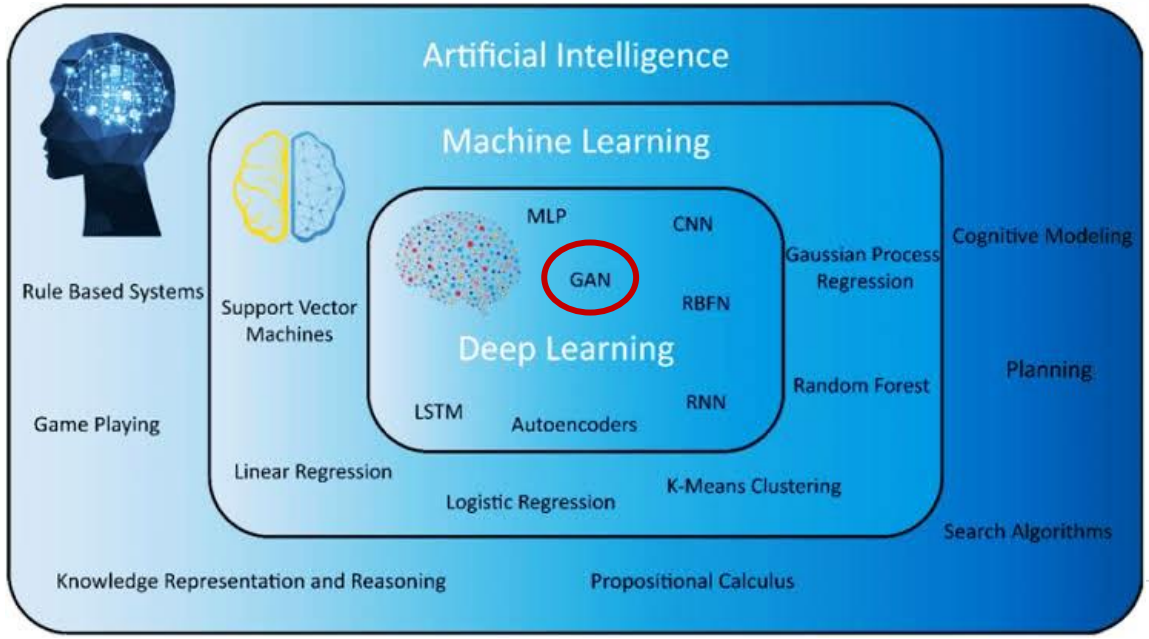

Figure 10.
Structure of Generative Adversarial Networks (GANs). Starting from random noise, the generator (G) uses the feedback from the discriminator (D) and learns to create images that are similar to the provided ground truth.

Which one is AC / NAC ?

skeletal

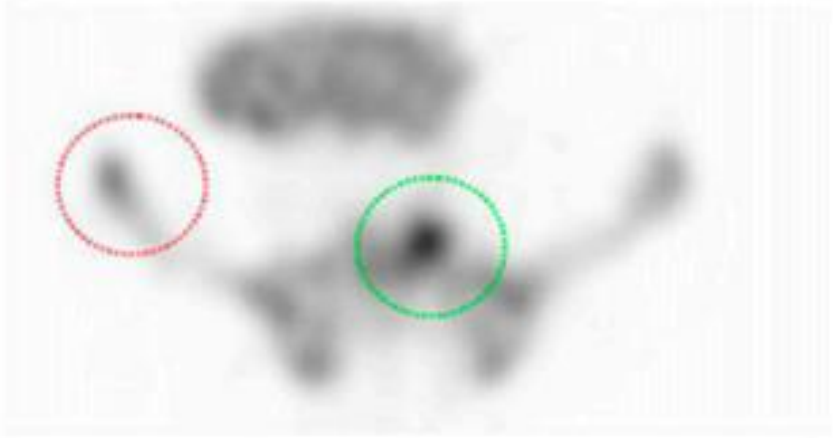

Which one is AC / NAC ?

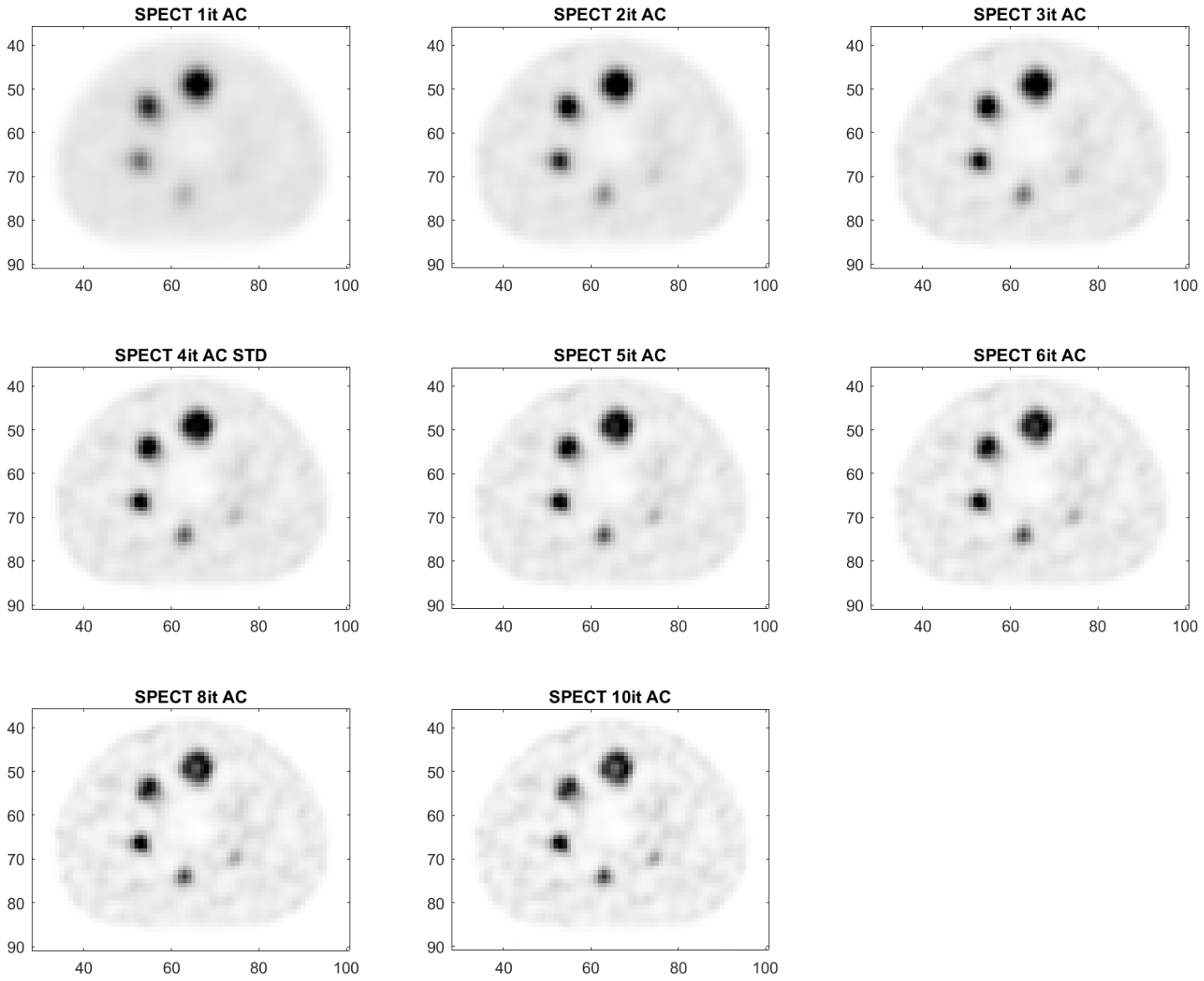

Which one is AC / NAC ?

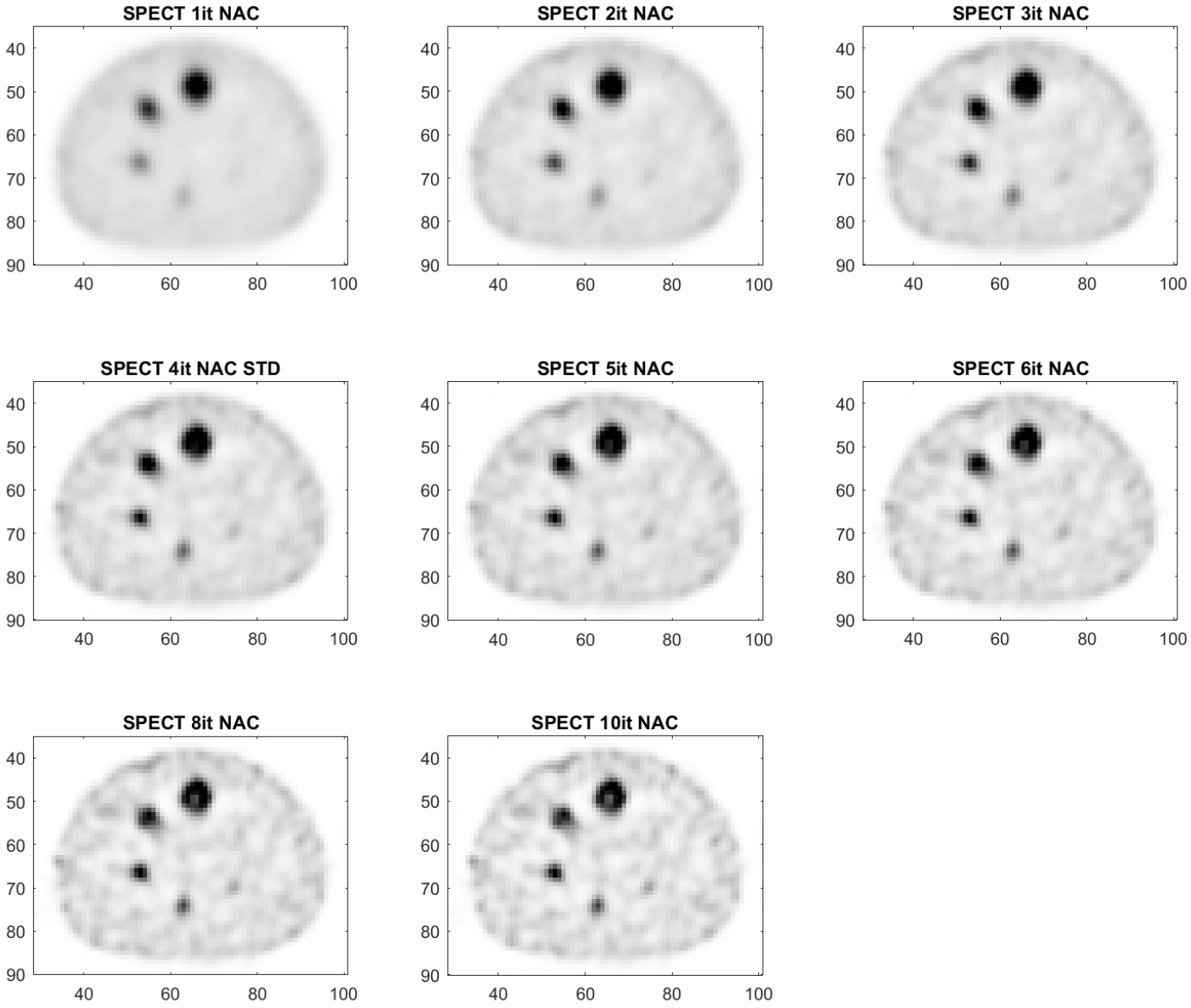

Scatter correction in SPECT

← scatter correction by energy discrimination

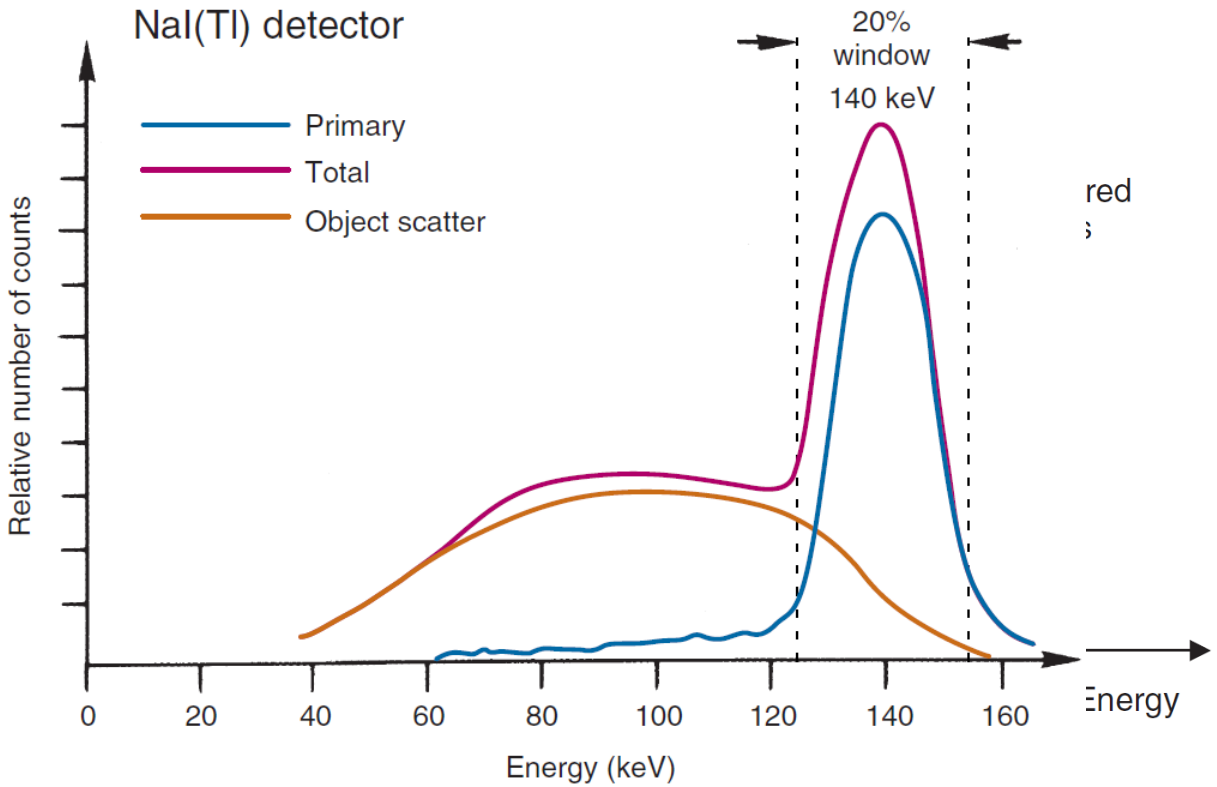

- Two energy windows: one for scatter and one for the photopeak.
- Scatter projection profiles are multiplied by a weighting factor and subtracted from the photopeak.
- Weighting factor needs to be determined experimentally (depends on source size, energy windows, system resolution).
- ***Ex: Scatter vs attenuation correction … which one comes first?***

- For most diagnostic examinations, activity administered to patient in NM depends on the patient mass.
- Activity can be ≠ depending on the system performances and particular situations, but some reference values are provided by the **Diagnostic Reference Levels (DRL).**
- Defined by the Federal Office of Public Health.
- DLR: 75 percentile of the dose indicator distribution for a given examination (e.g. CT) or median value (injected activity).

Tableau 1.1 Niveaux de référence diagnostiques lors d'examens de médecine nucléaire chez les adultes

Examen	Nucléide	Produit radiopharmaceutique	NRD (activite) (median)		CT Absorption/Localisation NRD (75e percentile)		Dose effective E_{50} due au produit radiopharmaceutique
			pour 70 kg [MBq]	par poids [MBq/kg]	$CTDI_{vol}$ [mGy]	DLP [mGy·cm]	[mSv]
Système osseux	Tc-99m	DPD (Teceos), MDP (Lenoscint), HDP	700	10,0	10 (bassin) 5 (CV) 5 (extr.)	410 (bassin) 190 (CV) 160 (extr)	4,0
Thyroïde	I-123	Iodure	10		4	160	2,2[1]
Tumeur (TEP)	F-18	FDG (2D)	350	5,0	5 (corps entier) 6 (tronc)	760 (corps entier) 620 (tronc)	
	F-18	FDG (3D)	250	3,5			4,8

Figure 7 : Représentation schématique visant à déterminer les niveaux de référence diagnostiques

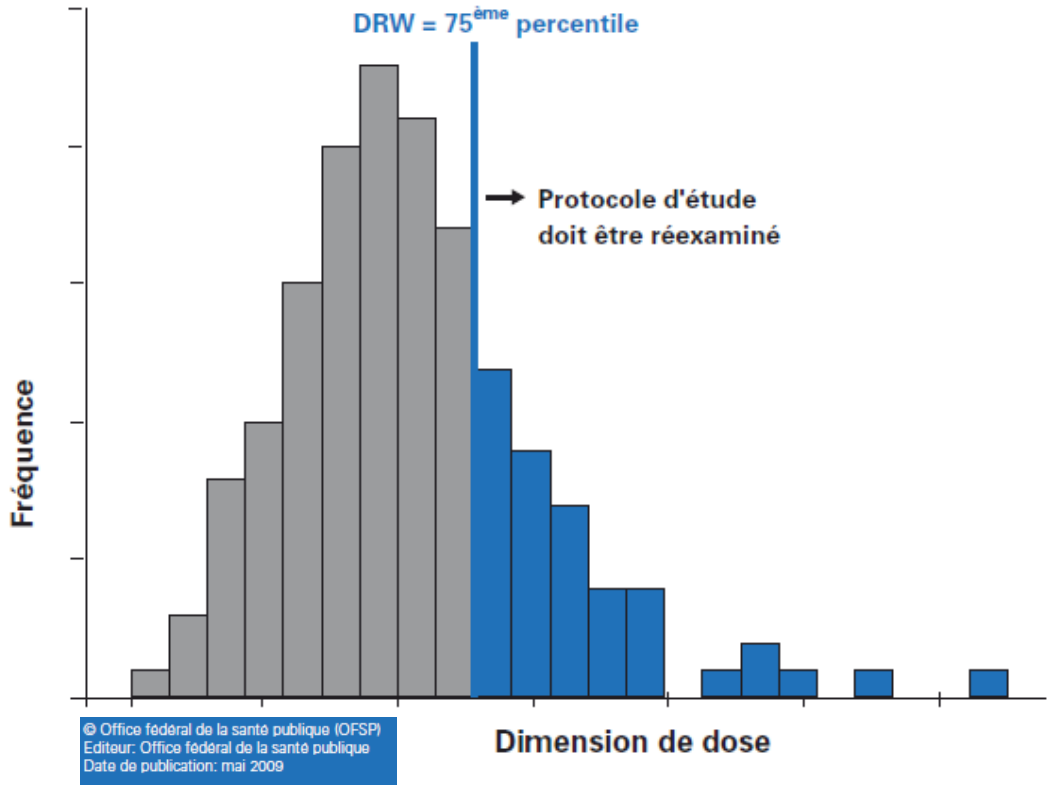

Image quality in NM also depends on the image statistics, hence the product of the acquisition time and the patient administered activity:

Time x mass-activity product (TAP)

Some applications of SPECT (examples)

Heart, kidney, brain, lungs, parathyroid, bones, digestive system, infections, tumors …

Sentinel Lymph Node

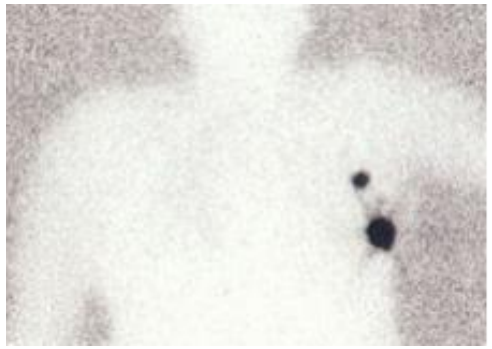

Renal scintigraphy

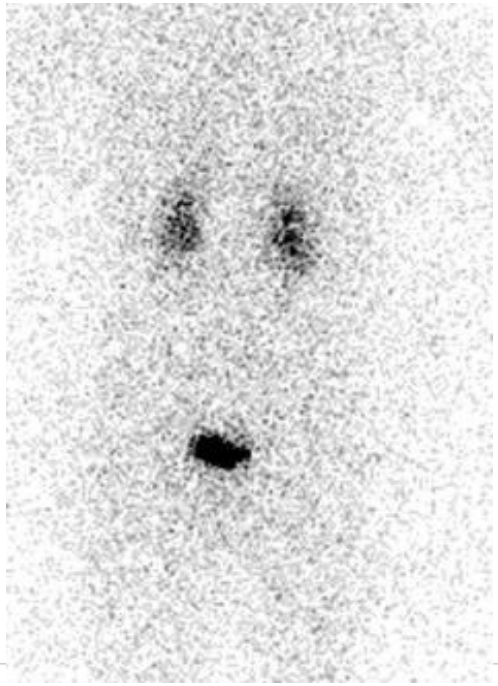

Bone scintigraphy

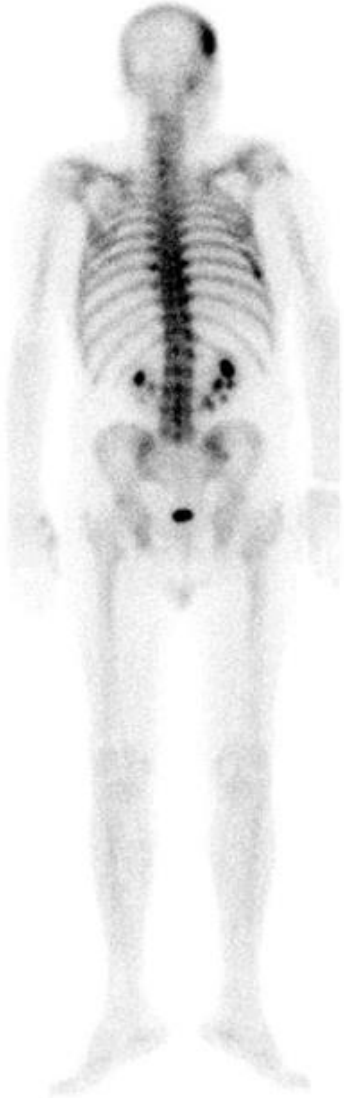

Cardiac (myocardial perfusion imaging)
Rest/stress study.
SPECT images are gated to ECG (movement correction).

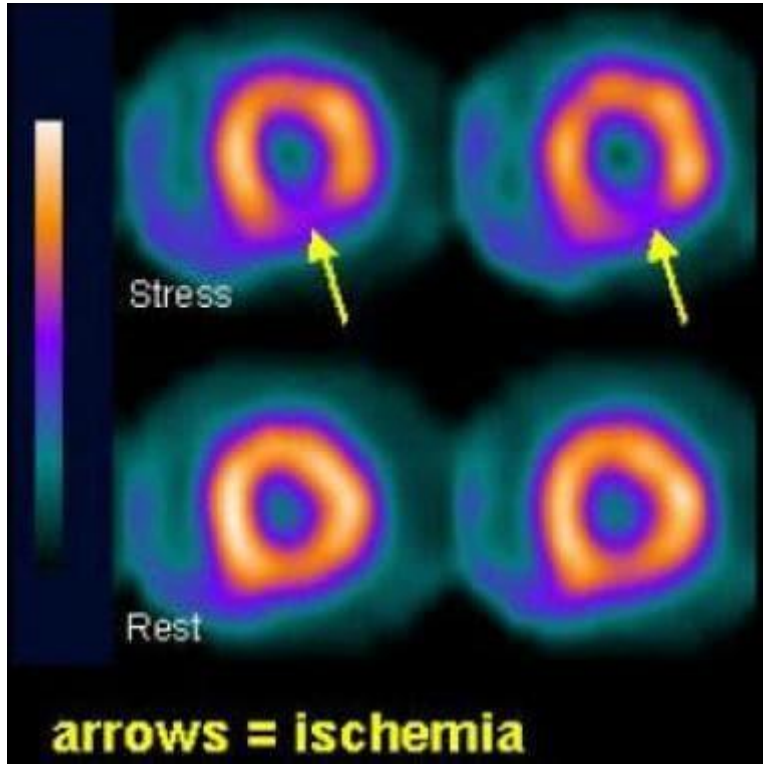

Some applications of SPECT (examples)

Cerebral perfusion studies
(radiotracer can be bound to specific receptors, e.g. dopamine → Parkinson's disease)

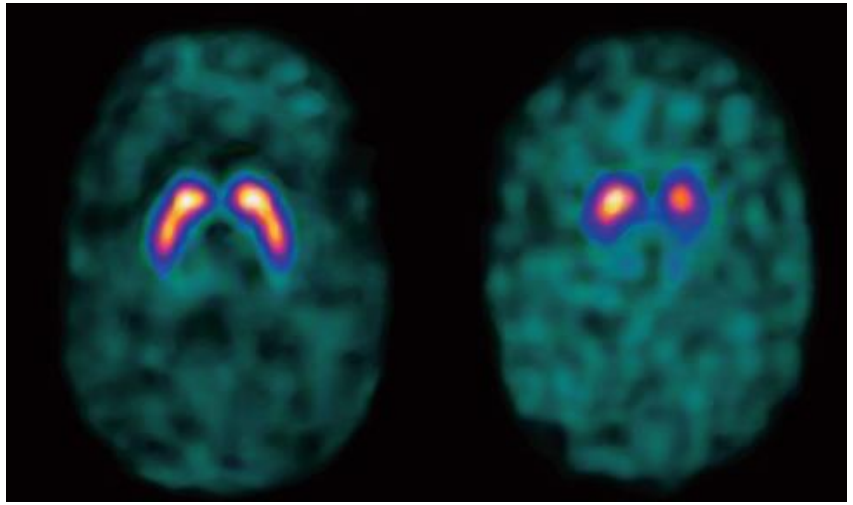

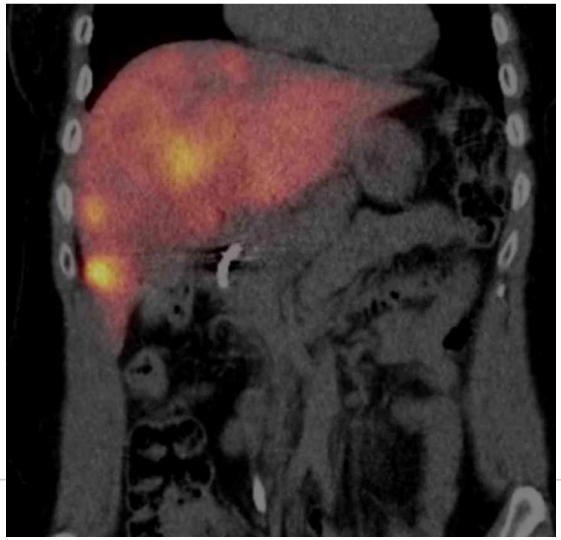

Liver treatment planning for hepatocellular carcinoma

Gastric emptying (dynamic study)

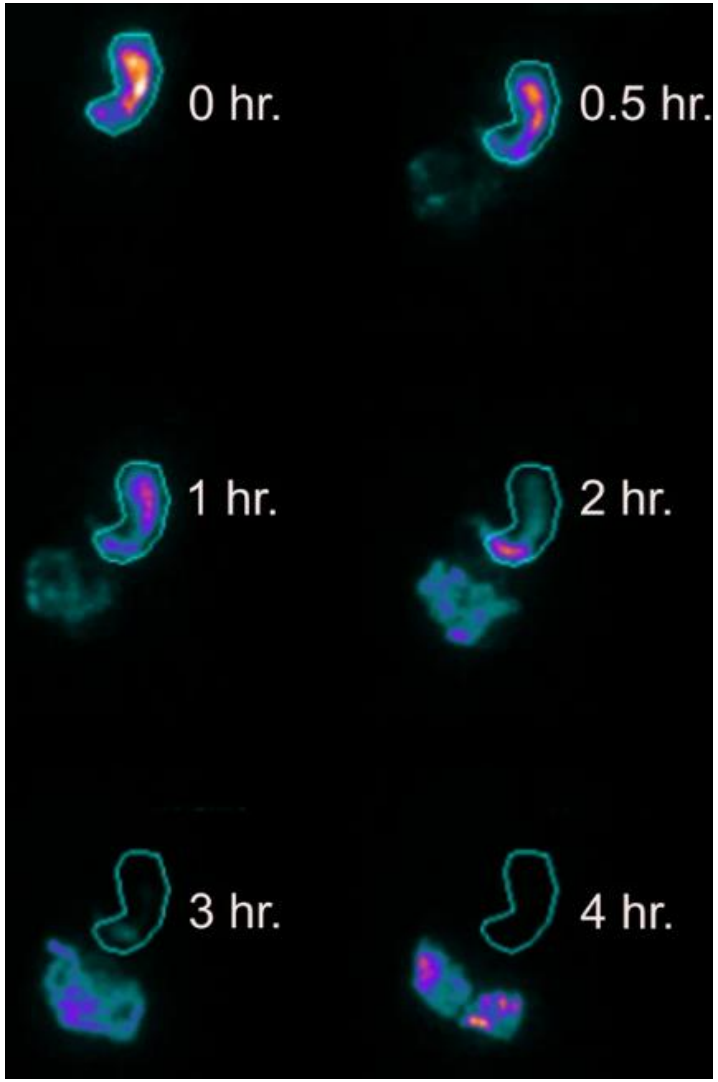

BONUS: radionuclide therapy, the future of NM?

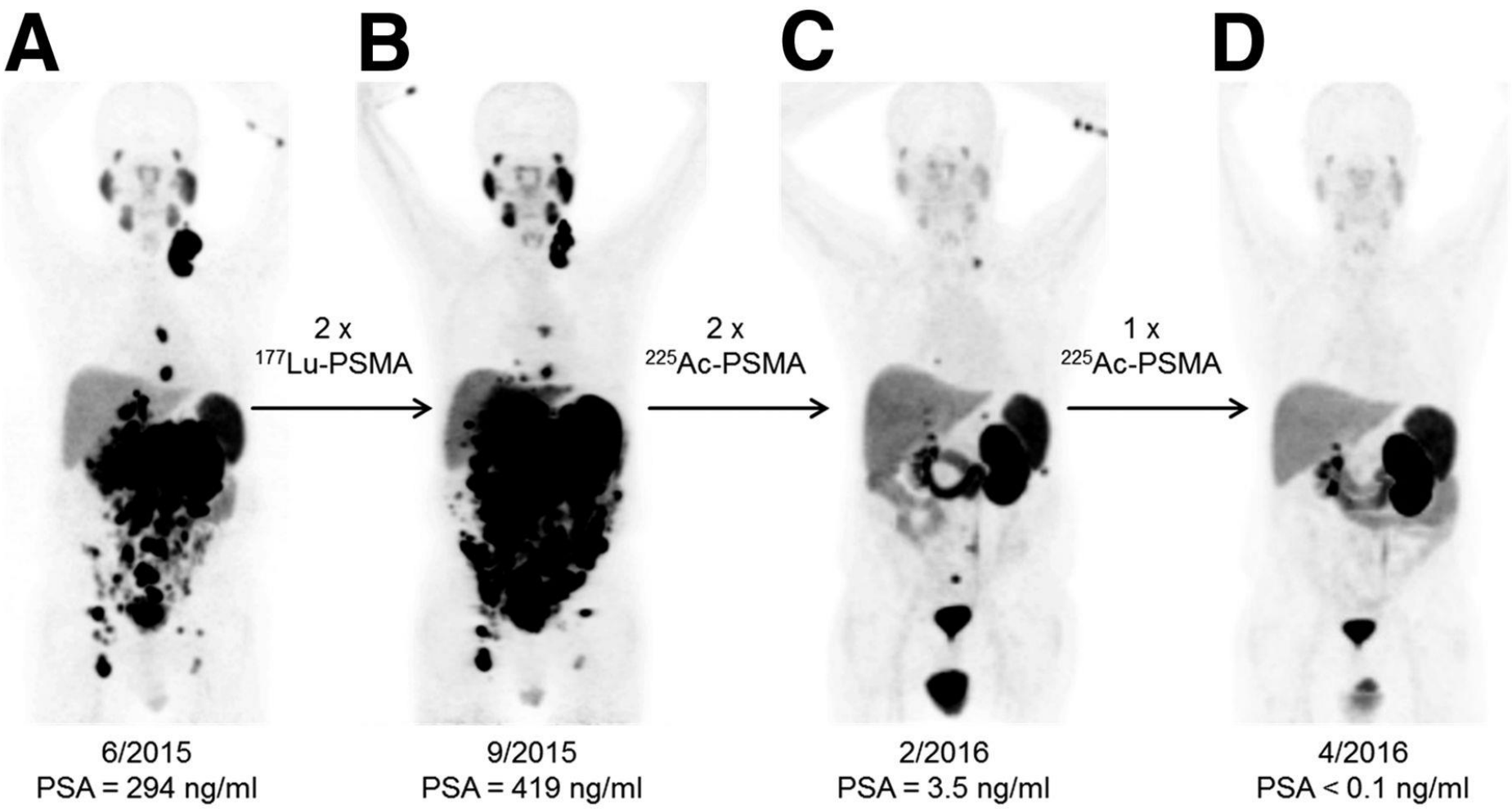

68Ga-PSMA-11 PET/CT scans of patient B. In comparison to initial tumor spread (A), restaging after 2 cycles of β-emitting 177Lu-PSMA-617 presented progression (B). In contrast, restaging after second (C) and third (D) cycles of α-emitting 225Ac-PSMA-617 presented impressive response.

https://jnm.snmjournals.org/content/57/12/1941

Example of medical physicist task : optimisation

NEMA phantom:

Background (BG), 6 hot spheres, 1 cold region

Activity concentration spheres/BG = 10:1

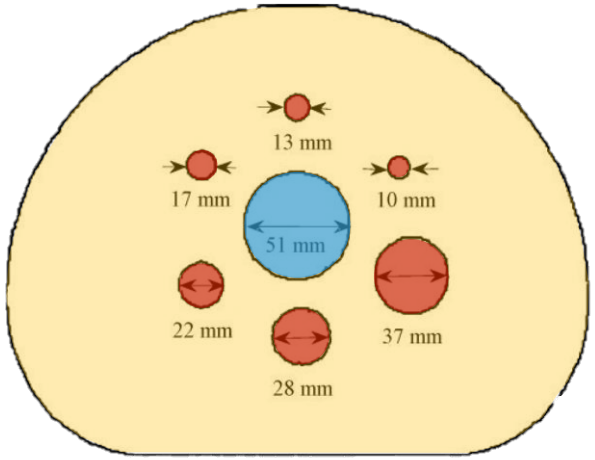

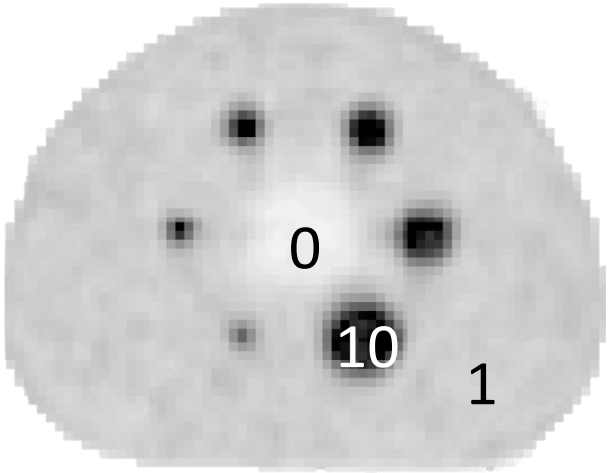

S. Medici, S. Gnesin. Impact of clinical protocol optimization in SPECT and PET: a multi-centre and multi-device study. Swiss Congress of Radiology 2023

Protocol optimisation

$$CNR_{\text{sphere}} = \frac{\bar{S}_{\text{sphere}} - \bar{S}_{\text{BG}}}{SD_{\text{BG}}}$$

$$Q_H(\%) = \left(\frac{\frac{S_{\text{sphere,meas}}}{S_{\text{BG,meas}}} - 1}{\frac{S_{\text{sphere,true}}}{S_{\text{BG,true}}} - 1} \right) \cdot 100$$

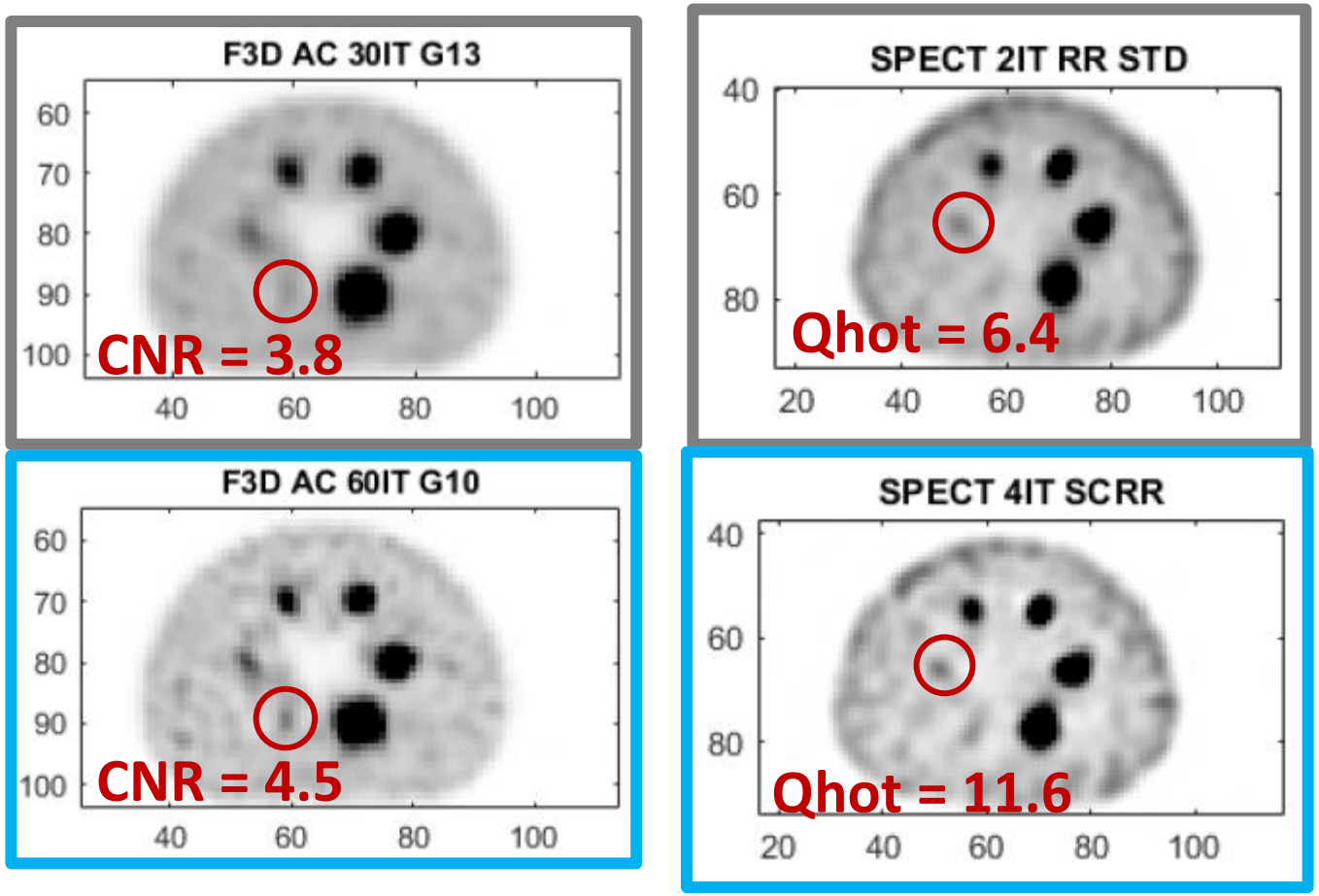

Examples of image quality improvement (CNR and Q_{hot}) by optimising reconstruction parameters

S. Medici, S. Gnesin. Impact of clinical protocol optimization in SPECT and PET: a multi-centre and multi-device study. Swiss Congress of Radiology 2023

Statistics vs. IQ

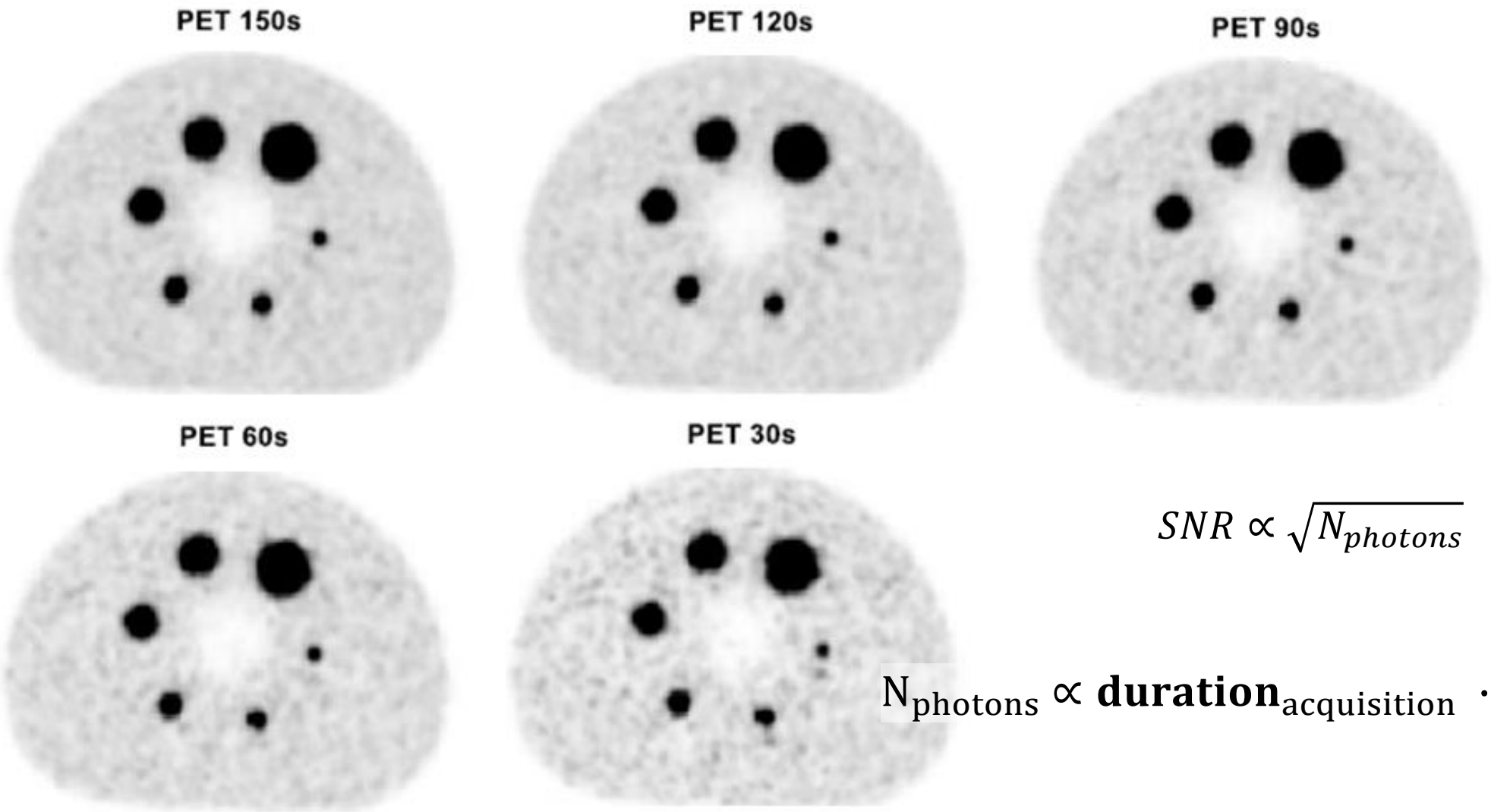

$$SNR \propto \sqrt{N_{photons}}$$

$$\mathrm{N}_{\mathrm{photons}} \propto \mathbf{duration}_{\mathrm{acquisition}} \cdot \mathbf{activity}_{\mathrm{injected}}$$

S. Medici, S. Gnesin. Impact of clinical protocol optimization in SPECT and PET: a multi-centre and multi-device study. Swiss Congress of Radiology 2023

Statistics vs. IQ

IQ preserved → margin for **dose reduction**

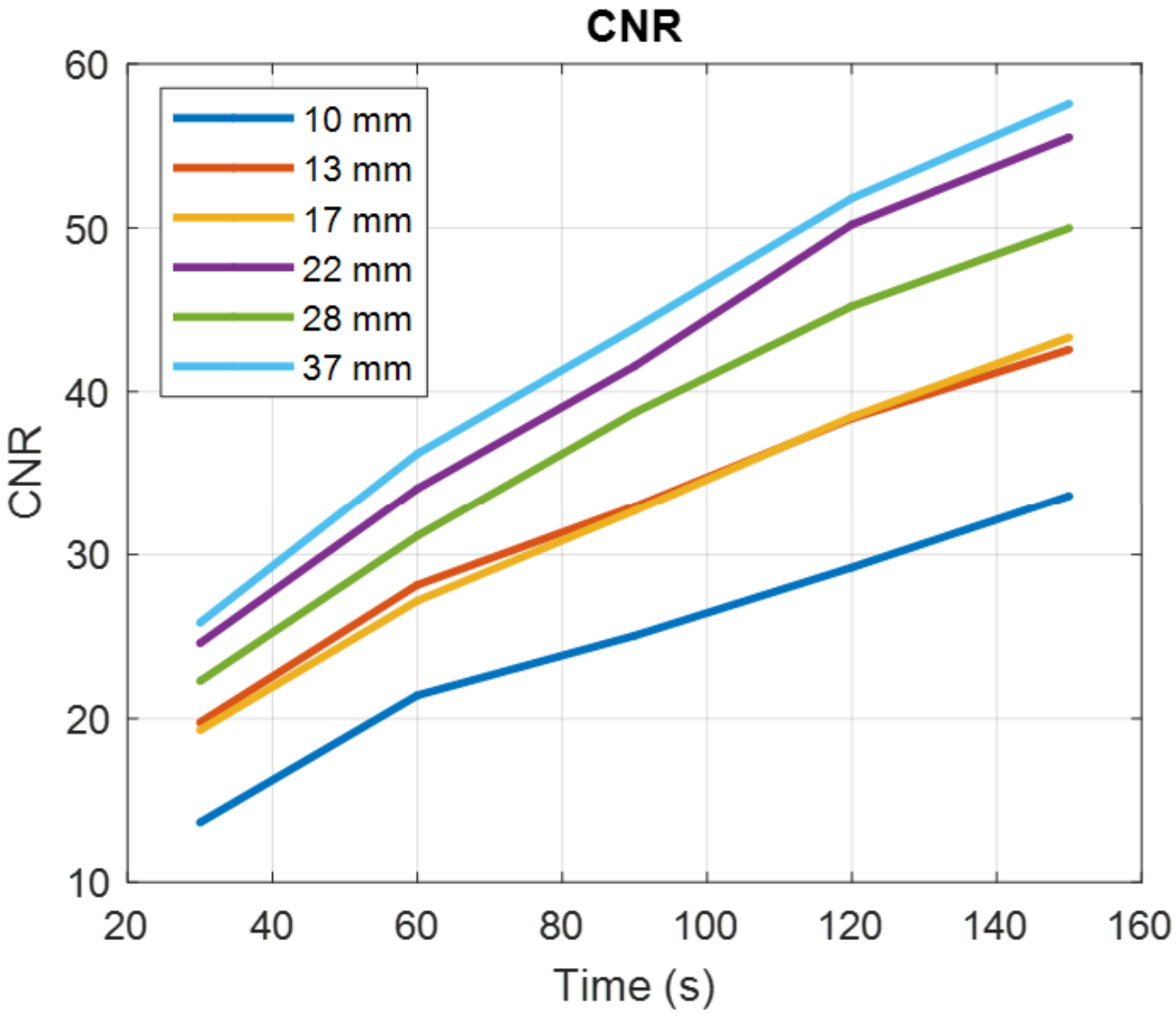

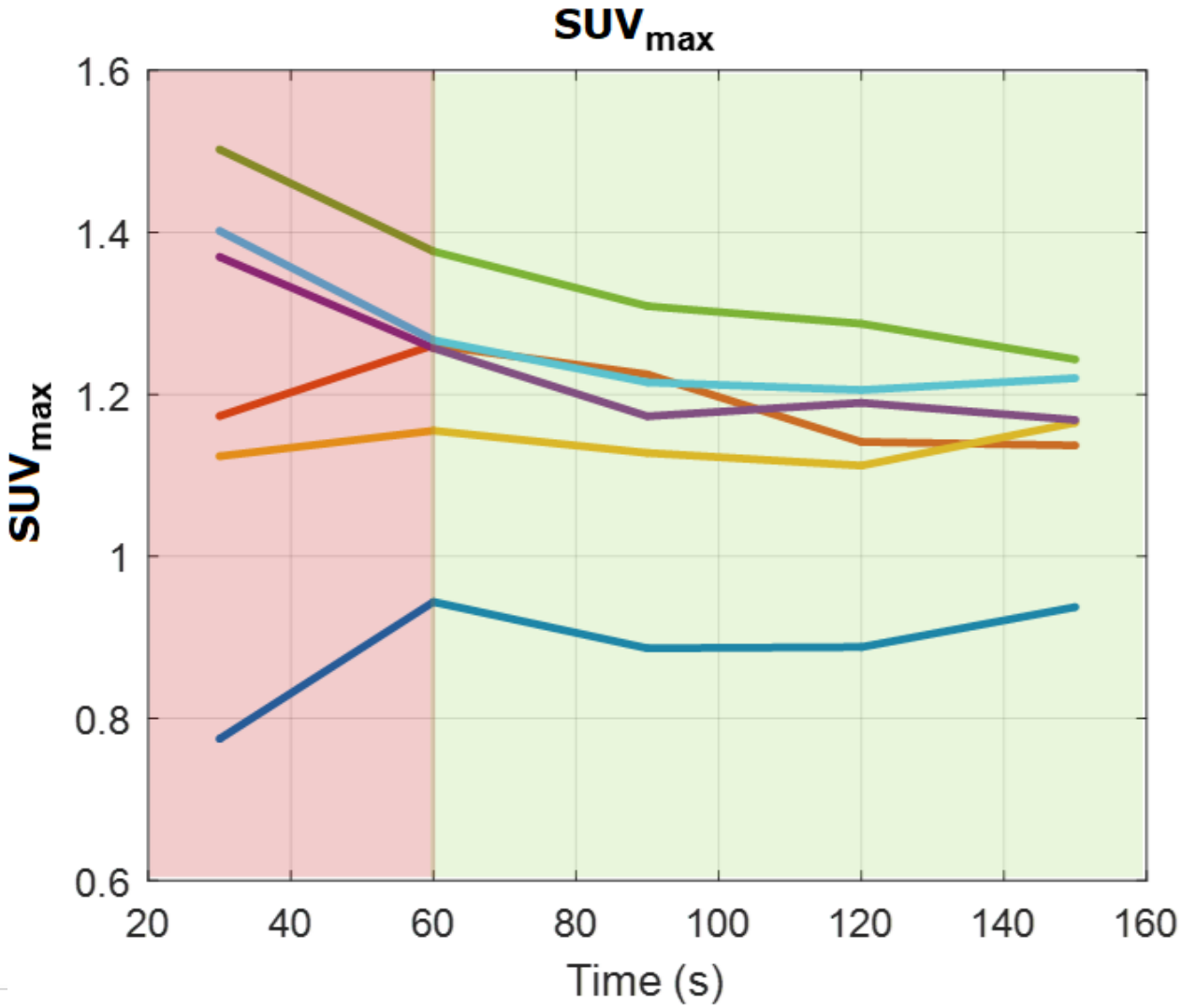

S. Medici, S. Gnesin. Impact of clinical protocol optimization in SPECT and PET: a multi-centre and multi-device study. Swiss Congress of Radiology 2023

Résumé (1/2)

- The gamma camera is the main component of SPECT devices.
- It features a large scintillation detector (usually NaI) that produces amount of scintillation light ∝ to the energy of incoming radiation that is then converted into an electric signal.
- Scatter also contribute to even mislocation in SPECT images and thus degradation of image quality.
- The energy discrimination allowed by scintillation detectors makes it possible to identify and ignore photons that underwent scattering within the patient.
- The detector crystal should be thick enough to allow the photons emitted from the patient to interact with it (ideally through photoelectric effect) but not too thick to lose spatial resolution.
- SPECT devices rely on the use of collimators to discriminate between wanted and unwanted events that may be recorded by the detector and allow for the localisation of the activity distribution within the patient.
- Different collimators are used for different purposes (e.g. minimisation or maximisation of certain anatomical regions).
- Collimators should be adapted to the energy of the incoming radiation (e.g. ≠ collimators for Tc-99m and for Lu-177).
- The spatial resolution of the gamma camera is highly impacted by the use of collimators and by the distance between the patient and the detector (typical spatial resolution ~ 10 mm).
- The use of absorptive collimation reduces the sensitivity (efficiency) of the gamma camera.
- Studies can be either static or dynamic (activity distribution over time) and acquisitions can be gated (e.g. to match certain phases of the cardiac cycle and correct for patient breathing motion).

Résumé (2/2)

- Tomographic reconstruction allows to retrieve the activity distribution within an object and allows for 3D imaging.
- The aim is to retrieve the unknown activity distribution within the patient starting from projections acquired at different angles, that are stored in sinograms. Each image slice has its own sinogram.
- Different methods exist (e.g. simple and filtered back-projection) to reconstruct the original activity distribution, but nowadays the most widely used is through iterative algorithms.
- Iterative algorithms compare the measured sinograms with the one obtained from an estimated image. The estimated image is updated until the measured and the computed sinogram converge → the estimated image is now a good approximation of the real activity distribution.
- Artifacts in SPECT may be given (among others) by linear and angular undersampling and missing or incomplete projections.
- Attenuation within the patient causes important loss of signal and many methods have been deployed to limit its impact.
- Nowadays, the most common way to correct for attenuation is by exploiting the attenuation information obtained through a transmission computed tomography (CT) scan.
- Protocol optimisation is needed to provide the best clinical information and should be adapted to the clinical question.

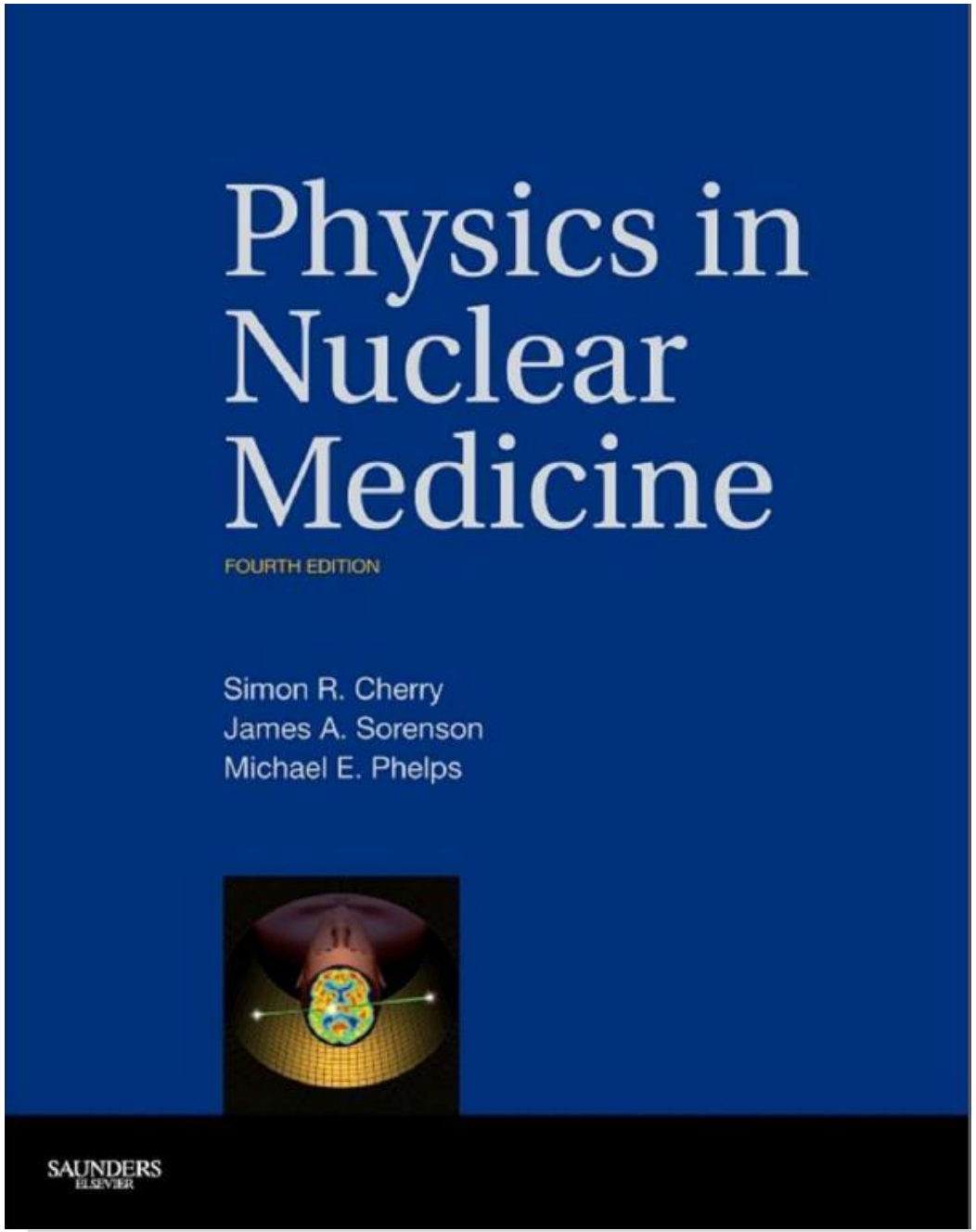

Main reference textbook:
Physics in Nuclear Medicine (4th edition)
by Simon R. Cherry, James A. Sorenson, and Michael E. Phelps
ISBN: 978-1-4160-5198-5

Other sources:
«Cours de Radiophysique Medicale - Médecine nucléaire & Radiochimie», IRA / HESAV TRM.

Some animations from:
Floris HP van Velden (EANM Milan 2012).